

การเลือกตัวทำละลายเพื่อแยก 1,3-โพรเพนไดออลที่ได้จากกระบวนการทางชีวภาพ

นาย ฐาปกรณ์ บุญส่งสวัสดิ์

วิทยานิพนธ์นี้เป็นส่วนหนึ่งของการศึกษาตามหลักสูตรปริญญาวิศวกรรมศาสตรมหาบัณฑิต

สาขาวิชาวิศวกรรมเคมี ภาควิชาวิศวกรรมเคมี

คณะวิศวกรรมศาสตร์ จุฬาลงกรณ์มหาวิทยาลัย

ปีการศึกษา 2550

ลิขสิทธิ์ของจุฬาลงกรณ์มหาวิทยาลัย

SOLVENT SELECTION FOR SEPARATION OF BIOLOGICALLY
DERIVED 1,3-PROPANEDIOL

Mr. Thapagorn Boonsongsawat

A Thesis Submitted in Partial Fulfillment of the Requirements
for the Degree of Master of Engineering Program in Chemical Engineering

Department of Chemical Engineering

Faculty of Engineering

Chulalongkorn University

Academic Year 2007

Copyright of Chulalongkorn University

Thesis Title SOLVENT SELECTION FOR SEPARATION OF BIOLOGICALLY
DERIVED 1,3-PROPANEDIOL
By Mr. Thapagorn Boonsongsawat
Field of Study Chemical Engineering
Thesis Advisor Associate Professor Chirakarn Muangnapoh, Dr.Ing.
Thesis Co-advisor Assistant Professor Artiwan Shotipruk, Ph.D.

Accepted by the Faculty of Engineering, Chulalongkorn University in Partial
Fulfillment of the Requirements for the Master's Degree

..... Dean of the Faculty of Engineering
(Professor Direk Lavansiri, Ph.D.)

THESIS COMMITTEE

..... Chairman
(Associate Professor Seeroong Prichanont, Ph.D.)

..... Thesis Advisor
(Associate Professor Chirakarn Muangnapoh, Dr.Ing.)

..... Thesis Co-advisor
(Assistant Professor Artiwan Shotipruk, Ph.D.)

..... Member
(Assistant Professor Muenduen Phisalaphong, Ph.D.)

..... Member
(Chaiya Chandavas, Ph.D.)

ฐานปรกรณ์ บุญส่งสวัสดิ์: การเลือกตัวทำละลายเพื่อแยก 1,3-โพรเพนไดออลที่ได้จากกระบวนการทางชีวภาพ. (SOLVENT SELECTION FOR SEPARATION OF BIOLOGICALLY DERIVED 1,3-PROPANEDIOL) อ. ที่ปรึกษา : รศ. ดร. จิรกานต์ เมืองนาโพธิ์, อ.ที่ปรึกษาร่วม : ผศ. ดร. อาทิวรรณ โชติพฤกษ์, 90 หน้า.

งานวิจัยนี้มีวัตถุประสงค์ที่จะเลือกตัวทำละลายที่เหมาะสมสำหรับการแยก 1,3 โพรเพนไดออลออกจากน้ำโดยพิจารณาข้อมูลจากการทดลองที่สมดุลของสารผสม 1,3 โพรเพนไดออล น้ำ และตัวทำละลาย การเลือกตัวทำละลายที่เหมาะสมสำหรับการสกัด 1,3 โพรเพนไดออลจากน้ำพิจารณาจากการเลือกตัวทำละลายในทางทฤษฎีโดยใช้แบบจำลองแอสเซน แล้วประเมินความเหมาะสมของตัวทำละลายจากค่าสัมประสิทธิ์การกระจายตัวและค่าการละลายของตัวทำละลายในน้ำ โดยเปรียบเทียบข้อมูลที่ได้จากการทดลองกับข้อมูลที่ได้จากการคำนวณด้วยสมการของยูนิเฟค พบว่าข้อมูลเส้นเชื่อมเฟสแสดงความสัมพันธ์ร่วมด้วยวิธีการของโอเมอร์-โทเบียสและแฮนด์มีค่าสัมประสิทธิ์ความสัมพันธ์อยู่ที่ 0.94 และ 0.99 ตามลำดับ จากการทดลองพบว่าเอทิลอะซิเตทเป็นตัวทำละลายที่เหมาะสมให้ค่าสัมประสิทธิ์การกระจายตัวของ 1,3 โพรเพนไดออลอยู่ที่ 0.22 ที่อุณหภูมิ 303.15 เคลวิน งานวิจัยนี้ยังศึกษาผลกระทบของอุณหภูมิ(303.15 ถึง 303.15 เคลวิน) และการเพิ่มกลีเซอรอล (4, 8, 12 g/L) ในสายป้อนเข้าระบบ พบว่าค่าสัมประสิทธิ์การกระจายตัวมีค่าเพิ่มขึ้นตามอุณหภูมิที่ลดลงและค่าสัมประสิทธิ์การกระจายตัวมีค่าเพิ่มขึ้นเมื่อความเข้มข้นของกลีเซอรอลเพิ่มขึ้น นอกจากนี้ได้ศึกษาตัวทำละลายผสมเพื่อลดปริมาณตัวทำละลายที่ใช้ในการสกัด พบว่าตัวทำละลายร่วมระหว่างเอทิลอะซิเตทและเอทานอลที่สัดส่วน 90:10 โดยปริมาตรให้ค่าสัมประสิทธิ์การกระจายตัวของ 1,3 โพรเพนไดออลมีค่าเพิ่มขึ้นเป็น 0.31 จากการคำนวณขึ้นการแยกในทางทฤษฎีของการสกัด 1,3 โพรเพนไดออลโดยอาศัยข้อมูลที่ได้จากการทดลองพบว่าจำนวนขึ้นการแยกในทางทฤษฎีอยู่ที่ 7.6 ขึ้นแต่การสกัดด้วยตัวทำละลายร่วมสามารถลดลงเหลือ 5.8 ขึ้น ที่อัตราการไหลของตัวทำละลายต่อสารป้อนเข้าระบบเท่ากับ 10 สำหรับการแยก 1,3 โพรเพนไดออลออกจากน้ำ

ภาควิชา.....วิศวกรรมเคมี..... ลายมือชื่อนิสิต.....
 สาขาวิชา.....วิศวกรรมเคมี..... ลายมือชื่ออาจารย์ที่ปรึกษา.....
 ปีการศึกษา...2550..... ลายมือชื่ออาจารย์ที่ปรึกษาร่วม.....

4870277921 : MAJOR CHEMICAL ENGINEERING

KEY WORD: 1,3-PROPANEDIOL / HANSEN MODEL / LIQUID-LIQUID EQUILIBRIUM / ETHYLACETATE / EXTRACTION

THAPAGORN BOONSONGSAWAT: SOLVENT SELECTION FOR SEPARATION OF BIOLOGICALLY DERIVED 1,3-PROPANEDIOL THESIS ADVISOR: ASSOC. PROF. CHIRAKARN MUANGNAPOH, Dr.Ing., THESIS COADVISOR: ASST. PROF. ARTIWAN SHOTIPRUK, Ph.D., 90 pp.

For the recovery of 1,3-propanediol from aqueous solution, a suitable solvent was selected and the experimental equilibrium data on 1,3-propanediol-water-solvent mixture was investigated. The theoretical solvent screening using Hansen model was applied to select the possible solvents for extracting 1,3-propanediol from aqueous solution. Then the experimental data were determined for evaluating the solvent based on the distribution coefficients and mutual solubility of the solvent and were compared with the calculating data by unific equation. The tie line data were correlated using the methods of Othmer-Tobias and Hand and their correlation coefficient (R^2) were 0.94 and 0.99, respectively. This results revealed that ethyl acetate would be suitable solvent and the distribution coefficient of 1,3-propanediol is 0.22 at temperature of 303.15 K. Furthermore, the effects of temperature (303.15 to 323.15 K) and glycerol addition in feed aqueous stream (4, 8, 12 g/L) were studied. For this results, the distribution coefficient of 1,3-propanediol increases with decrease in temperature; moreover, the distribution coefficient of 1,3--propanediol increases when the amount of glycerol increases. In order to decrease the amount of solvent, the solvent mixtures were also investigated. It was found that the distribution coefficient increases to 0.31 using the solvent mixture between ethyl acetate and ethanol at volume ratio of 90:10. The number of theoretical stages decreases from 7.6 to 5.8 stages at S/F of 10 for extracting 1,3-propanediol from aqueous phase with solvent mixture.

Department.....Chemical Engineering.....Student's signature.....

Field of study....Chemical Engineering..... Advisor's signature.....

Academic year2007..... Co-advisor's signature.....

ACKNOWLEDGMENTS

I would like to express my sincere gratitude to my adviser Assoc. Prof. Dr. Chirakarn Muangnapoh for her support, encouragement, and guidance throughout my work.

I am thankful to my co-advisor Asst. Prof. Artiwan Shotipruk, Ph.D. for her encouragement and guidance through my work.

Thanks to Assoc. Prof. Seeroong Prichanont, Ph.D., Asst. Prof. Muenduen Phisalaphong, Ph.D., and Chaiya Chandavas, Ph.D. for helpful suggestions.

This work was supported in part by PTT Chemical Public Company Limited for financial supports.

Sincere thanks are given to all members of the Biochemical Engineering Research Laboratory for all of their help and support.

Especially, I would like to express the highest gratitude to my parents, my sister, and everyone in my family for their support and encouragement.

CONTENTS

	Page
ABSTRACT IN THAI.....	iv
ABSTRACT IN ENGLISH.....	v
ACKNOWLEDGMENTS.....	vi
LIST OF TABLES.....	ix
LIST OF FIGURES.....	x
CHAPTER	
I. INTRODUCTION.....	1
1.1 Rationale.....	1
1.2 Objectives.....	3
1.3 Working Scopes.....	3
1.4 Expected benefits.....	3
II. BACKGROUND AND LITERATURE REVIEW.....	4
2.1 1,3-propanediol and its Application.....	4
2.2 Production of 1,3-propanediol.....	4
2.2.1 Chemical processes for 1,3-propanediol.....	4
2.2.2 Biotechnological process for 1,3-propanediol.....	5
2.3 Property of 1,3-propanediol and by-products.....	7
2.4 Literature review.....	9
2.5 Strategies for solvent selection.....	20
2.5.1 Hansen Model.....	20
2.5.2 Unifac Model.....	21
2.6 Solutions and molecules.....	23
2.7 Liquid-liquid extraction.....	24
2.7.1 Liquid-liquid equilibria.....	24
2.7.2 Ternary liquid-liquid systems.....	25
2.7.3 Mode of operation.....	29

CHAPTER	Page
III. MATERIALS AND METHODS.....	31
3.1 Chemicals.....	31
3.2 Experimental set-up and procedure.....	31
3.3 Analysis.....	32
3.3.1 Chemical analysis.....	32
3.3.2 Data analysis.....	32
IV. RESULT AND DISSCUSSION.....	33
4.1 Selected solvent for 1,3-propanediol extraction.....	34
4.2 Preliminary equilibrium measurements.....	38
4.3 Solvent characterization: result and data correlation.....	39
4.4 Effect of temperature for 1,3-propanediol extraction.....	45
4.5 Influence of residual glycerol from fermentation.....	48
4.6 1,3-propanediol with co-solvent extraction.....	51
4.7 Calculation of the number of theoretical stages.....	54
V CONCLUSION AND RECOMMENDATIONS.....	57
5.1 Conclusions.....	57
5.2 Recommendation.....	58
REFERENCES.....	59
APPENDICES.....	62
APPENDIX A.....	63
APPENDIX B.....	84
VITA.....	90

LIST OF TABLES

	Page
Table 2.1 Profile by-products of the actual fermentation.....	6
Table 2.2 Profile property of 1,3-propanediol and by-products.....	8
Table 2.3 Review on glycerol fermentation for producing 1,3-propanediol.....	14
Table 2.4 Review of separation methods for 1,3-propanediol from fermentation broth.....	15
Table 2.5 Advantages and disadvantages of different separation methods.....	17
Table 2.6 Profile Hansen parameters for solvents at 25°C.....	21
Table 4.1 Profile properties of the possible solvents for 1,3-propanediol extraction..	36
Table 4.2 The solubility curve data for the 1,3-Propanediol(1)-water(2)- ethyl acetate(3) System at 303.15 K.....	40
Table 4.3 The tie line compositions for the 1,3-Propanediol-water- ethyl acetate System at 303.15 K.....	40
Table 4.4 The correlation coefficients and correlation factors for the Othmer-Tobias and Hand correlations at 303.15 K.....	44
Table 4.5 The final concentration of fermentation broth.....	49
Table 4.6 The calculated distribution ratio of 1,3-propanediol and glycerol from extraction at 303.15 K.....	51
Table 4.7 Profile the calculated solubility parameters of solvent mixture at 25°C.....	52
Table A-1.1 Standard calibration curve data of 1,3-propanediol.....	63
Table A-1.2 Standard calibration curve data of glycerol.....	64
Table A-3.1 Liquid-liquid equilibria of the system 1,3-propanediol (1) + water (2) + ethyl acetate (3) at 303.15 K.....	65
Table A-3.2 Liquid-liquid equilibria of the system 1,3-propanediol (1) + water (2) + butanol (3) at 303.15 K.....	66
Table A-4.1 Equilibrium time data for extracting 1,3-propanediol and glycerol from aqueous solution with ethyl acetate.....	66
Table A-4.2 Mass fraction of 1,3-propanediol and glycerol in raffinate phase at different mixing time.....	67

LIST OF TABLES

	Page
Table A-5 Experimental solubility curve of the system 1,3-propanediol (1) + water (2) + ethyl acetate (3) at 303.15 K.....	67
Table A-6.1 Experimental tie line data of the system 1,3-propanediol (1) + water (2) + ethyl acetate (3) at 303.15 K.....	68
Table A-6.2 Experimental mass of the system 1,3-propanediol (1) + water (2) + ethyl acetate (3) at 303.15 K in raffinate phase.....	69
Table A-7 Experimental tie line data correlation to plot Othmer-Tobias and Hand.....	69
Table A-8 Experimental solubility of 1,3-propanediol in ethyl acetate at 303.15 K, 313.15 K, 323.15 K.....	70
Table A-9.1 Liquid-liquid equilibrium of the system 1,3-propanediol (1) + water (2) + ethyl acetate (3) at 313.15 K.....	70
Table A-9.2 Liquid-liquid equilibrium of the system 1,3-propanediol (1) + water (2) + ethyl acetate (3) at 323.15 K.....	71
Table A-10.1 Experimental data of the system 1,3-propanediol (1) + water (2) + ethyl acetate (3) at 313.15 K.....	72
Table A-10.2 Experimental mass of the system 1,3-propanediol (1) + water (2) + ethyl acetate (3) at 313.15 K.....	73
Table A-10.3 Liquid-liquid equilibrium of the system 1,3-propanediol (1) + water (2) + ethyl acetate (3) at 313.15 K.....	73
Table A-10.4 Experimental data of the system 1,3-propanediol (1) + water (2) + ethyl acetate (3) at 323.15 K.....	74
Table A-10.5 Experimental mass of the system 1,3-propanediol (1) + water (2) + ethyl acetate (3) at 323.15 K.....	75
Table A-10.6 Liquid-liquid equilibrium of the system 1,3-propanediol (1) + water (2) + ethyl acetate (3) at 323.15 K.....	75
Table A-11.1 Experimental data for extraction of 1,3-propanediol from aqueous solution with glycerol at mass ratio of 60 1,3-PDO/12 glycerol.....	76

LIST OF TABLES

	Page
Table A-11.2 Experimental mass for system of 1,3-propanediol with glycerol in feed stream at mass ratio of 60 1,3-PDO/12 glycerol.....	77
Table A-11.3 Liquid-liquid equilibrium of the system 1,3-propanediol (1) + water (2) + ethyl acetate (3) +glycerol (4) at 303.15 K at mass ratio of 60 1,3-PDO/12 glycerol.....	77
Table A-11.4 Experimental data for extraction of 1,3-propanediol from aqueous solution with glycerol at mass ratio of 60 1,3-PDO/8 glycerol.....	78
Table A-11.5 Experimental mass for system of 1,3-propanediol with glycerol in feed stream at mass ratio of 60 1,3-PDO/8 glycerol.....	79
Table A-11.6 Liquid-liquid equilibrium of the system 1,3-propanediol (1) + water (2) + ethyl acetate (3) +glycerol (4) at 303.15 K at mass ratio of 60 1,3-PDO/8 glycerol.....	79
Table A-11.7 Experimental data for extraction of 1,3-propanediol from aqueous solution with glycerol at mass ratio of 60 1,3-PDO/4 glycerol.....	80
Table A-11.8 Experimental mass for system of 1,3-propanediol with glycerol in feed stream at mass ratio of 60 1,3-PDO/4 glycerol.....	81
Table A-11.9 Liquid-liquid equilibrium of the system 1,3-propanediol (1) + water (2) + ethyl acetate (3) +glycerol (4) at 303.15 K at mass ratio of 60 1,3-PDO/4 glycerol.....	81
Table A-12.1 Experimental data for extraction of 1,3-propanediol from aqueous solution with solvent mixture at volume ratio 95:5 and 90:10 (ethyl acetate:ethanol).....	82
Table A-12.2 Experimental mass for 1,3-propanediol + water + solvent mixture system at volume ratio 95:5 and 90:10 (ethyl acetate:ethanol).....	82
Table A-12.3 Liquid-liquid equilibrium of the system 1,3-propanediol (1) + water (2) + solvent mixture (3) at 303.15 K.....	83
Table B-3 Error analysis of experimental results from the effect of temperature.....	89

LIST OF FIGURES

	Page
Figure 2.1 Metabolic pathways of glycerol metabolism.....	6
Figure 2.2 Profile diagram of the novel process for purification of 1,3-propanediol....	13
Figure 2.3 Phase splitting of ternary mixture component A and C mutually insoluble.25	25
Figure 2.4 Phase splitting of ternary mixture component A and C partially soluble.....	26
Figure 2.5 Equilateral triangular diagram.....	27
Figure 2.6 Profile countercurrent extraction cascade.....	29
Figure 4.1 Comparison of solvents based on their δ_p and δ_h Hansen solubility parameters to 1,3-propanediol as origin (0,0).....	35
Figure 4.2 Predicted ternary diagram for the 1,3-propanediol-water-ethyl acetate using the unifac model at 303.15 K.....	37
Figure 4.3 Predicted ternary diagram for the 1,3-propanediol-water-N-Butanol using the unifac model at 303.15 K.....	38
Figure 4.4 Mass fraction of 1,3-propanediol and glycerol in raffinate phase versus stirring time.....	39
Figure 4.5 Liquid-liquid equilibrium data for 1,3-Propanediol-water-ethyl acetate Ternary at 303.15 K.....	41
Figure 4.6 Comparison of experimental and calculated ternary diagram for the 1,3-propanediol-water-ethyl acetate using the Unifac model at 303.15 K: (-) calculated data; (--) experimental data.....	42
Figure 4.7 Othmer and Tobias Plot for the 1,3-Propanediol (1)-Water (2)-Ethyl acetate (3) System at 303.15 K.....	43
Figure 4.8 Hand Plot for the 1,3-Propanediol (1)- Water (2)- Ethyl acetate (3) System at 303.15 K.....	43
Figure 4.9 Equilibrium mass fraction of 1,3-Propanediol as a function of the aqueous equilibrium mass fraction for the ternary system 1,3-Propanediol (1)- Water (2)- Ethyl acetate (3) at 303.15 K.....	45
Figure 4.10 Solubility of 1,3-Propanediol as function of temperature for ethyl acetate.....	45

LIST OF FIGURES

	Page
Figure 4.11 Organic equilibrium mass fraction of 1,3-Propanediol as a function of the aqueous equilibrium mass fraction at 303.15 K, 313.15 K, and 323.15 K calculated values using the Unifac model.....	46
Figure 4.12 Experimental organic equilibrium mass fraction of 1,3-Propanediol as a function of the aqueous equilibrium mass fraction at 303.15 K, 313.15 K and 323.15 K.....	47
Figure 4.13 Experimental results of glycerol addition in feed at 303.15 K.....	50
Figure 4.14 Comparison of solvents and solvent mixture based on their δ_p and δ_h Hansen solubility parameters to 1,3-propanediol as origin (0,0).....	53
Figure 4.15 Experimental distribution ratio from 1,3-propanediol extraction with co-solvent at different %volume of ethyl acetate and ethanol at 303.15 K.....	54
Figure 4.16 Experimental solvent loss for 1,3-propanediol extraction at 303.15 K.....	54
Figure 4.17 1,3-propanediol raffinate mass fraction at 303.15 K as function of NTS used in extraction at different solvent to feed ratio.....	56
Figure 4.18 1,3-propanediol raffinate mass fraction at 303.15 K as function of NTS used in extraction at different solvent	56
Figure A-1.1 Standard calibration curve of 1,3-propanediol.....	63
Figure A-1.2 Standard calibration curve of glycerol.....	64
Figure A-2.1 HPLC chromatogram of 1,3-propanediol and glycerol.....	65
Figure B-2.1 Ternary Diagram of 1,3-PDO+water+ethyl acetate system used to calculate P_{min} for designing an extractor.....	86
Figure B-2.2 Ternary Diagram of 1,3-PDO+water+ethyl acetate system showing the mixing point based on the (S/F) _{min} , m.....	87

CHAPTER I

INTRODUCTION

1.1 Rationale

For decade, 1,3-Propanediol (PDO) is one of the major monomer components for the production of high performance polyester such as polytrimethylene terephthalate (PTT). The PTT produced from 1,3-propanediol has excellent physical properties and is suitable for fiber and textile applications. In addition, PTT can be produced in an environmentally friendly way and at a price very competitive to that of polyethylene terephthalate (PET) and polybutylene terephthalate (PBT). Nowadays, 1,3-propanediol (PDO) can be produced either by a chemical method or a biotechnological method. In the chemical method, 1,3-propanediol (PDO) is obtained by hydration of acrolein and hydroformylation reaction of ethylene oxide. Acrolein and ethylene oxide must first be produced from propylene and ethylene which are derived from petroleum and the prices of these raw materials tend to increase continuously. Moreover the chemical process involves use of toxic chemicals and emission of these chemicals are of high environmental concerns. On the other hand, 1,3-propanediol (PDO) can be produced by the biotechnological method through the conversion of glycerol to PDO using microorganisms such as *Klebsiella pneumoniae*, *Citrobacter freundii*, *Enterobacter agglomerans*, *Clostridium butyricum*. This bioconversion is of increasing interest as a result of the growing volume of glycerol, a by-product in biodiesel production and a minor by-product in ethanol fermentation. Moreover, this method operates at environmentally benign conditions (Zeng et al., 2002).

The study focused on separation and concentration of 1,3-PDO produced by the biological process. Separation and purification of 1,3-PDO from fermentation broth is not straightforward because 1,3-PDO has low volatility and hydrophilic characteristics in dilute aqueous solutions. Ames (2002) disclosed a process for separation and purification of 1,3-propanediol by evaporation and distillation whereas the necessity for a large amount of heat energy made this process unprofitable. Compared with distillation, solvent extraction requires lower energy consumption. Malinowski (1999) reported the theoretical evaluation of the downstream separation

of 1,3-propanediol from dilute aqueous solutions by liquid-liquid extraction with aliphatic aldehydes and alcohols. However, the distribution of 1,3-PDO into extraction solvents based on aldehyde and alcohol group appeared to be not good enough to make simple extraction efficient. Alternatively, Malinowski (2000) developed the 1,3-propanediol purification process based on the reactive extraction, using aldehydes to first convert 1,3-PDO to alkyl 1,3-dioxane, which was then extracted with organic solvent such as toluene, o-xylene, and ethylbenzene. Yan et al. (2005) proposed similar but improved reactive extraction process using aldehydes as both for reactant and extraction solvent. Although high extraction yield was resulted, the 1,3-dioxane product needs to be converted back to 1,3-PDO by extraction process hydrolysis reaction which is operated at high temperature and separating 1,3-propanediol from mixture of 1,3-propanediol and aldehyde is then again required. Such procedures were too complicated to achieve satisfactory yield of 1,3-propanediol. Alternatively, Shiguang Li et al. (2001) used a ZSM-5 zeolite membrane by pervaporation for separation of 1,3-propanediol from glycerol and glucose in aqueous solution. This method has some drawback such as a low flux and low selectivity. Roturier et al. (2002) and Hilaly et al. (2002) used the chromatographic column packed with cation exchange resin for the recovery of 1,3-propanediol. This method consumed less energy and satisfied the environmental protection standards; however, it was difficult to obtain 1,3-propanediol with high purity and the process required the dewatering step. Corbin et al. (2003) suggested the separation of 1,3-propanediol, glycerol, and a mixture of 1,3-propanediol and glycerol from a biological mixture using a molecular sieve. They discovered that using any of molecular sieves and ethanol in an elution step achieves a yield greater than 90%. However, the mixture must still be purified further using conventional separation methods such as distillation.

Recently, Cho et al. (2006) developed a novel isolation and purification method for producing 1,3-propanediol with high purity and high yield. This method employed phase separation with ethyl acetate to concentrate 1,3-propanediol from fermentation broth and chromatography through silica gel column to separate and purify 1,3-propanediol from the mixture of 1,3-PDO and 1,2-PDO. The author suggested that the phase separation proposed was simple and efficient for the isolation of 1,3-propanediol from the other components in the fermentation mixture, however no clear evidence such as extraction yield into ethyl acetate was given. In this work,

we proposed to concentrate 1,3-PDO from the fermentation broth using phase separation. First, the suitability as phase separation solvent for 1,3-propanediol of ethyl acetate and other solvents such as butanol will be evaluated based on the solute distribution ratio, selectivity and mutual solvent solubility of liquid-liquid systems. Then experimental liquid-liquid equilibrium data will be experimentally measured in order to evaluate process performance. In addition, the extraction factor and the number of theoretical stages will be calculated to determine the commercial feasibility of the process.

1.2 Objectives

1.2.1 To select suitable solvents for separating 1,3-propanediol from model mixture of fermentation broth.

1.2.2 To investigate the extraction performance in term of the extraction factor and the number of theoretical stages.

1.3 Working Scopes

1.3.1 Empirical and theoretical screening and selection of suitable solvents for concentrating and separating 1,3-propanediol from model mixture of fermentation broth.

1.3.2 Prediction of liquid-liquid equilibria of the mixture at a temperature of 303.15 K with the UNIFAC group-contribution method.

1.3.3 Experimental investigation of liquid-liquid equilibria (LLE) for systems of ternary mixture at a temperature of 303.15 K and comparison with values predicted by the UNIFAC group-contribution method.

1.3.4 Calculation of extraction factor and the number of theoretical stages (NTS) for evaluation of extraction performance.

1.4 Expected benefits

1.4.1 Provide the suitable separation process for 1,3-propanediol from aqueous glycerol fermentation broth.

CHAPTER II

BACKGROUND AND LITERATURE REVIEWS

2.1 1,3-propanediol and its Applications (Zeng et al., 2002)

1,3-propanediol (PDO) is a valuable chemical used mainly as a monomer to synthesize poly(trimethylene terephthalate) (PTT) which has excellent properties such as good resilience, stain resistance, low static generation, and is particularly suitable for fiber and textile applications. It also has the potential to replace the traditional polyethylene terephthalate (PET) and polybutylene terephthalate (PBT) because it can be produced in an environmentally friendly way and at a price very competitive to that of PET and PBT.

1,3-propanediol also has a number of other interesting applications. It improves properties for solvents, adhesives, laminates, resins, detergents and cosmetics. It can even be used to produce biocides for industrial disinfection and treatment of industrial circulation water, and freshness-keeping agents for cut flowers. In a recent patent, 1,3-propanediol was also used as a component of animal feed.

2.2 Production of 1,3-propanediol (Zeng et al., 2002)

Generally, there are two methods of producing 1,3-propanediol. One is the chemical method and the other is biotechnological method.

2.2.1 Chemical processes for 1,3-propanediol

Nowadays, PDO is produced mainly by two different chemical processes. The first process starts from acrolein which is obtained by catalytic oxidation of propylene. Acrolein is first hydrated at moderate temperature and pressure to 3-hydroxypropionaldehyde which, is then hydrogenated to 1,3-propanediol over a rubidium catalyst under high pressure. The second process starts from ethylene oxide, which is prepared by oxidation of ethylene. Ethylene oxide is transformed with synthesis gas in a hydroformylation process at very high pressure to 3-hydroxypropanal which is extracted from the organic phase with water and subjected to hydrogenation using nickel as a catalyst at high pressure.

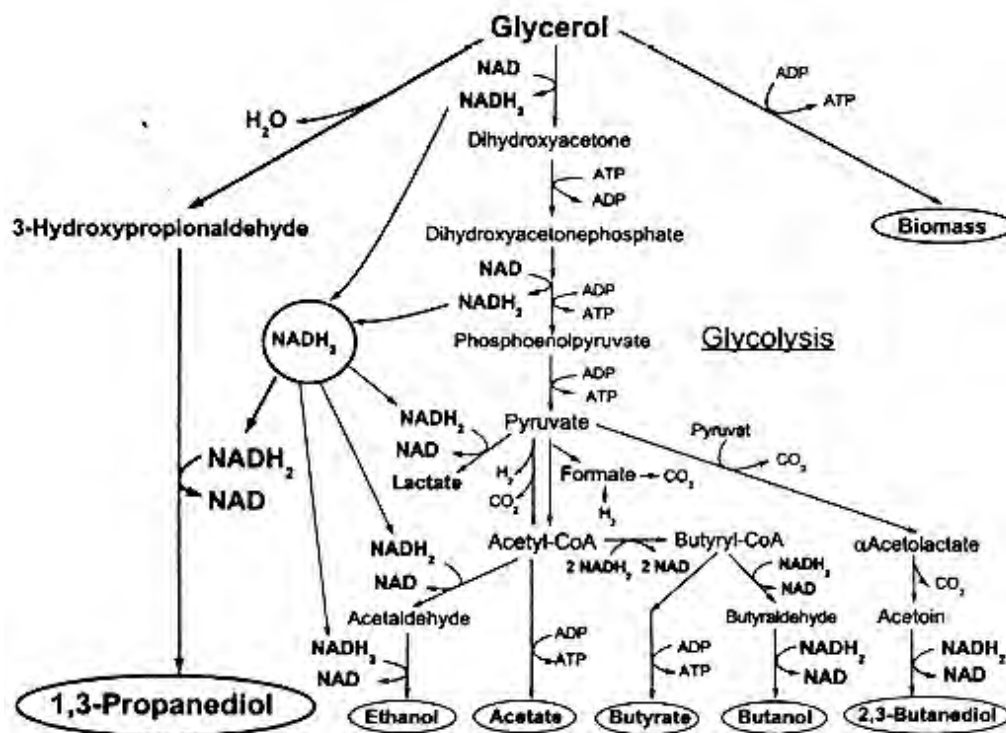


Figure 2.1 Metabolic pathways of glycerol metabolism (Zeng et al., 2002)


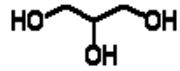
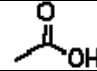

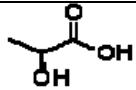
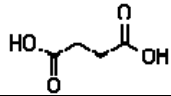
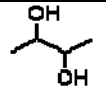
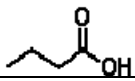

Table 2.1 Profile by-products of the actual fermentation (Zeng et al., 2002)

Microorganisms	By-products of 1,3-propanediol fermentation	
<i>Klebsiella pneumoniae</i>	Acetic acid, Ethanol, Lactic acid, Succinic acid, and 2,3-Butanediol	CO ₂ , H ₂
<i>Citrobacter freundii</i>	Acetic acid, Ethanol, Lactic acid, Succinic acid, and 2,3-Butanediol	CO ₂ , H ₂
<i>Enterobacter agglomerans</i>	Acetic acid, Ethanol, Lactic acid, Succinic acid, and 2,3-Butanediol	CO ₂ , H ₂
<i>Clostridium butyricum</i>	Acetic acid, Butyric acid	CO ₂ , H ₂
<i>Clostridium pasteurianum</i>	Acetic acid, Butanol	CO ₂ , H ₂
<i>Clostridium acetobutylicum</i>	Acetic acid, Butyric acid	CO ₂ , H ₂

2.3 Property of 1,3-propanediol and by-products

For separation of 1,3-PDO from the fermentation broth, it is important to know the properties of the product and other existing by-products. The general characteristics of 1,3-propanediol and the by-products, listed in Table 2.1, resulted from the fermentation are summarized in Table 2.2.

Table 2.2 Profile property of 1,3-propanediol and by-products

Name	Synonyms	Molecular Formula	Molecular Weight	Melting point (°C)	Boiling point (°C)	Density (g/cm ³)	Solubility in water	Structure
1,3-propanediol	1,3 propylene glycol	C ₃ H ₈ O ₂	76.09	-32 °C	214 °C	1.052	complete	
Glycerol	Propane-1,2,3-triol	C ₃ H ₈ O ₃	92.09	18°C	290°C	1.216	>500 g/l	
Acetic acid	Ethanoic acid	C ₂ H ₄ O ₂	60.05	16 °C	117 °C	1.048	miscible	
Ethanol	Ethyl Alcohol	C ₂ H ₆ O	46.0688	-114.1 °C	78.3 °C	0.789	slightly soluble	
Lactic acid	2-Hydroxy propanoic acid	C ₃ H ₆ O ₃	90.07	53 °C	122 °C	1.05	miscible	
Succinic acid	Butanedioic acid	C ₄ H ₆ O ₄	118.08	185 °C	235 °C	1.552	80g/l	
2,3-butanediol	2,3-Butylene glycol	C ₄ H ₁₀ O ₂	90.12	19 °C	180 °C	1.01	miscible	
Butyric acid	n-Butyric acid	C ₄ H ₈ O ₂	88.1	-7 °C	162°C	0.96	miscible	
Butanol	n-Butyl alcohol	C ₄ H ₁₀ O	74.12	-89.5 °C	117.6 °C	0.81	80 g/l	
Carbon dioxide	-	CO ₂	44.01	-57 °C	-78 °C	1.98	-	-
Hydrogen	-	H ₂	2	-259.14°C	-252.87°C	0.089	-	-

2.4 Literature review

For almost 120 years a bacterial fermentation has been known in which glycerol is converted to 1,3-PDO, but only very recently, since 1990, has its biotechnological significance been recognized, and more directed research initiated. The review on biological production of propanediol is summarized in Table 2.3. Barbirato et al. (1998) investigated and compared the fermentation of glycerol by the bacterial species *Klebsiella pneumoniae*, *Citrobacter freundii*, *Enterobacter agglomerans*, and *Clostridium butyricum* under similar culture conditions. Their results showed that fermentation of glycerol by *E. agglomerans*, *C. freundii* and *K. pneumoniae* revealed the occurrence of inhibitory phenomena which was observed during broth cultures, followed by the cessation of growth and the decrease of the rates of substrate consumption and products formation. This was assigned to the accumulation in the fermentation medium of a strongly inhibitory compound, 3-hydroxypropionaldehyde, the only intermediate of the 1,3-propanediol metabolic pathway. In their study, the inhibitory effect was however not observed with *C. butyricum* and thus it was chosen for test of 1,3-PDO production from glycerol containing wastewaters. A high efficiency of conversion yield to 1,3-propanediol was 0.59 mol/mol glycerol and 0.69 mol/mol glycerol, respectively, with glycerin coming from the ester production and from wine stillage. In contrary to Barbirato et al., Saint-Amans et al. (1994) observed inhibitory phenomena with *C. butyricum* and proposed to solve the problem by employing in a simple controlled fed-batch system. Their results showed that the concentration of 1,3-propanediol obtained and the productivity were significantly higher than those reached in batch culture. They found that 65 g/l of 1,3-propanediol was produced with a productivity of 1.21 g/l.h and a yield of 0.561 mol/mol glycerol. Reimann et al. (1997) suggested that the productivity of 1,3-PDO from glycerol by *Clostridium butyricum* could be further improved by a factor of four in a continuous fermentation with cell recycling, in comparison to the continuous culture without cell recycling. In their study, cell recycling was achieved by filtration using hollow-fiber modules made from polysulphone. Its performance was checked at a retention ratio of 5, dilution rates between 0.2 h⁻¹ and 1.0 h⁻¹ and glycerol input concentrations of 32 g/l and 56 g/l glycerol. The optimum 1,3-propanediol concentration of 26.5 g/l (for 56 g/l glycerol) was maintained up to dilution rate of 0.5 h⁻¹ and the 1,3-propanediol concentration decreased while the 1,3-propanediol productivity was the highest at 0.7 h⁻¹.

In general, by-products produced by glycerol fermentation are such as acetic acid and butyric acid. These make pH value decline and inhibits the growth of microorganisms. To keep the pH value of fermentation broth at 7.0, potassium hydroxide is added, and thus organic acid salts are formed, which required desalination. These can be achieved by a number of means as suggested by Yan et al. (2004) and Ames (2002) who proposed the desalination of 1,3-PDO fermentation broth by Electrodialysis method and vacuum distillation, respectively.

After desalination, the purification of 1,3-propanediol can be proceeded and various methods have been reported in many of studies. The reviews of the studies in the separation process are summarized in table 2.4 and the advantages and disadvantages of these methods were summarized in Table 2.5. Generally, purification of product from fermentation broth is carried out by distillation and liquid-liquid extraction. However for the recovery of 1,3-PDO from fermentation broth, these processes could be somewhat difficult because 1,3-PDO has low volatility and strong hydrophilic characteristics in dilute aqueous solutions.

Ames (2002) proposed to separate 1,3-PDO from fermentation broth by evaporation and distillation. They found that yield and purity for recovery 1,3-PDO were high, however, distillation used the high energy consumption for separating 1,3-propanediol from fermentation broth.

A less energy intensive alternative for separation of 1,3-PDO from dilute aqueous solutions is by liquid-liquid extraction which was investigated by Malinowski (1999). Employing group contribution theory, they reported that the aldehydes have the most suitable solvent characteristics, with high distribution coefficient and selectivity. Thus aliphatic alcohols and aldehydes were selected for experimental testing. However, the distribution of 1,3-PDO into extraction solvents appeared to be not good enough to make simple extraction efficient. Based on their finding, Malinowski (2000) later proposed the technically feasible and attractive downstream separation of 1,3-propanediol by reactive extraction in which 1,3 propanediol was first reacted with acetaldehyde to form 2-methyl-1,3-dioxane, which can be easily extracted by organic solvent such as toluene, o-xylene, and ethylbenzene. He found that the dioxane yield was 91-92 %, the overall conversion of 1,3-propanediol was 98 %, and recovery of dioxane into the organic solvent was 75%. Subsequent study by Hao et al. (2005) demonstrated improved recovery of 1,3-propanediol by reactive extraction using aldehyde as both reactant and extractant.

Three aldehydes: propionaldehyde, butyraldehyde, or isobutyraldehyde were tested in this study. First the excess amount of aldehyde was added to the fermentation broth to form substituted 1,3-dioxane, which was then extracted from the aqueous phase into the aldehyde phase. Compared with using different solvent as extractant, this method reduce the step to separate acetals from aldehyde and because the aldehyde concentration in the aqueous phase remained at a high level while that of acetal remains at the low level, the conversion rate of PDO could be enhanced. In this study, the recovery rates of PDO were found to be 65%, 85%, and 87% for propionaldehyde, butyraldehyde, and isobutyraldehyde, respectively. In this study, the reaction equilibrium constants of isobutyraldehyde and the mass distribution coefficients of its substituted 1,3-dioxanes achieved were found to be the highest. Although the acetalization reaction gave rather high yield, the hydrolysis of acetals to convert to propanediol which was then needed to be separated out again by distillation. Such procedures were too complicated to achieve satisfactory yield of 1,3-propanediol .

Alternatively, Roturier et al. (2002) investigated the purification of 1,3-propanediol from a fermentation medium by chromatography using a cationic resin, consisting of lanthanum, lead, zinc, iron, and aluminum with water as eluent. The maximum yield was found for lanthanum which was still only 57.9%. The reason for low yield was due to the lack of ionic properties of propanediol and the other compounds involved. In addition to the above study, Hilaly et al. (2002) proposed a method of recovering 1,3-propanediol from fermentation broth by ion exclusion resins and utilized simulated moving bed technology to effect the recovery of 1,3-propanediol from a liquid composition. They found that the size of cationic resin was preferably between about 200-350 microns and water was the eluent. Its flow rate was preferably about 2.6 ml/min in a 100 ml column. Their results showed that purity was 88.1% and the recovery of PDO was 86.7% when their test was carried out in a column containing 100 ml of a cation exchange resin (CS11GC350). In addition, their SMB experiments were carried out wherein 12 columns, were loaded with 300 ml of cationic resin (CS11GC350). The experiments resulted in a product with 89.4% purity and the yield was 99.5%. Despite the high purity and yield, SMB was too complicated to be applied in a large scale.

Due to the drawback of the cation exchange chromatography, Corbin et al. (2003) developed separation process of 1,3-propanediol, glycerol, and a mixture of 1,3-propanediol and glycerol from a biological mixture using a molecular sieve

chromatography. They used Na-ZSM-5 zeolite to separate 1,3-propanediol from a cell free broth and elute the column with ethanol, and found that the yield of 1,3-propanediol was increased by increasing the concentration of ethanol and total recovery of 1,3-propanediol product was calculated to be as high as 94.7%. Despite the high yield, the elution mixture requires further purification using conventional separation methods such as distillation.

Shiguang Li et al. (2001) investigated separation process for 1,3-propanediol from glycerol and glucose using a ZSM-5 zeolite membrane by pervaporation. Such membrane operation have advantages over a packed bed in that its operation is continuous and it does not require an additional separating agent such as ethanol used for a packed bed, which means that the distillation step can be eliminated. In their results, it was found that 1,3-propanediol/glycerol selectivity decreased over the temperature range 308-328 K, whereas the 1,3-propanediol/glucose selectivity increased for the same range. In addition, they showed that the presence of glycerol inhibited glucose permeation and thus increased the 1,3-propanediol/glucose selectivity. Furthermore, the presence of glucose was found to decrease the total flux but increased the 1,3-propanediol/glycerol selectivity. Despite the advantages of ZSM-5 zeolite membrane pervaporation over the packed bed, the technique carries some drawbacks such as low flux and selectivity.

Recently, Cho et al. (2006) studied a novel isolation and purification method for producing 1,3-propanediol with high purity and high yield from mixture containing 1,3-propanediol, 1,2-propanediol, glycerol, glucose. Their method consisted of phase separation to remove glucose and glycerol from the mixture and chromatography for purification of 1,3-propanediol from 1,2-propanediol as shown in the diagram in Figure 2.2. The propose technique was claimed to be a simple and efficient for the isolation and purification of 1,3-propanediol from the other components in the mixture. For the phase separation step, they found that the optimal feed concentration in the phase separation step was 40 g/L on the basis of 1,3-propanediol when their solvent was ethyl acetate. In the chromatographic separation, a column packed with silica resin was used. The elution condition was attained by using ethyl acetate/methanol (98/2, v/v) as a mobile phase in an isocratic mode. Their study showed that the over all purity and yield of 1,3-propanediol were 98% and 82% in the purification process, respectively.

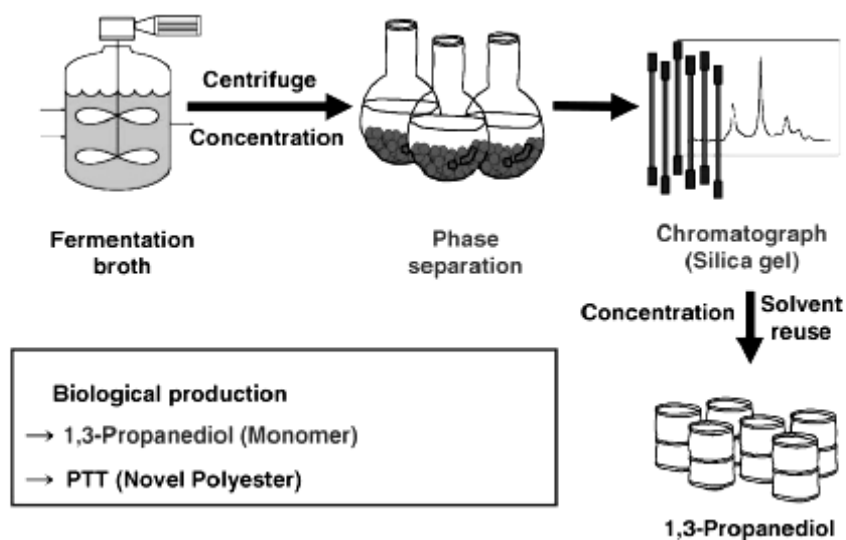


Figure 2.2 Profile diagram of the novel process for purification of 1,3-propanediol.

In this work we propose to determine equilibrium phase composition of the system and evaluate solvent for continuous column extraction to separate 1,3-propanediol from mixture.

Table 2.3 Review on glycerol fermentation for producing 1,3-propanediol

Author	Bacterial species	Materials	Analysis	Objective
1. Barbirato et al., 1998	<i>Klebsiella pneumoniae</i> <i>Citrobacter freundii</i> <i>Enterobacter agglomerans</i> <i>Clostridium butyricum</i>	Wine distillation stillage, Glycerol issued from the esterification of coza oil	HPLC GC-8A	To demonstrate the advantages and the limitations encountered during anaerobic cultures with glycerol as carbon source by 1,3-propanediol producing bacteria in order to reveal the microorganism exhibiting the better abilities for an industrial application.
2. Saint-Amas et al., 1994	<i>Clostridium butyricum</i>	Glycerol	HPLC	To develop production of 1,3-propanediol from glycerol by <i>Clostridium butyricum</i> VPI3266 in a simple controlled fed-batch system
3. Reimann et al., 1998	<i>Clostridium butyricum</i>	Glycerol	GC Enzymatic method	To apply the method of cell recycling by continuous filtration.

Table 2.4 Review of separation methods for 1,3-propanediol from fermentation broth

Author	Separation method	Feed materials	Analysis	Objective
Malinowski., 1999	Liquid-liquid Extraction	1,3-propanediol/ Glycerol	HPLC HP5890(II)GC	To evaluate the potentials of liquid extraction for downstream separation of 1,3-propanediol.
Malinowski., 2000	Reactive extraction	1,3-propanediol/ Glycerol	HP5890(II)GC	To study the downstream separation of 1,3-propanediol from dilute aqueous solution.
Jian hao et al., 2005	Reactive extraction	1,3-propanediol	GC	To study reactive extraction, using propionaldehyde, butyraldehyde, and isobutyraldehyde as both reactant and extractant to recover 1,3-propanediol from a dilute aqueous solution.
Shiguang Li et al., 2001	Pervaporation using ZSM-5 zeolite membrane	Glucose/Glycerol/ 1,3-propanediol	HPLC HP5890(II)GC	To study a Na-ZSM-5 (Si/Al = 25) membrane for separation of 1,3-propanediol from glycerol and glucose in aqueous solutions.

Author	Separation method	Feed materials	Analysis	Objective
Ames, 2002	Evaporation and distillation	Glucose fermentation broth	GC	To study a process of adding base to the fermentation broth to raise the pH to a suitable level for reduction of impurity formation during isolation of 1,3-propanediol by evaporation and distillation.
Roturier et al., 2002	Chromatography using a cationic resin	Glucose fermentation broth	HPLC	To study the purification of 1,3-propanediol from a fermentation medium by chromatography using a cationic resin.
Hilaly et al., 2002	Ion exclusion resins and simulated moving bed (SMB) technology	Glucose fermentation broth	N/A	To study a method of recovering 1,3-propanediol from fermentation broth by ion exclusion resins and utilized simulated moving bed technology.
Corbin et al., 2003	Molecular sieve	1,3-propanediol and glycerol from a biological mixture	HPLC	To study the separation of 1,3-propanediol and glycerol from a mixture of 1,3-propanediol and glycerol from a biological mixture using a molecular sieve.
Cho et al., (2006)	Phase separation and chromatography	1,3-propanediol/ 1,2-propanediol/ Glycerol/Glucose	HPLC	To study phase separation step and chromatographic column packed with silica resin to recover 1,3-propanediol from model mixture containing some of the compounds obtained by biotechnological production.

Table 2.5 Advantages and disadvantages of different separation methods

Author	Separation method	Extractant	Reactant	Advantage	Disadvantage
Breitkopf et al., 1991	Liquid-liquid Extraction	Cyclohexane	-	(1) Energy efficient	(1) 1,3-PDO had a very low solubility in cyclohexane.
Malinowski J., 1999	Liquid-liquid Extraction	Aliphatic alcohols and aldehyde	-	(1) Energy efficient	(1) Mass distribution coefficient of 1,3-PDO appeared to be not good enough to make simple extraction.
Malinowski J., 2000	Reactive extraction	aromatic solvent; o-xylene toluene ethylbenzene	acetaldehyde	(1) High yield (91-92%) (2) High conversion in range of 91-94%	(1) This method was too complicated to achieve satisfactory yield of 1,3-PDO. (2) Acetaldehyde dissolved in the extractant so that it decreased the conversion rate of PDO and had to be separated through distillation. (3) Acetaldehyde has low boiling point (bp = 20 °C) which was difficult to condense.
Jian Hao et al., 2005	Reactive extraction	propionaldehyde butyraldehyde isobutyraldehyde	propionaldehyde butyraldehyde isobutyraldehyde	(1) High recovery rate of PDO (87%). (2) Improved conversion rate of PDO. (3) No problem condensing the solvent during distillation.	(1) This method was too complicated to achieve satisfactory yield of 1,3-PDO. (2) It requires hydrolysis reaction unit that operated at high temperature (80-100°C).

Author	Separation method	Feed materials	Advantage	Disadvantage
Shiguang Li et al., 2001	Pervaporation using ZSM-5 zeolite membrane	Glucose/Glycerol/1,3-propanediol	(1) Energy efficient (2) Requires no an additional separation agent such as ethanol	(1) Low 1,3-propanediol flux and selectivity.
Ames, 2002	Evaporation and distillation	Glucose fermentation broth	(1) High yield of 95%, base addition. (2) High purity of 99%.	(1) High energy consumption.
Roturier et al., 2002	Chromatography using a cationic resin	Glucose fermentation broth	(1) Energy efficient (2) The process meet clean and satisfied the environmental protection standards.	(1) Low yield. (2) Difficult in obtaining 1,3-propanediol with high purity. (3) Requirement for the dewatering step for high purity of 99%.
Hilaly et al., 2002	Ion exclusion resins and simulated moving bed (SMB) technology	Glucose fermentation broth	(1) Energy efficient (2) It was favorable for environmental protection. (3) High yield of 99.5% and purity of 89.4% for SMB.	(1) Difficult in obtaining 1,3-propanediol with high purity. (2) Requirement for the dewatering step for high purity of 99%.

Author	Separation method	Feed materials	Advantage	Disadvantage
Corbin et al., 2003	Molecular sieve	1,3-propanediol and glycerol from a biological mixture	(1) Energy efficient (2) Increased total production rate of 1,3-propanediol. (3) It resolved the major problem of the high cost of adsorbents. (4) High yield of greater than 90%.	(1) Requirement of two-step adsorption for high purity. (2) Requirement of dewatering step for high purity of 99%
Cho et al., 2006	Phase separation and chromatography	1,3-propanediol/ 1,2-propanediol/ Glycerol/Glucose	(1) The use of phase separation allows rapid separation of 1,3-propanediol from interfering compounds. (2) The use of phase separation reduces solvent usage compared to alter native methods. (3) High yield of 82% and a purity of 98%. In chromatography step.	(1) Requirements of eluting agents and chromatography difficult to operate in a continuous industrial scale.

2.5 Strategies for solvent selection

The solvent selection needs to be carefully evaluated when optimizing the design and operation of the extraction. The selection of alternative solvents can be performed empirically, theoretically or experimentally. Empirical methods generally compare one or more properties of solvents to classify them and to assess the solvent capacity. These methods can only identify possible alternative solvent classes, but the selection of a specific solvent is not possible. Theoretical screening methods are based on a thermodynamic description of the investigated system. Here, solvent selection is based on the solute distribution ratio, selectivity, and mutual solvent solubility of liquid-liquid system, which can be calculated using various thermodynamic models. For an overview of possible alternative solvents, the Hansen model was used by plotting the δ_p against the δ_h parameter for each solvents, representing the dipole and hydrogen bonding interactions of this solvent, respectively. Furthermore, the Unifac model was initially applied for the prediction of distribution and mutual solubility data.

2.5.1 Hansen Model (Burke, 1984)

The most widely accepted three component system to date is the three parameter system developed by Charles M. Hansen in 1966. Hansen parameters divide the total Hildebrand value into three parts: a dispersion force component, a hydrogen bonding component, and a polar component. This means that Hansen parameters are additive:

$$\delta_t^2 = \delta_d^2 + \delta_p^2 + \delta_h^2 \quad (2.1)$$

Where

δ_t^2 = Total Hildebrand parameter

δ_d^2 = dispersion component

δ_p^2 = polar component

δ_h^2 = hydrogen bonding component

Hansen parameters are reasonably accurate in predicting solubility behavior because precise values for all three component parameters are utilized. Hansen's three dimensional volumes can be similarly illustrated in two dimensions by plotting a cross-section through the center of the solubility sphere in a graph that uses only two

of the three parameters, most commonly p and h . Hansen parameters for solvents are shown in Table 2.6.

Table 2.6 Profile Hansen parameters for solvents at 25°C (Barton. 1983)

Solvent	Δ (MPa ^{1/2})			
	δ_t	Δd	δ_p	Δh
Water	47.8	15.6	16.0	42.3
1,3-Propanediol	31.1	12.5	14.1	27.0
Glycerol	36.1	17.4	12.1	29.3
n-Butane	14.1	14.1	0.0	0.0
n-Pentane	14.5	14.5	0.0	0.0
n-Hexane	14.9	14.9	0.0	0.0
Cyclohexane	16.8	16.8	0.0	0.2
Benzene	18.6	18.4	0.0	2.0
Toluene	18.2	18.0	1.4	2.0
Chloroform	19.0	17.8	3.1	5.7
Acetone	20.0	15.5	10.4	7.0
Methyl ethyl ketone	19.0	16.0	9.0	5.1
Ethyl acetate	18.1	15.8	5.3	7.2
n-Butyl acetate	17.4	15.8	3.7	6.3
Ethanol	26.5	15.8	8.8	19.4
1-Butanol	23.1	16.0	5.7	15.8
Acetic acid	10.5	7.1	3.9	6.6
Acetaldehyde	20.3	14.7	8	11.3
Butanal	17.1	14.7	5.3	7
1-Pentanol	10.6	7.8	2.2	6.8
Hexanol	10.2	6.9	4.2	6.2
Cyclohexanol	22.4	17.4	4.1	13.5

2.5.2 Unifac Model (Fredenslund et al., 1975)

UNIFAC model, a group-contribution method, is presented for the prediction of activity coefficients in non-ideal liquid mixtures. UNIFAC model follows Derr and Deal's (1969) ASOG model, wherein activity coefficients in mixtures are related to interactions between structural groups. Derr and Deal separate the molecular activity coefficient into two parts: one part provides the contribution due to differences in molecular size and the other provides the contribution due to molecular interactions. Much of the arbitrariness is removed by combining the solution-of-groups concept

with the UNIQUAC equation. In a multi component mixture, the UNIQUAC equation for the activity coefficient of component i is

$$\ln \gamma_i = \ln \gamma_i^C + \ln \gamma_i^R \quad (2.2)$$

combinatorial + residual

where

$$\ln \gamma_i^C = \ln \frac{\Phi_i}{x_i} + \frac{z}{2} q_i \ln \frac{\theta_i}{\Phi_i} + l_i - \frac{\Phi_i}{x_i} \sum_j \alpha_j l_j \quad (2.3)$$

And

$$\ln \gamma_i^R = q_i \left[1 - \ln \left(\sum_j \theta_j \tau_{ji} \right) - \sum_j \left(\theta_j \tau_{ij} / \sum_k \theta_k \tau_{kj} \right) \right] \quad (2.4)$$

$$l_i = \frac{z}{2} (r_i - q_i) - (r_i - 1); z = 10$$

$$\theta_i = \frac{q_i x_i}{\sum_j q_j x_j}; \Phi_i = \frac{r_i x_i}{\sum_j r_j x_j}$$

$$\tau_{ji} = \exp \left[- \frac{u_{ji} - u_{ii}}{RT} \right]$$

In the UNIFAC method, the combinatorial part of the UNIQUAC activity coefficients, Equation (2.3), is used directly. Whereas the residual part of the activity coefficient, Equation (2.4), is replaced by the solution-of-groups concept.

$$\ln \gamma_i^R = \sum_k \nu_k^{(i)} \left[\ln \Gamma_k - \ln \Gamma_k^{(i)} \right] \quad (2.5)$$

all groups

$$\ln \Gamma_k = Q_k \left[1 - \ln \left(\sum_m \Theta_m \Psi_{mk} \right) - \sum_n \left(\Theta_m \Psi_{kn} / \sum_n \Theta_n \Psi_{nn} \right) \right] \quad (2.6)$$

$$\Theta_m = \frac{Q_m X_m}{\sum_n Q_n X_n} \quad (2.7)$$

$$\Psi_{mn} = \exp \left[- \frac{U_{mn} - U_{nm}}{RT} \right] = \exp \left(- a_{mn} / T \right) \quad (2.8)$$

Parameters are given for eighty-three different group interactions in the temperature region 275 to 400 K. Prediction of liquid-phase activity coefficients is demonstrated for a variety of binary and ternary mixtures including those containing alcohols, water, or other polar liquids.

2.6 Solutions and molecules (Burke, 1984)

A solvent is a substance that is capable of dissolving other substances and forming a uniform mixture called a solution. The substance dissolved is called the solute. For the solution to occur, the solvent molecules must overcome this intermolecular stickiness in the solute and find their way between and around the solute molecules. At the same time, the solvent molecules themselves must be separated from each other by the molecules of the solute. This is accomplished best when the attractions between the molecules of both components are similar. If the attractions are sufficiently different, the strongly attracted molecules will cling together, excluding the weakly attracted molecules, and immiscibility will result. These sticky forces between molecules are called Van der Waals forces that are the result of intermolecular polarities. These differences in polarity are directly responsible for the different degrees of intermolecular stickiness from one substance to another. The accurate predictions of solubility behavior will depend not only on determining the degree of intermolecular attractions between molecules, but also in discriminating between different types of polarities as well. Thus, substances will dissolve in each other not only if their intermolecular forces are similar, but if their composite forces are made up in the same way. The types of component interactions include hydrogen bonds, induction and orientation effects, and dispersion forces. It is mentioned that van der Waals forces result from the additive effects of several different types of component polarities.

This is an introduction to the three types of polar interactions that are commonly used in solubility theories: dispersion forces, polar forces, and hydrogen bonding forces. For nonpolar liquids, the intermolecular forces between nonpolar molecules are entirely due to dispersion forces which are related to surface area: the larger the molecule, the greater the intermolecular attractions. Dispersion forces are present to some degree in all molecules, but in polar molecules there are also stronger forces at work. Polar molecules tend to arrange themselves head to tail, positive to negative, and these orientations lead to further increases in intermolecular attraction. These dipole-dipole forces, called Keesom interactions, are attractions that depend on the same properties in each molecule. Because Keesom interactions are related to molecular arrangements, they are temperature dependent. Higher temperatures cause increased molecular motion and thus a decrease in Keesom interactions. On the other hand, any molecule, even if nonpolar, will be temporarily polarized in the vicinity of a

polar molecule, and the induced are permanent dipoles will be mutually attracted. These dipole-induced dipole forces, called Debye interactions, are not as temperature dependant as Keesom interactions. Furthermore, the strong type of polar interaction occurs in molecules where a hydrogen atom is attached to an extremely electron-hungry atom such as oxygen, nitrogen, or fluorine. This type of polarity is so strong compared to other van der Waals interactions.

2.7 Liquid-liquid extraction

Liquid-liquid extraction is a process for separating components in solution by their distribution between two immiscible liquid phases. It is an extraction of a substance from one liquid phase into another liquid phase. The liquid-liquid extraction may provide the most cost-effective separation process; however, its economic utility depends strongly on the solvent selected and on the procedures used for solvent recovery and raffinate desolventizing.

2.7.1 Liquid-liquid equilibria

The separation of components by liquid-liquid extraction depends primarily on the thermodynamic equilibrium partition of those components between the two liquid phases. Knowledge of these partition relationships is essential for selecting the ratio of extraction solvent to feed that enters an extraction process and for evaluating the mass transfer rates or theoretical stage efficiencies achieved in process equipment.

Equilibrium partition ratios

The weight fraction of solute in the extract phase y divided by the weight fraction of solute in the raffinate phase x at equilibrium is called the partition ratio, K .

$$K = y/x \quad (2.5)$$

Thermodynamically the partition ratio K° is derived in mole fractions y° and x° .

$$K^\circ = y^\circ/x^\circ \quad (2.6)$$

The relative separation, or selectivity between two components, b and c , can be described by the ratio of the two partition ratios.

$$\alpha(b/c) = K_b^\circ / K_c^\circ = K_b / K_c \quad (2.7)$$

Thermodynamic basic of liquid-liquid equilibria

In a ternary liquid-liquid system, all three components are present in both liquid phases. At equilibrium the activity A° of any component is the same in both phases by definition.

$$A_r^\circ = \gamma_r x^\circ = A_e^\circ = \gamma_e y^\circ \quad (2.8)$$

where A° = activity of solute

γ = activity coefficient of solute

r = raffinate phase

e = extract phase

Consequently, the partition ratio in mole-fraction units K° is a result of the ratio of activity coefficients in two layers

$$K^\circ = y^\circ / x^\circ = \gamma_r / \gamma_e \quad (2.9)$$

2.7.2 Ternary liquid-liquid systems

Ternary mixtures that undergo phase splitting to form two separate liquid phases can differ as to the extent of solubility of the three components in each of the two liquid phases. The simplest case is shown in Figure 2.3, where only the solute, component B, has any appreciable solubility in either the carrier, A, or the solvent, C, both of which have negligible solubility in each other. In this case, it assumes that the entering solvent contains no solute. Then the solute material balance is

$$X_B^{(F)} F_A = X_B^{(E)} S + X_B^{(R)} F_A \quad (2.10)$$

and the distribution of solute at equilibrium is given by

$$X_B^{(E)} = K'_{D,B} X_B^{(R)} \quad (2.11)$$

where F_A = feed rate of carrier A

S = flow rate of solvent C

X_B = ratio of mass (or moles) of solute B, to mass (or moles) of the other component in the feed (F), raffinate (R), or extract (E)

K'_{DB} = distribution coefficient defined in terms of mass or mole ratios.

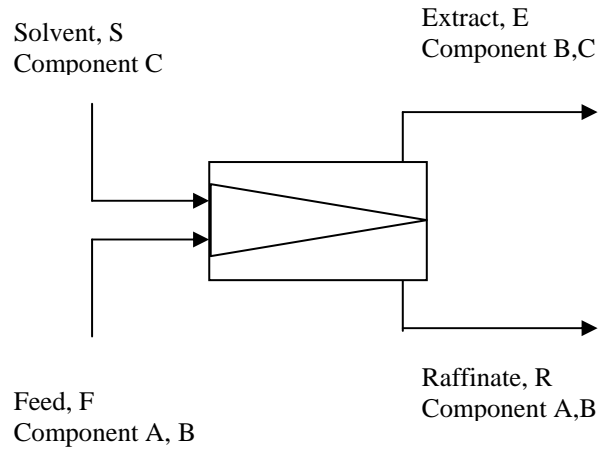


Figure 2.3 Phase splitting of ternary mixture component A and C mutually insoluble

Thus,

$$X_B^{(R)} = \frac{X_B^{(F)} F_A}{F_A + K'_{D,B} S} \quad (2.12)$$

It is convenient to define an extraction factor, E_B , for the solute B:

$$E_B = \frac{K'_{D,B} S}{F_A} \quad (2.13)$$

The larger the value of E , the greater the extent to which the solute is extracted. Large values of E results from large values of the distribution coefficient or large ratios of solvent to carrier.

From equation (2.13), the ratio is referred to as the distribution coefficient of liquid-liquid equilibrium ratio:

$$K_{D,i} \equiv \frac{x_i^{(1)}}{x_i^{(2)}} \quad (2.14)$$

Values of the distribution coefficient, $K'_{D,i}$, in terms of ratios, are related to $K_{D,i}$ in term of fractions:

$$K'_{D,i} = \frac{x_i^{(1)} / (1 - x_i^{(1)})}{x_i^{(2)} / (1 - x_i^{(2)})} = K_{D,i} \left(\frac{1 - x_i^{(2)}}{1 - x_i^{(1)}} \right) \quad (2.15)$$

When values of x_i are small, $K'_{D,i}$ approaches $K_{D,i}$. The distribution coefficient is a strong function of equilibrium phase compositions and temperature.

In the ternary liquid-liquid system, shown in figure 2.4, component A and C are partially soluble in each other and component B again distributes between the

extract and raffinate phases. Both of these exiting phases contain all components present in the feed and solvent. This case is by far the most commonly encountered, and a number of different phase diagrams and computational techniques have been devised to determine the equilibrium compositions.

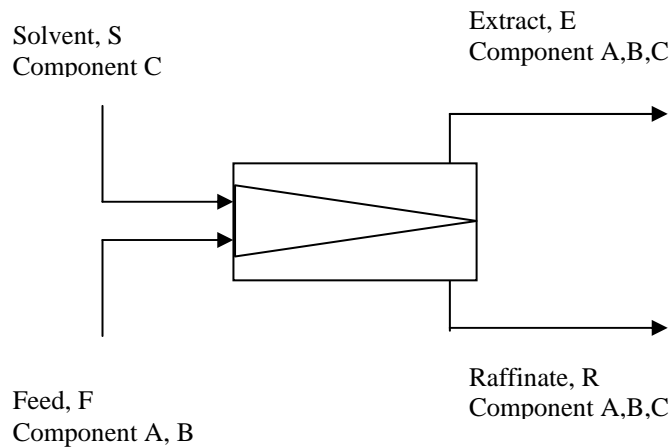


Figure 2.4 Phase splitting of ternary mixture component A and C partially soluble

An equilateral triangular diagram, shown in Figure 2.14, is the most common display of ternary liquid-liquid equilibrium data. Any point located within or on an edge of the triangle represents a mixture composition. The miscibility limits for the solvent-carrier binary system are at J and K. The miscibility boundary, represented by JDPEK in Figure 2.5, can be obtained experimentally by a cloud point titration. For example, a solution containing components A and C with some composition is made, and then component B is added until the onset of cloudiness due to the formation of a second phase occurs. Then the composition is known for the mixture and can be plotted onto the ternary phase diagram.

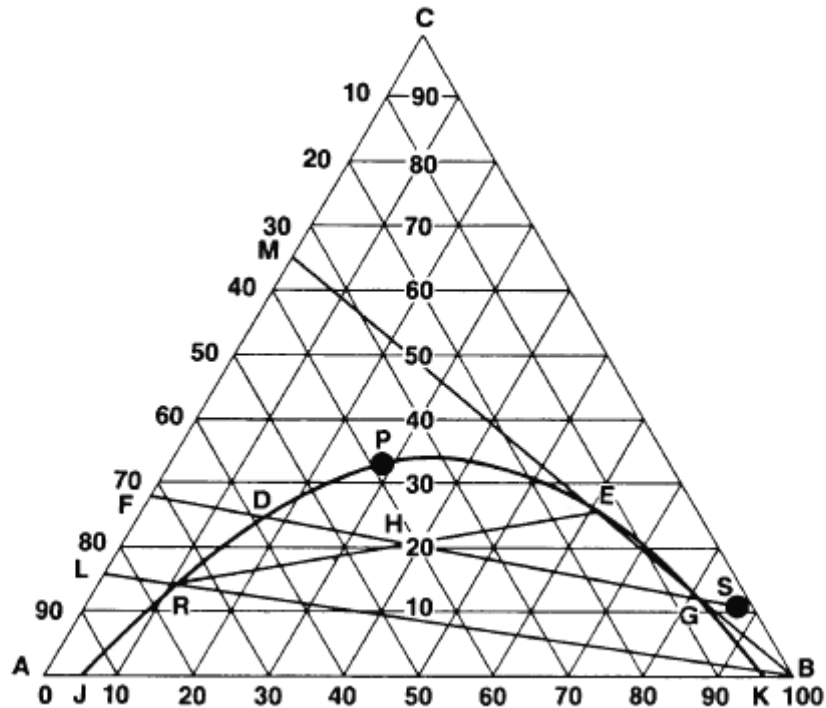


Figure 2.5 Equilateral triangular diagram

Tie lines are lines that connect points on the miscibility boundary. The tie lines may also be presented onto the ternary phase diagram from an experiment. A mixture may be prepared with composition that of point H (40% A, 40% C, 20% B) from Figure 2.5. If we allow it to equilibrate, then we can chemically analyze the final extract (E) phase and the raffinate (R) phase. Point F is a feed composition into the extractor while point S is the solvent feed to the extractor. Point H represents the composition of the two feeds at equilibrium. This point is determined by summing the feed (F) and Solvent (S) compositions for each component. Point R and E are the compositions of the raffinate and extract, respectively, and the line between them forms the tie line. The tie lines move above and below this line based on the relationship between the raffinate and extract. At point P, plait point, only one liquid phase exists and the compositions of the two effluents are equal. The curve represented by JRDPEK is the equilibrium between all three components. The area under the curve is the region where two liquid phases will exist. Above the curve, there will only be one liquid phase. If a line is drawn from F to E or from S to R, this will represent the operating line.

2.7.3 Mode of operation

Extractors can be operated in crosscurrent or counter-current. The operation in crosscurrent mode offers more flexibility; however, it is not very desirable due to the high solvent requirements and low extraction yields. On the other hand, countercurrent operation conserves the mass transfer driving force and hence gives optimal performance.

Countercurrent theoretical stages

The number of theoretical stages in the design of a liquid-liquid extraction process is calculated for evaluating the compromise between the size of the equipment and the ratio of extraction solvent to feed flow rate required to achieve the desired transfer of mass from one phase to the other. Shortcut method is used for determining the number of countercurrent theoretical stages of a ternary system. It assumes a constant flow rate of feed solvent F' and a constant flow rate of extraction solvent S' through the extractor. These concentrations and coordinates will essentially give a straight operating line on a XY diagram for stage 2 through $r-1$ in Figure 2.6.

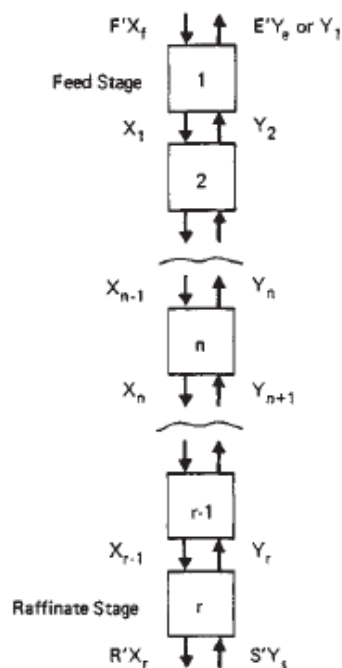


Figure 2.6 Profile countercurrent extraction cascade

The number of theoretical stages can be calculated with the Kremser equation, as shown below.

$$N = \frac{\ln \left[\left(\frac{X_f - Y_s/m}{X_r - Y_s/m} \right) \left(1 - \frac{1}{E} \right) + \frac{1}{E} \right]}{\ln E} \quad (2.16)$$

The value of m is the slope of the equilibrium line but m is equal to K' in equation 2.15 at low concentrations where the equilibrium line is straight. The values of E , the extraction factor, is calculated by dividing slope of the equilibrium, m by the slope of operating line, as shown below and same as equation 2.13 at low concentration.

$$E = mS'/F' \quad (2.17)$$

When the equilibrium line is not straight

$$m = \sqrt{m_l m_r} \quad (2.18)$$

where m_l = the concentration leaving the feed stage

m_r = the raffinate concentration leaving raffinate stage

In this case, the solvents are partially miscible, and the miscibility is nearly constant through the extractor. This occurs when all solute concentrations are relatively low. The feed stream is assumed to dissolve extraction solvent only in the feed stage and to retain the same amount throughout the extractor. Likewise, the extraction solvent is assumed to dissolve feed solvent only in the raffinate stage. With these assumptions the primary extraction-solvent rate moving through the extractor is assumed to be S' , and the primary feed-solvent is assumed to be F' . The extract rate E' is less than S' , and the raffinate rate R' is less than F' because of solvent solubilities. The two pseudo inlet concentrations X_f^B and Y_s^B can be used in equation 2.19 and 2.20 with the actual value of X_r and E to calculate rapidly the number of theoretical stages required.

$$X_f^B = X_f + \frac{S' - E'}{F'} Y_e \quad (2.19)$$

$$Y_e^B = Y_s + \frac{F' - R'}{S'} X_r \quad (2.20)$$

CHAPTER III

MATERIALS AND METHODS

3.1 Chemicals

The feed material in this study was a mixture of 1,3-propanediol and glycerol in aqueous solution. 1,3-propanediol with purity 98% was purchased from Acros Organic Co. Glycerol with purity of 99.5% was supplied from Ajax Finechem. Ethyl acetate analytical grade was obtained from Fisher Scientific, UK. Ethanol with purity of 99.7% was supplied from VWR International Ltd., UK.

3.2 Experimental set-up and procedure

To study liquid-liquid equilibrium data, data for the solubility curve of the ternary systems were determined by the cloud point method (D. Ozmen et al., 2004). Determinations of solubility curve data were made in an equilibrium cell equipped with a magnetic stirrer at isothermal condition. The temperature was controlled by a bath within an accuracy of ± 0.02 °C. The cell was filled with homogeneous water-1,3-propanediol mixtures prepared by weighing. Then the solvent was added into the cell until the end point was reached, as indicated by the onset of permanent turbidity. The tie lines data were obtained using the equilibrium cell into which 20 mL of an organic solvent and 20 mL of an aqueous mixture containing 1,3-propanediol are introduced. The temperature of the system is controlled at 30 ± 0.02 °C by refrigerated bath. The content of the two phases is stirred at 150 rpm for at least 40 min in order to reach equilibrium. The mixture is then centrifuge in centrifuge for 30 min at 30 °C and 500 rpm to complete phase separation. The organic and aqueous phases are separated and measured volume. Finally, the aqueous phase is evaporated with vacuum rotary evaporator at 35 °C for 10 min to separate the solvent that dissolves in aqueous phase and then the aqueous phase is analyzed with HPLC analytic column.

The solubility of 1,3-propanediol in water and solvent were determined by using a synthetic method. A weighed amount of the first substance was introduced into cell and then the second was added until permanent turbidity was observed.

3.3 Analysis

3.3.1 Chemical analysis

An HPLC (Lichrocart-C18) system was used to measure the concentration of 1,3-propanediol and glycerol in both the extract (solvent phase) and raffinate (aqueous) phase. Lichrocart-C18 column (250 mm x 4 mm I.D.) was used as a HPLC analytic column and the mobile phase was 5%MeOH. The flow rate of mobile phase was maintained at 0.5 ml/min and an injection volume of 20 μ L was used. The column effluent was monitored with RI detector. Each analysis was carried out at room temperature. For the sample of the extract phase, organic solvent was first removed by evaporation in a rotary vacuum evaporator, and the dried sample was then redissolved again in distilled water, and the sample solution in distilled water was injected into the HPLC analytic column.

3.3.2 Data analysis

Using the described analytical methods, the mass fraction of solute was determined in the aqueous phase. The mass balance was calculated in the mass fraction of solute in the solvent phase. The distribution ratio of a solute i , $K_{D,i}$, was calculated based on its definition as the ratio of the determined solute mass fraction in the organic phase, $w_{i,org}$, and that in the aqueous phase, $w_{i,aq}$, at equilibrium:

$$K_{D,i} = \frac{w_{i,org}}{w_{i,aq}}$$

The distribution ratio represents the capacity of a solvent system in the extraction of 1,3-propanediol and was used for evaluation of the experimental results.

CHAPTER IV

RESULTS AND DISCUSSION

In previous studies, a number of methods for the recovery of 1,3-propanediol from aqueous solution have been reported (Hao et al., 2005; Ames, 2002; Corbin et al., 2003). Cho et al. (2006) employed a phase separation process using ethyl acetate for the recovery of 1,3-propanediol from the other components in the mixture. Although, this method was found to be simple and efficient procedure, the experimental data of the liquid-liquid equilibrium to separate 1,3-propanediol from other contaminants: glycerol, 1,2-propanediol, and glucose in dilute aqueous solution was not reported. In addition, the information on the effects of parameters which are useful the evaluation of the feasibility of extraction process for separation and concentration of 1,3-propanediol was not available.

The objective of this study is to select suitable solvents and to determine the extraction potentials for 1,3-propanediol separation from aqueous solution. First, solvent screening was conducted on the theoretical basis in order to determine a suitable solvent for separating 1,3-propanediol from aqueous solution. Then the experimental liquid-liquid equilibrium data at a temperature of 303.15 K were obtained and presented in terms of distribution coefficients and mutual solubility. The tie line data are correlated using the methods proposed by Other-Tobias and Hand (Othmer and Tobias, 1942; G. S. Laddha, 1978). Furthermore, this study investigated the influence of the presence of glycerol at different concentration and the effect of temperature on extraction process. Finally, the extraction factor and the number of theoretical stages would be calculated to determine the commercial feasibility of the process.

4.1 Solvent selection for 1,3-propanediol extraction

In the selection procedure for a suitable solvent for a liquid-liquid extraction process, several factors have to be taken into account. The solvent must have favorable selectivity in order to give a good separation and high capacity in order to reduce the amount of solvent required. Therefore, the selection of effective solvent can be performed theoretically, empirically or experimentally based on the solute distribution ratio, which represents the solvent's capacity of the product and mutual solvent solubility of liquid-liquid system. For an overview of possible solvents, the Hansen solubility parameter theory could be used to classify solvents in term of their nonpolar, polar and hydrogen bonding characteristics. The total solubility parameter value is presented by three components; namely dispersion of nonpolar (δ_d), polar (δ_p), and hydrogen bonding (δ_h) (Burke, 1984).

In this work, the Hansen model was used by plotting the δ_p against the δ_h parameter for each solvents in Table 2.6. The comparison of solvent characteristics relative to 1,3-propanediol, which is presented as (0,0), is shown in Figure 4.1. These parameters represent the dipole and hydrogen bonding interactions of the solvent that are important in determining the selectivity, distribution ratio, and mutual solubility, which depends on the distance between solute and solvent. The distribution ratio is defined as the ratio of the 1,3-propanediol mass fraction in the solvent to the 1,3-propanediol mass fraction in the aqueous solution, at equilibrium. As the distribution ratio increase, less solvent is required for effective extraction. Furthermore, the mutual solubility of the suitable solvent would be minimized. In Figure 4.1, it is shown that the distribution ratio of 1,3-propanediol in methanol is high since methanol is the closest to the origin point. However, its point is also close to glycerol and water, indicating that methanol is not suitable solvent for 1,3-propanediol extraction from dilute aqueous solution due to low selectivity and high mutual solubility.

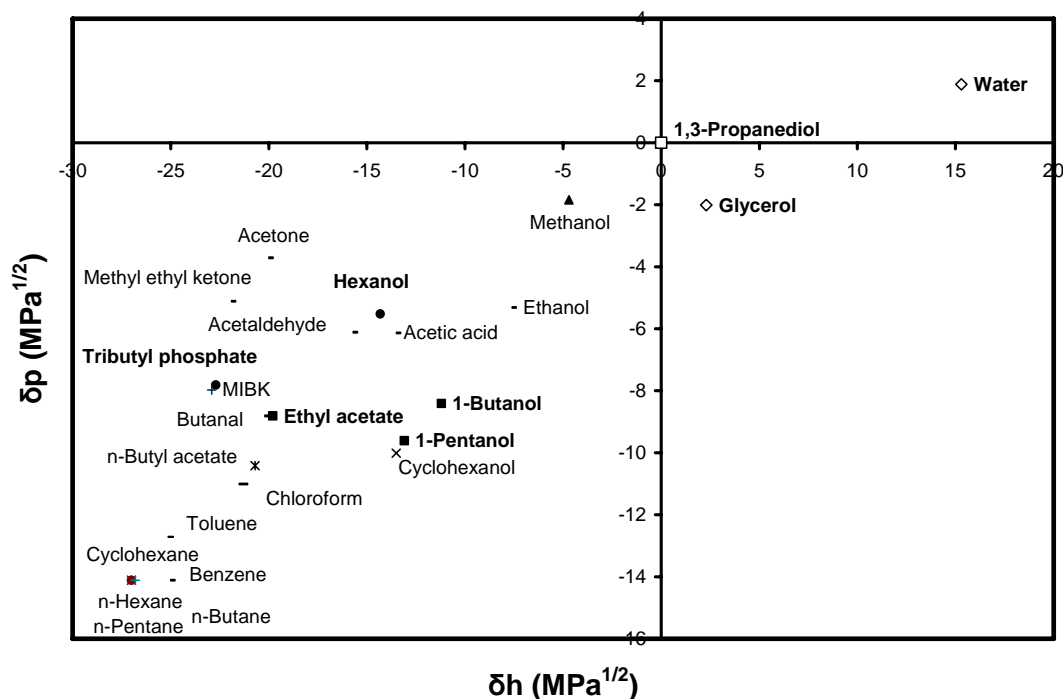


Figure 4.1 Comparison of solvents based on their δ_p and δ_h Hansen solubility parameters to 1,3-propanediol as origin (0,0)

Ethyl acetate, proposed by Cho et al. (2006) was used for solvent extraction of 1,3-propanediol from mixture and was claimed to be good for glycerol and glucose separation. Thus we select a group of possible solvents whose points are located close to ethyl acetate such as butanol, pentanol, cyclohexanol, butyraldehyde, and ethyl acetate itself. These point are close to 1,3-propanediol but they are far from glycerol and water.

In general solvent selection, the solvent must preferably be chemically stable, of low toxicity, non-corrosive, inexpensive, available in large quantities, and easily recoverable from the extract. The solvent properties that affect the ease of 1,3-propanediol recovery include density, viscosity, and the solvent boiling point are shown in Table 4.1.

Table 4.1 Profile properties of the possible solvents for 1,3-propanediol extraction

Name	Ethyl acetate	1-Butanol	Cyclohexanol	Butyraldehyde	Pentanol
Synonyms	Acetic acid ethyl ester	n-Butanol; n-Butyl alcohol	-	Butanal	-
Molecular Formula	C ₄ H ₈ O ₂	C ₄ H ₁₀ O	C ₆ H ₁₂ O	C ₄ H ₈ O	C ₅ H ₁₂ O
Molecular Weight	88.1	74.12	100.16	72.1	88.14
Melting point (°C)	-83.5 °C	-89.5 °C	23 °C	-96 °C	-78 °C
Boiling point (°C)	75-77.5 °C	117.6 °C	161 °C	75 °C	137 °C
Density (g/cm ³)	0.902	0.81	0.96	0.817	0.811
Solubility in water	80 g/L	80 g/L	36g/L	71 g/L	2.2 g/100 ml
Price (USD/L)	24.5 (99%)	21.7 (99%)	23 (98%)	24.4 (99%)	21.3(99%)
Risk Description	Highly flammable. Irritating to eyes. Repeated exposure may cause skin dryness or cracking. Vapors may cause drowsiness and dizziness.	Flammable. Harmful if swallowed. Irritating to respiratory system and skin. Risks of serious damage to eyes. Vapors may cause drowsiness and dizziness.	Harmful by inhalation and if swallowed. Irritating to respiratory system and skin.	Highly flammable.	Flammable. Harmful by inhalation. Irritating to respiratory system. Repeated exposure may cause skin dryness or cracking

From the properties in table 4.1, pentanol and cyclohexanol are difficult to recover from the extract phase because of their high boiling point. Furthermore, butyraldehyde has low flash point and highly flammable solvent are not appropriate solvents. Of the selected solvents, ethyl acetate and 1-butanol might be most suitable for 1,3-propanediol extraction from dilute aqueous phase due to low boiling point. Furthermore, the Unifac model was initially applied for the prediction of phase composition to determine distribution and mutual solubility data (D. Ozmen et al., 2004; Doulabi et al., 2006). Using the Unifac model, phase compositions are calculated for the systems of water+1,3-propanediol+ethyl acetate and water+1,3-propanediol+1-butanol at 303.15 K. The predicted liquid-liquid equilibrium data at 303.15 K are presented in Figure 4.2 and Figure 4.3.

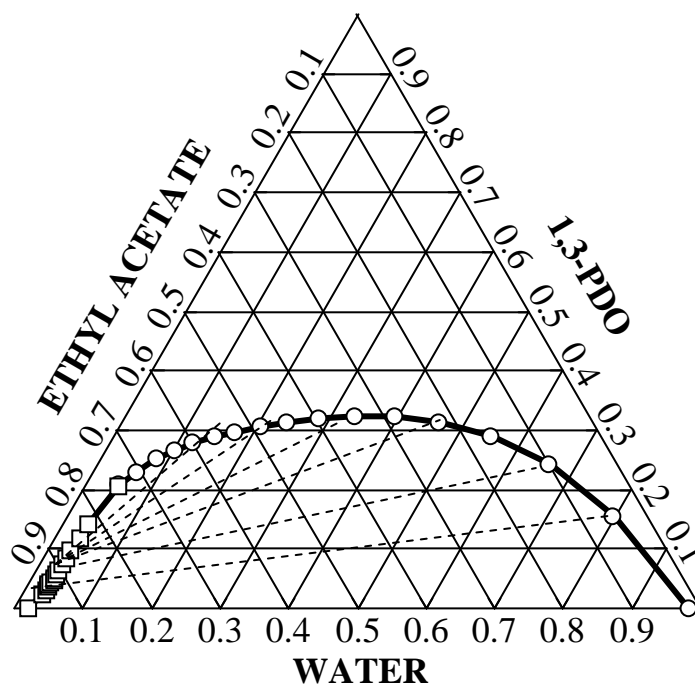


Figure 4.2 Predicted ternary diagram for the 1,3-propanediol-water-ethyl acetate using the Unifac model at 303.15 K

From Figure 4.2, it is shown that the binodal curve of 1,3-propanediol-water-ethyl acetate system has a large two-phase area, with a minimum mutual solubility but the distribution of 1,3-propanediol is favor of aqueous phase. However, we find that the mutual solubility of 1,3-propanediol-water-1-butanol system as shown in Figure 4.3 was higher because of smaller the two-phase area than one. From this result, using the 1-butanol as a solvent is not suitable to extract 1,3-propanediol from aqueous solution but ethyl acetate might be suitable for extracting 1,3-propanediol due to lower mutual solubility. Furthermore, ethyl acetate have been used to concentrate and separate 1,3-propanediol from glycerol fermentation mixture (Cho et al., 2006).

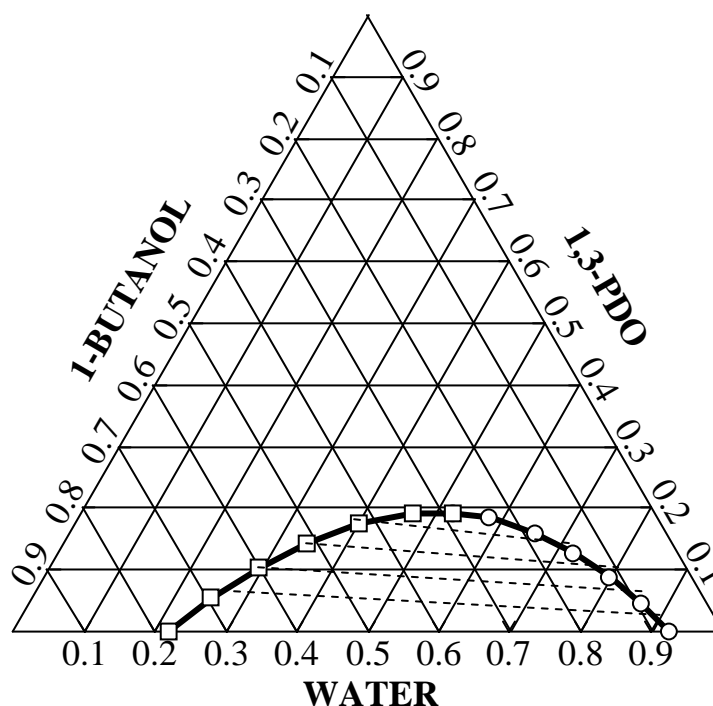


Figure 4.3 Predicted ternary diagram for the 1,3-propanediol-water-1-Butanol using the Unifac model at 303.15 K

Although, using the unifac model is able to predict the phase compositions, however it might be possible to improve the accuracy by experimental results. Thus ethyl acetate would be experimentally evaluated potential for 1,3-propanediol based on the equilibrium distribution and mutual solvent solubility.

4.2 Preliminary equilibrium measurements

The liquid-liquid equilibrium phase composition data was measured for the system of water+1,3-propanediol+ethyl acetate at 303.15 K to investigate the equilibrium distribution and mutual solvent solubility. Thus the time of agitation required to reach equilibrium was determined by measuring the change in 1,3-propanediol and glycerol concentration for different stirring time among solvent and aqueous phase (20, 40, 60 min). The experimental setup consisted of an equilibrium tank of 100 mL whose mixture temperature was controlled by refrigerated bath at 303.15 ± 0.02 K and stirred at 150 rpm. Equilibrium measurements were performed as followed. The solvent (20 mL ethyl acetate) and 20 mL of an aqueous 1,3-propanediol and glycerol solution were introduced in the tank. The concentration of 1,3-

propanediol and glycerol in the initial aqueous solution were 60 g/L and 10 g/L, respectively. The mixture was then stirred at different stirring time after which the mixture was centrifuged to achieve complete phase separation. The raffinate (aqueous) phases were analyzed by HPLC. The mass fraction of 1,3-propanediol and glycerol at different stirring time are shown in Figure 4.4.

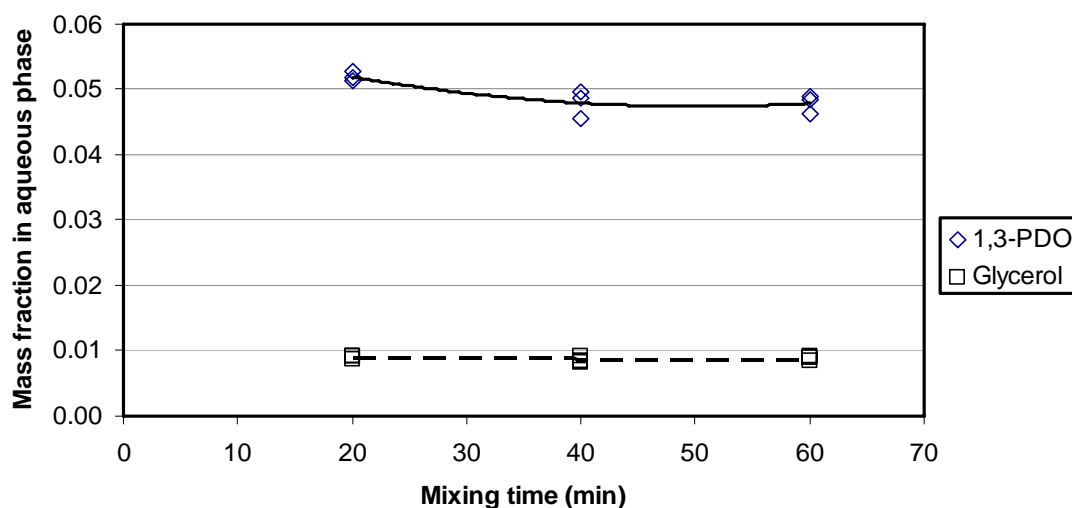


Figure 4.4 Mass fraction of 1,3-propanediol and glycerol in raffinate phase versus stirring time.

Figure 4.4 shows that mass fraction of 1,3-propanediol in raffinate phase tends to decrease slightly when the time of agitation increased and reached a constant value after 40 min, while the mass fraction of glycerol in the raffinate phase achieves to equilibrium at 20 min. From these results, we concluded that 40 min of mixing time would experimentally be sufficient to approach the equilibrium state. Thus the experimental liquid-liquid equilibrium data would taken after 40 min of extraction of 1,3-propanediol from mixture, provided the same degree of mixing degree was applied.

4.3 Results and data correlation

To evaluate the suitable solvent that posses a favourable interaction with 1,3-propanediol, experimental liquid-liquid equilibrium data were determined for 1,3-propanediol-water-solvent ternary mixtures at a temperature of 303.15 K. The plot ternary diagram shows the binodal curve, representing the boundary line between the

liquid single-phase region and the two-phase area. Every point on the binodal curve is in equilibrium with conjugated binodal point. The lines connecting the two points are called tie lines. In general extraction operation, the solvent should have a large two-phase area, with a minimum mutual solubility and distribution in favor of the solvent. In this study, the measured values of the binodal (solubility) curve for 1,3-propanediol-water-ethyl acetate (solvent) are reported in Table 4.2 and the tie line compositions for this system are given in Table 4.3.

Table 4.2 The solubility curve data for the 1,3-Propanediol(1)-water(2)-ethyl acetate(3) System at 303.15 K.

Exp. No.	Water-rich phase			Solvent-rich phase		
	W_{12}	W_{22}	W_{32}	W_{13}	W_{23}	W_{33}
1,3-Propanediol (1)- Water (2)- Ethyl acetate (3) System						
1	0.00	0.95	0.05	0.00	0.17	0.82
2	0.09	0.84	0.07	0.02	0.16	0.82
3	0.22	0.71	0.07	0.05	0.16	0.79
4	0.35	0.50	0.15	0.07	0.15	0.78
5	0.40	0.40	0.20	0.09	0.17	0.74

Table 4.3 The tie line compositions for the 1,3-Propanediol-water-ethyl acetate System at 303.15 K.

Exp. No.	Overall			Water-rich phase			Solvent-rich phase		
	W_1	W_2	W_3	W_{12}	W_{22}	W_{32}	W_{13}	W_{23}	W_{33}
1,3-Propanediol (1)- Water (2)- Ethyl acetate (3) System									
1	3.21	49.44	47.35	5.50	85.05	9.45	1.09	16.53	82.39
2	11.85	41.00	47.15	19.74	66.38	13.89	3.93	15.80	80.26
3	14.87	38.06	47.08	24.86	61.82	13.31	5.40	16.07	78.53
4	21.17	31.90	46.93	35.67	50.48	13.86	7.43	15.09	77.48
5	27.11	26.10	46.79	44.40	37.00	18.60	9.71	16.65	73.65

W_{13} and W_{12} are the mass fractions of 1,3-propanediol in the solvent and aqueous phases at equilibrium, respectively. For ethyl acetate, the two-phase on ternary diagram and the tie-lines are plotted in Figure 4.5 to demonstrate the distribution behavior of 1,3-propanediol and the mutual solubility at 303.15 K.

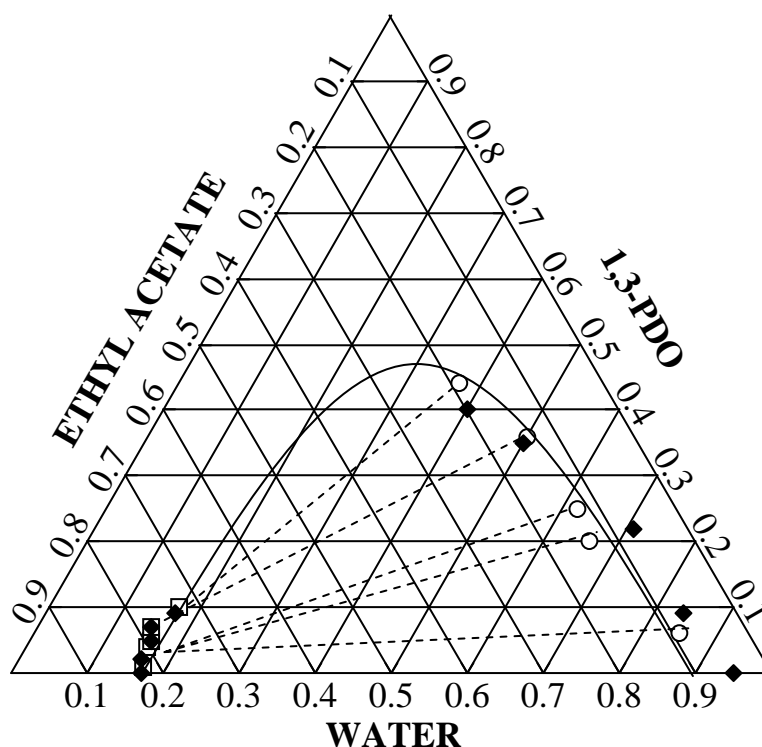


Figure 4.5 Liquid-liquid equilibrium data for 1,3-Propanediol-water-ethyl acetate Ternary at 303.15 K.

According to Figure 4.5, the tie lines show the distribution of 1,3-propanediol at equilibrium is in favor of the aqueous phase and show a similar behavior to the prediction using unifac equation. Nevertheless, the experimental mutual solubility of 1,3-propanediol from extraction with ethyl acetate is higher than the calculated mutual solubility due to the smaller two-phase area of ternary system as shown in Figure 4.6. To calculate phase equilibrium data using the unifac model, liquid-phase activity coefficients are related to interactions between their functional groups instead of interaction between molecules. Therefore, the phase equilibrium data from experiment and calculation by unifac equation are different for estimation of ternary system.

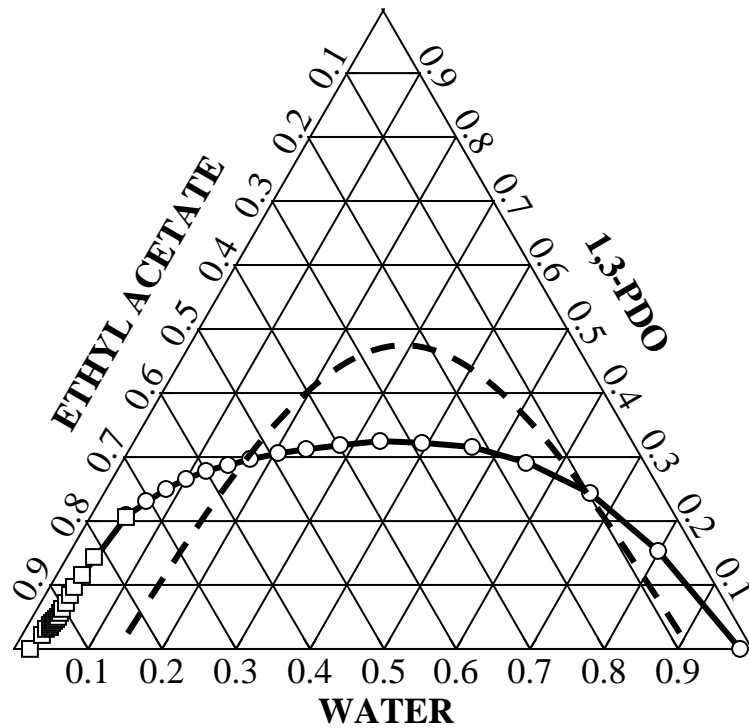


Figure 4.6 Comparison of experimental and calculated ternary diagram for the 1,3-propanediol-water-ethyl acetate using the Unifac model at 303.15 K: (-) calculated data; (--) experimental data.

In this work, the reliability of experimentally measured tie-line data is determined by making a Othmer and Tobias (Eq. 1) and Hand (Eq. 2) correlation. The linearity of the plots indicates the degree of consistency of the related data (Othmer and Tobias, 1942; G. S. Laddha, 1978).

$$\ln\left(\frac{(1-W_{33})}{W_{33}}\right) = a_1 + b_1 \ln\left(\frac{(1-W_{22})}{W_{22}}\right) \quad (1)$$

$$\ln\left(\frac{W_{13}}{W_{33}}\right) = a_2 + b_2 \ln\left(\frac{W_{12}}{W_{22}}\right) \quad (2)$$

The Othmer and Tobias plot is shown in Figure 4.7 and the Hand plot is shown in Figure 4.8 to determine a and b coefficients.

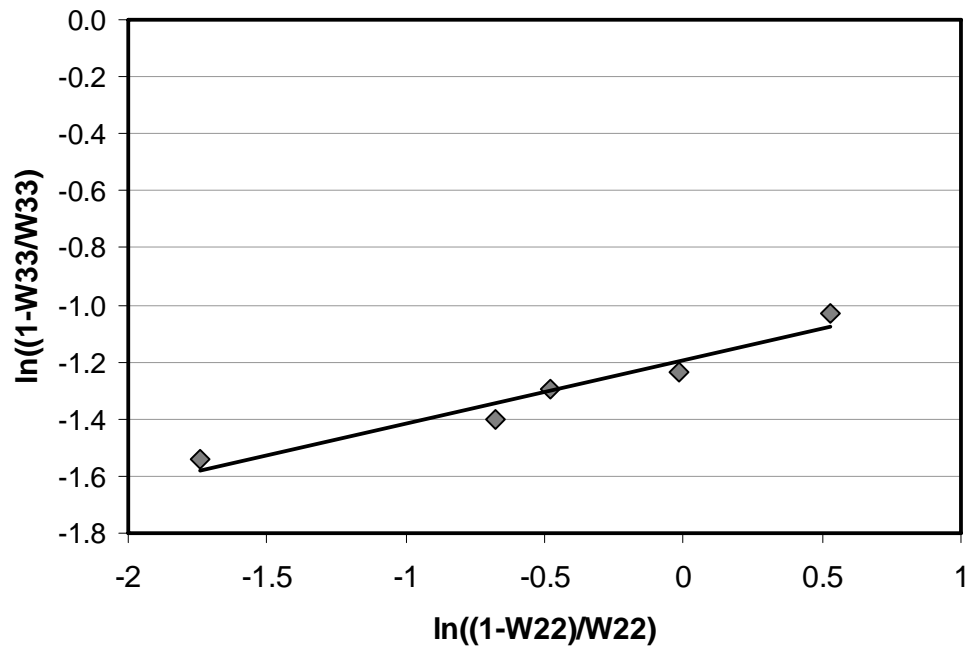


Figure 4.7 Othmer and Tobias Plot for the 1,3-Propanediol (1)-Water (2)- Ethyl acetate (3) System at 303.15 K

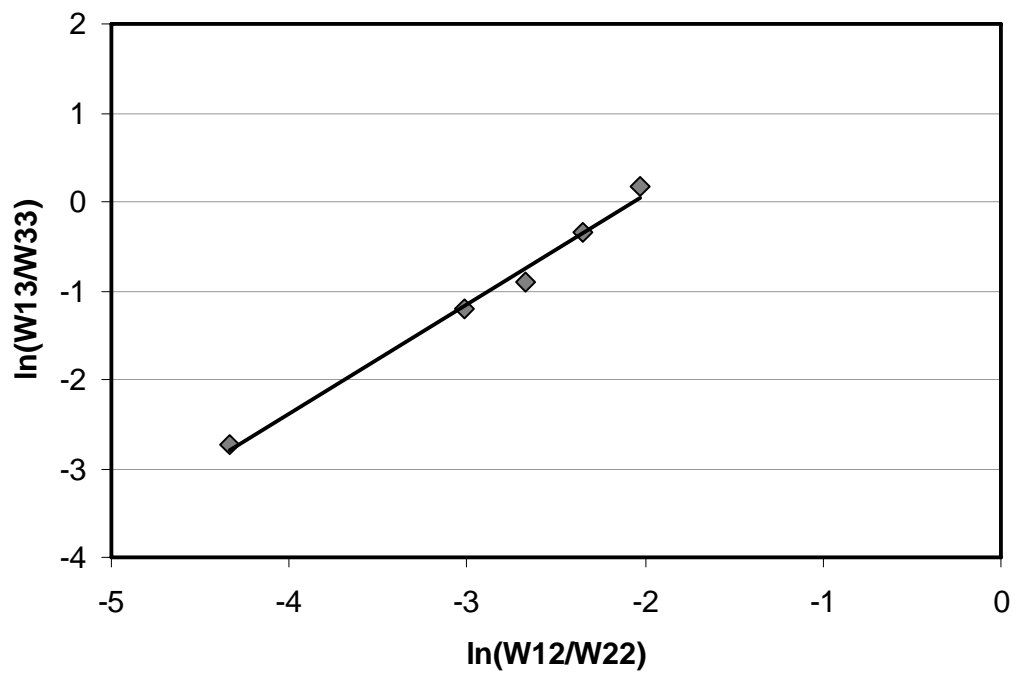


Figure 4.8 Hand Plot for the 1,3-Propanediol (1)- Water (2)- Ethyl acetate (3) System at 303.15 K

The values of the parameters a, b, and correlation coefficients (R^2) are given in Table 4.4. The proximity of the correlation coefficient (R^2) to 1 indicates the degree of consistency of the related data. In this study, correlation coefficient (R^2) for the Othmer-Tobias and Hand are 0.9428 and 0.9904, respectively; therefore, this data are sufficient for the determination of the tie line compositions.

Table 4.4 The correlation coefficients and correlation factors for the Othmer-Tobias and Hand correlations at 303.15 K.

System	Othmer-Tobias coefficients			Hand coefficients		
	a1	b1	R^2	a2	b2	R^2
1,3-Propanediol-Water-Ethyl acetate	- 1.1957	0.2207	0.9428	2.5518	1.2357	0.9904

The experimentally determined equilibrium distribution data of 1,3-propanediol are plotted in Figure 4.9. The distribution of 1,3-propanediol between the two phases represents the capacity of a solvent system for the extraction of 1,3-propanediol. From Figure 4.9, it can be concluded that the distribution of 1,3-propanediol is most in favor of the aqueous phase for ethyl acetate and the distribution ratio determined from slope of Figure 4.9 is about 0.2201. From previous literature, tributyl phosphate was used for extracting 1,3-propanediol from aqueous solution and its distribution ratio was reported to be 0.203 (Avraham M. Baniel et al., 2006). Although, the mutual solubility of extraction with tributyl phosphate is lower than the mutual solubility of extraction with ethyl acetate due to higher hydrophobic parameter, tributyl phosphate is difficulty to separate from extract phase in order to purification of 1,3-propanediol due to its high boiling point. On the other hand, ethyl acetate can be easily separated 1,3-propanediol from extract phase since the boiling point of ethyl acetate is low. From these results, we can conclude that ethyl acetate is a potential alternative solvent for extracting 1,3-propanediol from aqueous solution.

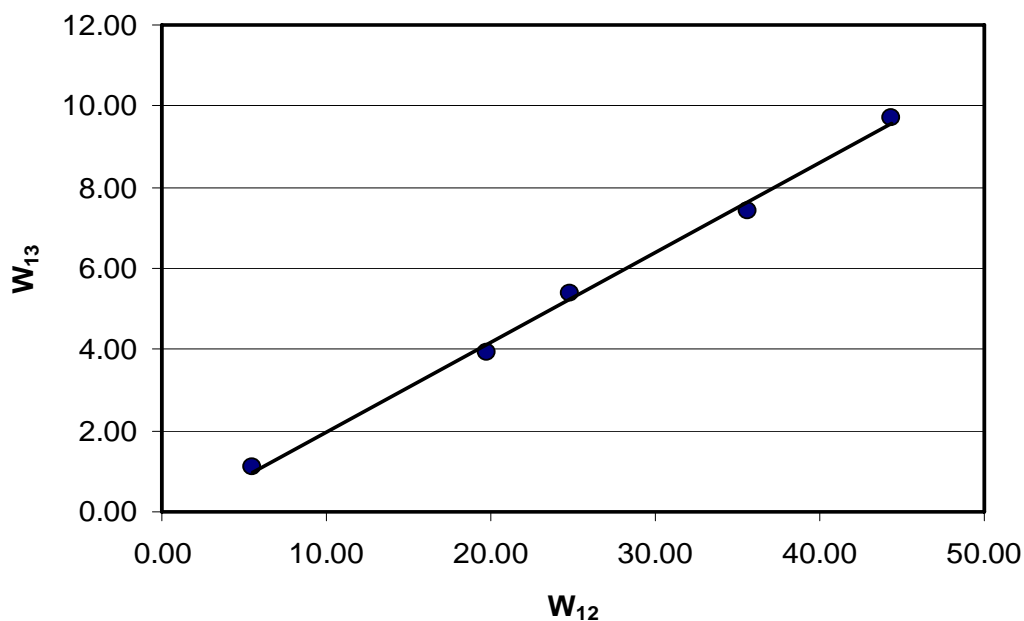


Figure 4.9 Equilibrium mass fraction of 1,3-Propanediol as a function of the aqueous equilibrium mass fraction for the ternary system 1,3-Propanediol (1)- Water (2)- Ethyl acetate (3) at 303.15 K

4.4 Effect of temperature for 1,3-propanediol extraction

In general, the solubility of a solute is an indication of the extraction capacity of a solvent. The 1,3-Propanediol solubility as function of temperature for ethyl acetate is shown in Figure 4.10.

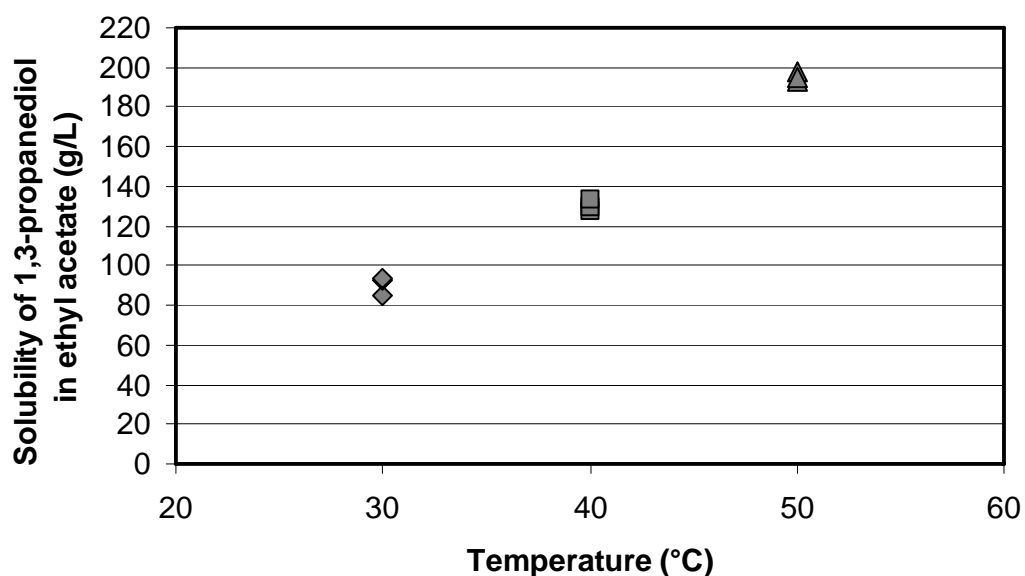


Figure 4.10 Solubility of 1,3-Propanediol as function of temperature for ethyl acetate.

Figure 4.10 shows that the solubility of 1,3-Propanediol in ethyl acetate increases as temperature is increased due to polarity of 1,3-Propanediol. The polarity of a molecule is related to its atomic composition, its geometry, and its size (John Burke, 1984). Because of geometry of 1,3-propanediol molecule, the 1,3-propanediol molecule is high polar molecule and is completely miscible with water. The interaction between 1,3-propanediol molecule is Keesom interactions that depend on temperature (John Burke, 1984). The higher temperature causes increased the molecular motion and thus a decrease in Keesom interactions. Therefore, the Keesom interaction between 1,3-propanediol molecule is decreased and then the solubility of 1,3-propanediol in ethyl acetate is increased when the temperature of extraction increases. For 1,3-propanediol, it is found to be completely miscible in water due to strong hydrophilic property of 1,3-propanediol. In addition, the phase equilibrium data depend upon the temperature. In this work, we first investigate the influence of temperature for 1,3-Propanediol extraction using the unifac model. To study distribution of 1,3-Propanediol as function of temperature, the temperature for extracting 1,3-Propanediol was varied at 303.15 K, 313.15 K, and 323.15 K and the distribution data are plotted as shown in Figure 4.11.

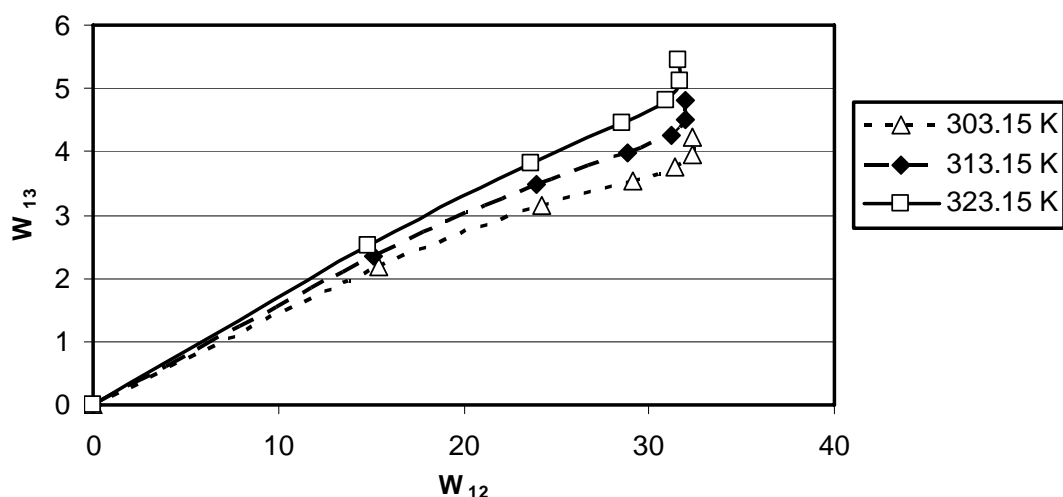


Figure 4.11 Organic equilibrium mass fraction of 1,3-Propanediol as a function of the aqueous equilibrium mass fraction at 303.15 K, 313.15 K, and 323.15 K calculated values using the Unifac model

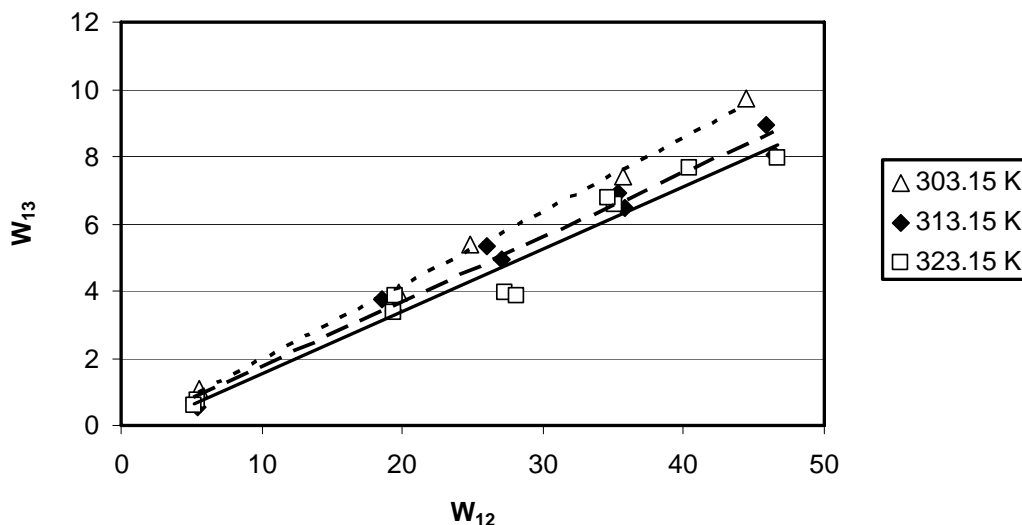


Figure 4.12 Experimental organic equilibrium mass fraction of 1,3-Propanediol as a function of the aqueous equilibrium mass fraction at 303.15 K, 313.15 K and 323.15 K

Figure 4.11 shows that the mass fraction of 1,3-Propanediol in organic solvent phase, calculated from slope of this figure is increased considerably at elevated temperatures. This result from the model does, however, not guarantee the accuracy in the prediction of liquid-liquid equilibrium due to assumption of unifac equation. From equation 2.8, the group interaction parameters, Ψ_{mm} are assumed to be independent of temperature and thus there are two group interaction parameters for each pair of the groups. Furthermore, the parameters are not back-calculated from experimental liquid-liquid equilibrium data. Thus the unifac model can be used but should not be expected to give accurate estimates.

From Figure 4.12, the experimental results are not consistent with the calculated results. Even though the solubility of 1,3-propanediol is increased at higher temperature, the mass fraction of 1,3-Propanediol in organic solvent phase is decreased due to solubility behavior of 1,3-propanediol. The solubility behavior of substances will depend not only on determining the degree of intermolecular attractions between molecules, but also in discriminating between different types of polarities as well. The types of polarities are the results of the component interactions that include hydrogen bonds, orientation effect, and dispersion forces. In this study, we considered the solubility behavior from the polar and hydrogen bonding

characteristics of 1,3-propanediol molecule. From Table 2.6, we found that polar components (δ_p) of 1,3-Propanediol and water that are 15.6 and 14.1, respectively which are closely plotted on the solubility parameter diagram as shown in Figure 4.1. Both water and 1,3-propanediol molecules are highly polar molecules that result from polar force and hydrogen bonding force between interaction of molecule 1,3-propanediol and water. When the temperature increases, the interaction between molecules, Keesom interaction from polar force decreases due to increased molecular motion and then the solvent molecules should separate 1,3-propanediol from water easily. However, there are other molecular interactions between 1,3-propanediol and water in term of hydrogen bonding, this interaction between 1,3-propanediol and water increases according to increase of temperature. Moreover, the molecular interaction between ethyl acetate and 1,3-propanediol decrease as the temperature increase because of a decrease of polar force. Therefore, the distribution of 1,3-propanediol in solvent phase decrease as the temperature increases. Although, the distribution ratio of 1,3-propanediol increases to 0.03 when the temperature of extraction decreases to 10 K, but this extraction needs to supply more energy for decreasing the temperature lower than the ambient temperature (Appendix B). From this result, the extraction temperature at 303.15 K is suitable to extract 1,3-Propanediol from aqueous solution.

4.5 Influence of residual glycerol from fermentation

In the biotechnological process for producing 1,3-propanediol, bioconversion of glycerol to 1,3-propanediol is already known for several bacterial strains such as *Klebsiella pneumoniae*, *Citrobacter freundii*, *Enterobacter agglomerans*, *Clostridium butyricum*, and *Clostridium acetobutylicum*. The type of strain, used for 1,3-propanediol production affects the type of products, their concentrations, productivity, and glycerol consumption. The glycerol consumption also depends on the type of fermentor. In batch culture, glycerol consumption is almost complete at low initial glycerol concentration but some strain such as *Enterobacter agglomerans* remained a lot of unconsumed glycerol in the broth (Barbirato et al., 1998). Furthermore, fed-batch and continuous operations were used for glycerol fermentation in order to increase initial glycerol concentration. In continuous culture, the culture presented high dilution rates gave the increased volumetric productivity whereas the amounts of residual glycerol in the fermentation broth increased (Papanikolaou et al., 2000).

Therefore, we need to investigate the effect of residual glycerol from fermentation. The final concentrations of fermentation broth were summarized in Table 4.5. The residual glycerol makes it difficult to separate 1,3-propanediol separation from fermentation broth due to its hydrophilic property and high boiling point near 1,3-propanediol. From the literature, the maximum residual glycerol is 12 g/L and the minimum residual glycerol is 0 g/L due in a batch fermentation process. Therefore, we investigated the effective of residual glycerol in three mass fractions. The mass ratio of 60 g 1,3-propanediol to 12 g glycerol, 60 g 1,3-propanediol to 8 g glycerol, and 60 g 1,3-propanediol to 4 g glycerol in 1 L solution were studied at different feed concentration for 1,3-propanediol extraction. Figure 4.13 shows the experimental results of glycerol addition in feed stream at 303.15 K.

Table 4.5 The final concentration of fermentation broth

Author	Type of fermentation process	Bacterial species	1,3-propanediol concentration (g/L)	Residual glycerol concentration (g/L)
Barbirato et al., 1998	Batch	<i>K. pneumoniae</i>	31.5	0.0
		<i>C. freundii</i>	31.0	0.0
		<i>E. agglomerans</i>	18.0	30.8
		<i>C. butyricum</i>	36.7	0.0
A. Reimann et al., 1998	Continuous	<i>C. butyricum</i>	35.8	2-4
S.Saint-Amans et al., 1994	Fed-batch	<i>C. butyricum</i>	60	10
Papanikolaou et al., 2000	Continuous	<i>C. butyricum</i>	41-46	1.5-8.6
Maria Gonzalez-Pajuelo et al., 2005	Continuous	<i>C. acetobutylicum</i>	60	7.6

In Figure 4.13, the distribution of 1,3-propanediol is increasingly in favor of solvent phase when the amounts of glycerol added to feed are increased. Due to the polarity and hydrogen bonding characteristics of glycerol, the increased amount of residual glycerol results in the intermolecular interactions between water and 1,3-propanediol. The glycerol molecules that are highly polar molecules have higher hydrogen bonding forces between water and glycerol than that between water and 1,3-propanediol because of their molecular structure. Thus the molecular interactions

between water and 1,3-propanediol tend to decrease in the case glycerol addition. Then the ethyl acetate molecules can overcome this interactions and find their way around 1,3-propanediol. From Figure 4.9 and 4.13, we can calculate the distribution ratio as reported in Table 4.6. This experimental data are also calculated in distribution ratio of glycerol and the selectivity of extraction of 1,3-propanediol as compared with glycerol. The selectivity is defined as the distribution ratio of 1,3-propanediol divided by the distribution ratio of glycerol.

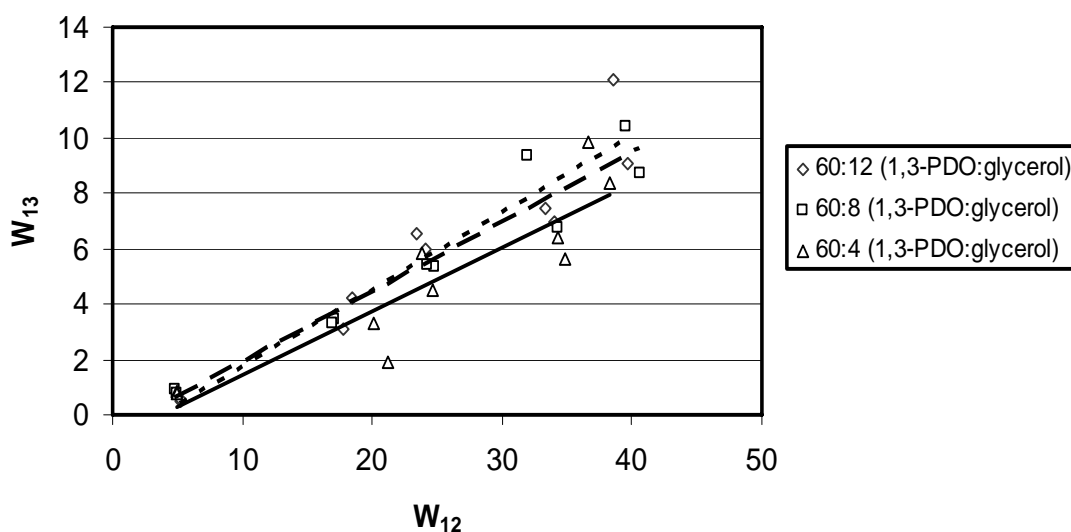


Figure 4.13 Experimental results of glycerol addition in feed at 303.15 K

In Table 4.6, the distribution ratio of 1,3-propanediol is slightly increased at low concentration of glycerol and the distribution is increased to 0.28 at high concentration of glycerol. Furthermore, the distribution ratio of glycerol at high glycerol concentration is higher than the distribution ratio of glycerol at low concentration due to the increased amounts of glycerol in water. When the amount of glycerol in aqueous solution was increased, the intermolecular interaction between glycerol and water was decreased and then ethyl acetate molecules can be stick glycerol molecules increasingly. However, the selectivity decreases as the distribution ratio of both 1,3-propanediol and glycerol increases. Based on this result, the extraction of 1,3-propanediol from fermentation broth should have the potential of residual glycerol between 0 g/L and 12 g/L in order to increase the distribution of 1,3-propanediol.

Table 4.6 The calculated distribution ratio of 1,3-propanediol and glycerol from extraction at 303.15 K

Final concentration of broth mass ratio (1,3-PDO:Glycerol)	Distribution ratio		Selectivity
	$K_{D,1,3-PDO}$	$K_{D,glycerol}$	
60:0	0.22	-	-
60:4	0.23	0.08	2.88
60:8	0.25	0.20	1.25
60:12	0.28	0.20	1.40

4.6 1,3-propanediol with co-solvent extraction

In our experiment, the extraction of 1,3-propanediol with ethyl acetate is a rather simple and efficient separation method; however, the distribution of 1,3-propanediol is in favor of aqueous phase. The distribution ratios of 1,3-propanediol from extraction without the addition of glycerol and with the addition of glycerol at 303.15 K are 0.22 and 0.28, respectively. In this results, the solvent, ethyl acetate shows a low capacity, thus requiring a large amount of solvent to extract 1,3-propanediol from aqueous phase. To improve the efficiency of 1,3-propanediol separation, a solvent mixtures is investigated. From literature, Malinowski (1999) found that the aldehyde group has the best characteristics for the extraction of 1,3-propanediol; however, it is difficult to keep the solvent on safe storage because of its highly flammable property. Although, the alcohol group has lower distribution ratio than the aldehyde group, its distribution ratio and selectivity are potential for extraction of 1,3-propanediol. In addition, methanol and ethanol positions in Figure 4.1 are close to 1,3-propanediol and they can be used for blending solvent mixture to improve solvent polar. Due to safety aspect, we select ethanol for the solvent mixture in the extraction of 1,3-propanediol.

Solvents can easily be blended to exhibit selective solubility behavior, or to control such properties as evaporation rate, solution viscosity, the degree of toxicity and the environmental effects (Mathijs L. et al., 2006). Because solubility properties are the net results of intermolecular attractions, a mixture with the same solubility parameters as a single liquid will exhibit the same solubility behavior. Determining the solubility behavior of the solvent mixture, therefore, is simply a matter of locating the solubility parameter on the graph. There are two ways by which this may be accomplished: mathematically, by calculating the parameters of the mixture from the

parameters of the individual solvents, and geometrically, by simply drawing a line between the solvents and measuring the ratio of the mixture on the graph (Burke, 1984). In this study, we predicted the solubility behavior of the solvent mixture by the mathematical method that is the most accurate and present in Hansen solvent map as shown in Figure 4.12. To derive the solubility parameters of the solvent mixture, the simple mixing rule can be applied according to the following equations (Cheremisinoff, 2003).

$$\delta_p = \sum_1 \phi_i \delta_{pi} \quad (4.1)$$

$$\delta_h = \sum_1 \phi_i \delta_{hi} \quad (4.2)$$

Where δ_p = polar component

δ_{pi} = polar component of the i th solvent in a blend

δ_h = hydrogen bonding component

δ_{hi} = hydrogen bonding component of the i th solvent in a blend

ϕ_i = volume fraction of the i th solvent in a blend

From Table 2.6, we can calculate the solubility parameters of solvent mixture between ethyl acetate and ethanol as presented in Table 4.7. 95:5 volume fraction and 90:10 volume fraction of ethyl acetate and ethanol were investigated at 303.15 K. The comparison of solvent characteristics relative to 1,3-propanediol, which is presented as (0,0), is shown in Figure 4.14.

Table 4.7 Profile the calculated solubility parameters of solvent mixture at 25°C

Volume fraction		$\delta/\text{MPa}^{1/2}$	
Ethyl acetate	Ethanol	δ_p	δ_h
0.95	0.05	5.5	7.8
0.90	0.10	5.7	8.4

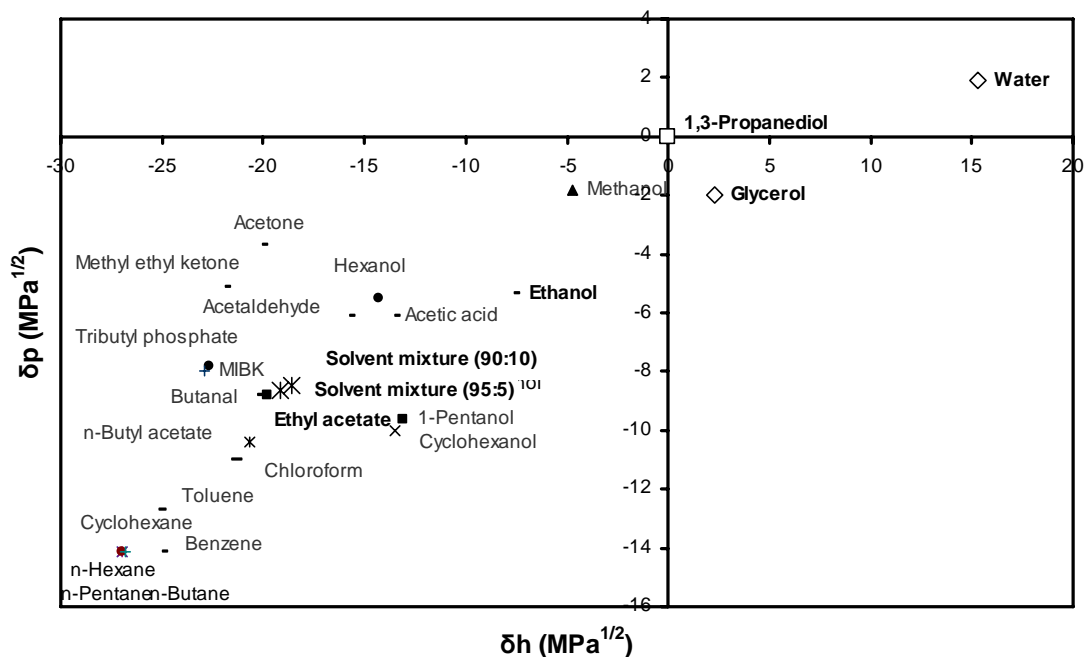


Figure 4.14 Comparison of solvents and solvent mixture based on their δ_p and δ_h Hansen solubility parameters to 1,3-propanediol as origin (0,0)

In Figure 4.15, it can be concluded that the more ethanol, the larger capacity toward 1,3-propanediol because the distance between solvent mixture and 1,3-propanediol is shorter than the distance of pure ethyl acetate. From experimental extraction with solvent mixture, it was found that the distribution ratio of 1,3-propanediol increased as the volume fraction of ethanol increased as shown in Figure 4.15. At 95:5 volume fraction of ethyl acetate and ethanol, the distribution ratio of 1,3-propanediol was found to be 0.26. Moreover, the distribution ratio of 1,3-propanediol was 0.31 when the volume fraction of ethyl acetate and ethanol was 90:10. The increased volume fraction of ethyl acetate could increase the polarity of the mixture solvent because of the high polarity of ethanol. However, Figure 4.16 shows that the loss of solvent into raffinate phase after extraction increases when we increase the fraction of ethanol in solvent stream before extraction. From these results, we can conclude that the additional of ethanol into solvent mixture can increase the distribution ratio of 1,3-propanediol from 0.22 to 0.31 by blending ethanol from 0 to 10 % volume. The mutual solubility, however, was increased due to increased solvent polarity.

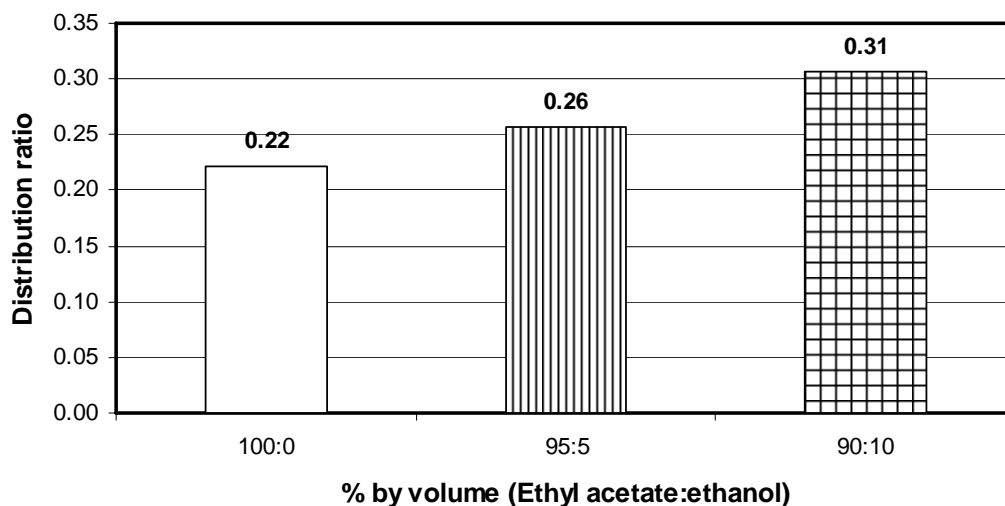


Figure 4.15 Experimental distribution ratio from 1,3-propanediol extraction with co-solvent at different % volume of ethyl acetate and ethanol at 303.15 K

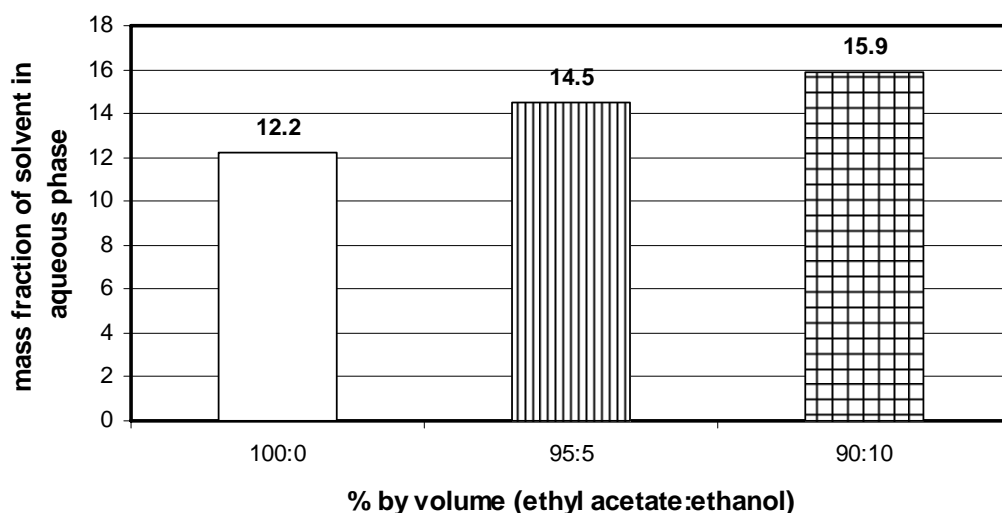


Figure 4.16 Experimental solvent loss for 1,3-propanediol extraction at 303.15 K

4.7 Calculation of the number of theoretical stages

From our experimental results, the solvent to feed ratio, S/F, and the number of theoretical stages, NTS for extracting 1,3-propanediol from aqueous solutions were calculated for single solvent and co-solvent extraction. As ethyl acetate was found to be a suitable solvent for 1,3-propanediol extraction and the experimental liquid-liquid equilibrium data at 303.15 K are presented as shown in Figure 4.5. The equilibrium composition and tie line data were used for calculating the minimum solvent to feed

ratio, $(S/F)_{\min}$ for the ethyl acetate by a graphical method (Appendix B). This the minimum solvent to feed ratio was calculated as $(S/F)_{\min} = 2.03$. Generally, the solvent to feed ratio for an extraction system is 1.5 times $(S/F)_{\min}$ (Seader J. D. et al., 1998). The actual solvent to feed ratio, S/F of 3.05 selected for 1,3-propanediol extraction with ethyl acetate. In this work, it was assumed that there was low concentration of glycerol and the mutual solubility of solvent remained nearly constant. Furthermore, it was assumed a constant flow rate of feed stream and a constant flow rate of extraction solvent through the extractor. From the Kremser equation (2.16), the mass fraction of 1,3-propanediol in the raffinate phase after extraction is shown in Figure 4.17 as function of the number of equilibrium stages. Figure 4.17 shows that the mass fraction of 1,3-propanediol in raffinate phase at 303.15 K was lower as the number of theoretical stages increases. Although, the number of theoretical stages is 13.9, the lowest mass fraction of 1,3-propanediol in raffinate phase is 0.03 when S/F is 3.05. To decrease the number of theoretical stages, the solvent to feed ratio is increased to 10 as shown in Figure 4.17. The number of stages that was used for extracting 1,3-propanediol from aqueous solutions is 7.6 stages in this case.

However, when ethanol co-solvent was blended between ethyl acetate at the ethyl acetate to ethanol ratio of 90 to 10 % by volume was used, the value of the distribution ratio was higher. The extraction with co-solvent requires only $NTS = 5.8$ stages in order to reach the same raffinate mass fraction at the $S/F = 10$ as shown in Figure 4.18. Nevertheless, using the number of theoretical stage tends to increase when we would like to decrease the mass fraction of 1,3-propanediol less than about 0.08 at S/F of 10 for both ethyl acetate and co-solvent. In order to decrease energy and cost for separation of 1,3-propanediol, the mass fraction of 1,3-propanediol in raffinate phase should be residual about 0.008 and then it can be concentrated for extraction again or separated by the lower energy and operating cost method such as pervaporation.

From the obtained experimental results, the liquid-liquid extraction presents good alternative method for separation of 1,3-propanediol. Although, rather high amount of solvent must be used in separation of 1,3-propanediol, this solvent can be easily recovered from extract stream and can be reused for extracting 1,3-propanediol from aqueous solutions.

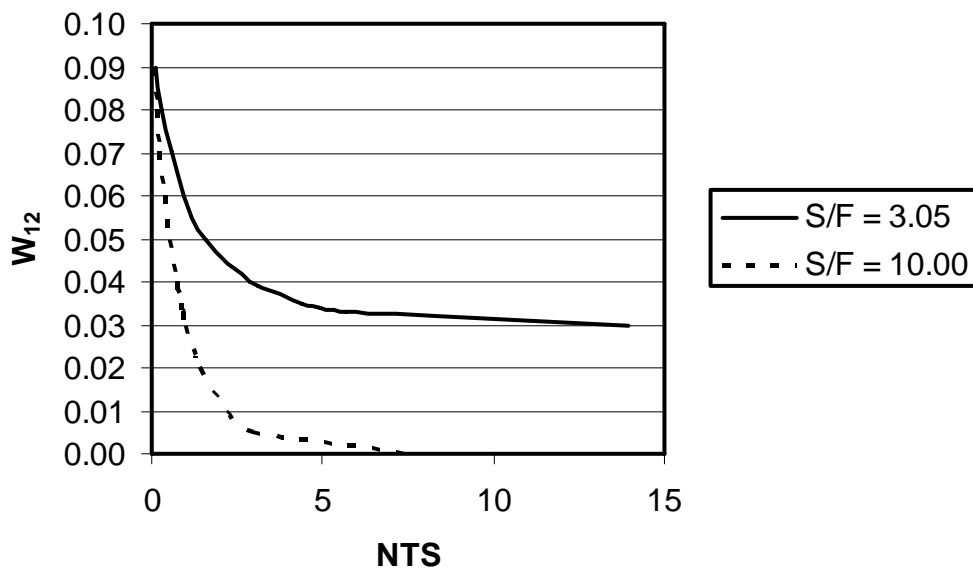


Figure 4.17 1,3-propanediol raffinate mass fraction at 303.15 K as function of NTS used in extraction at different solvent to feed ratio

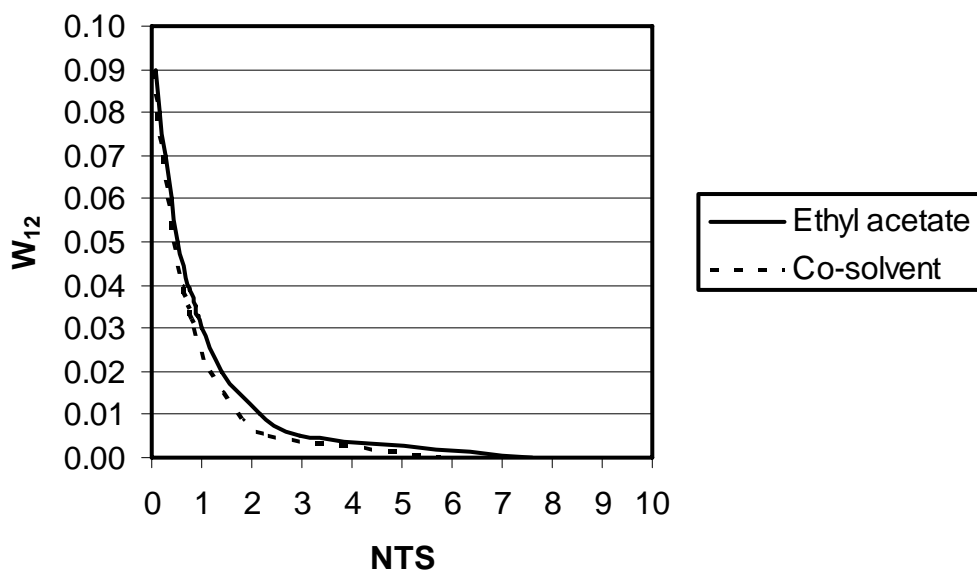


Figure 4.18 1,3-propanediol raffinate mass fraction at 303.15 K as function of NTS used in extraction at different solvent

CHAPTER V

CONCLUSIONS AND RECOMMENDATIONS

5.1 Conclusions

1. From theoretical screening methods, ethyl acetate would be suitable for recovery of 1,3-propanediol from aqueous solution.
2. In this study, ethyl acetate is used in extraction of 1,3-propanediol and the distribution ratio of 1,3-propanediol at 303.15 K is 0.22.
3. The solubility of 1,3-propanediol in ethyl acetate increases as the temperature increases because of the increased molecular motion and thus decreased interactions between 1,3-propanediol molecules.
4. The experimental distribution ratio of 1,3-propanediol decreases when the temperature for extracting 1,3-propanediol from aqueous solution with ethyl acetate increases due to the decrease in molecular interactions between 1,3-propanediol and ethyl acetate and the increase in molecular interactions between 1,3-propanediol and water from hydrogen bonds interactions.
5. The addition of glycerol in feed aqueous stream effects to increase the distribution ratio of 1,3-propanediol; however, the selectivity of extraction decreases when the concentration of glycerol increases.
6. The solvent mixture of ethyl acetate and ethanol can improve the distribution of 1,3-propanediol in solvent phase due to the increase in the polarity of solvent. The distribution ratio of 1,3-propanediol increases as the volume fraction of ethanol increases. Nevertheless, the mutual solubility of solvent mixture increases.
7. In this study, the NTS is 13.9 for decreasing mass fraction of 1,3-propanediol to 0.03 at S/F of 3.05. In order to extract the amount of 1,3-propanediol in raffinate phase completely, the S /F ratio is increased to 10. This extraction requires NTS = 7.6. Furthermore, the solvent mixture of ethyl acetate and ethanol can decrease NTS to 5.8 stages in similar required S/F. Although, the distribution ratio of 1,3-propanediol tends to increase at higher volume fraction of ethanol in solvent mixture, the

mutual solubility of solvent increases. Thus using amount of solvent mixture increases for extracting 1,3-propanediol from aqueous solution.

5.2 Recommendations

1. Using the solvent mixture of ethyl acetate and ethanol to decrease the amount of solvent for extracting 1,3-propanediol should be further studied the optimal volume ratio of solvents on the distribution coefficients and mutual solubility. Furthermore, the effect of glycerol addition, based on the distribution coefficients and selectivity should be investigated. The physical properties, being density, viscosity, and interfacial tension of liquid-liquid systems should be determined to design extraction column diameter and height of column.
2. The effects of the species of blending solvents should be studied and should select as high distribution coefficients and low mutual solubility.
3. The extraction with ethyl acetate tends to increase distribution ratio of 1,3-propanediol with increase in residual glycerol and thus the solvent biocompatible to cells should be considered to decrease products inhibition in fermentation process.
4. From this study, the number of theoretical stages is 7.6 stages at S/F of 10 for complete extracting 1,3-propanediol from aqueous solution at 303.15 K. The column extractor would set up and the efficiency of extraction should be determined.

REFERENCES

- A. Reimann, H. Biebl, W. D. Deckwer. Production of 1,3-propanediol by *Clostridium butyricum* in continuous culture with cell recycling. Appl Microbiol Biotechnol 49 (1998): 359-363.
- A. Reimann, S. Abbad-Andaloussi, H. Biebl and H. Petitdemange 1,3-Propanediol formation with product-tolerant mutants of *Clostridium butyricum* DSM 5431 in continuous culture: productivity, carbon and electron flow. Journal of Applied Microbiology 84 (1998): 1125-1130.
- Ames TT. Process for the isolation of 1,3-propanediol from fermentation broth. US Patent 6.361.983 B1 (2002).
- Avraham M. Baniel, Robert P. Jansen, Asher Vitner, Anthony Baiada. Process for producing 1,3-propanediol. US Patent 7.056.439 B2 (2006).
- Barton, Allan F.M. Handbook of Solubility Parameters, CSC Press, (1983): 153-157
- Corbin DR, Norton T. Process to separate 1,3-propanediol or glycerol, or a mixture thereof from a biological mixture. US Patent 6.603.048 (2003).
- D. Ozman, U. Dramur, B. Tatli. Liquid-liquid equilibria of propionic acid-water-solvent (n-hexane, cyclohexane, cyclohexanol and cyclohexyl acetate) ternaries at 298.15 K. Brazilian journal of chemical engineering 21 (2004): 647-657.
- D.M.T. Newsham, J.D Thornton (Ed). Science and Practice of Liquid-Liquid Extraction, Clarendon, Oxford (1992): 1-39.
- F.S. Mohammad Doulabi, M. Mohsen-Nia, H. Modarres. Measurements and modeling of quaternary (liquid+liquid) equilibria for mixtures of (methanol or ethanol+water+toluene+n-dodecane). J. Chem. Thermodynamics 38 (2006): 405-412.
- Fabien Barborato, El Hassan H., Theirry C., Andre B. 1,3-propanediol production by fermentation: An interesting way to valorize glycerin from the ester and ethanol industries. Industrial Crops and Products 7 (1998): 281-289.
- Fredenslund, Aa., R.L. Jones and J.M. Prausnitz, Group-Contribution Estimation of Activity Coefficients in Nonideal Liquid Mixtures, AIChE J. 21 (1975): 1086-1099.
- G. S. Laddha, T. E. Degaleesan. Transport phenomena in liquid extraction. McGraw-Hill Book Company. New York, (1978): 26-28.

- Hilaly AD, Thomas PB. Method of recovering 1,3-propanediol from fermentation broth. US Patent 6.479.716 (2002).
- John Burke. Solubility Parameter: Theory and Application. AIC Book and Paper Group Annual 3 (1984): 13-58.
- Malinowski J. Evaluation of liquid extraction potentials for downstream separation of 1,3-propanediol. Biotechnology Techniques 13 (1999): 127-130.
- Malinowski J. Reactive extraction for downstream separation of 1,3-propanediol. Biotechnol. Prog. (2000).
- Maria Gonzalez-Pajuelo, I. Meynial-Salles, F. Mendes, J. Carlo Andrade, I. Vasconcelos, P. Soucaille Metabolic of *Clostridium acetobutylicum* for the industrial production of 1,3-propanediol from glycerol. Metabolic Eng. 7 (2005): 329-336.
- Mathijs L., van Delden, Norbert J.M. Kuipers, Andre B. deHaan. Selection and evaluation of alternative solvents for caprolactam extraction. Separation and Purification Technology 51 (2006):219-231.
- Mi-Hae Cho, Sun Im Joen, Sang-Hyun Pyo, Sungyong Mun, Jin-Hyun Kim. A novel separation and purification process for 1,3-propanediol. Process Biochem 41 (2006): 739-744.
- Nicholas P. Cheremisinoff. Industrial solvent handbook. Marcel, Dekker, Inc. New York, (2003): 132-134.
- Othmer, T.F. and Tobias, P.E., Tie line Correlation, Ind. Eng. Chemistry 34 (1942): 693-696.
- Roturier JM, Fouache C, Berghmans E. Process for the purification of 1,3-propanediol from a fermentation medium. US Patent 6.428.992 B1 (2002).
- S. Papanikolaou, P. Ruiz-Sanchez, B. Pariset, F. Blanchard, M. Fick High production of 1,3-propanediol from industrial glycerol by a newly isolated *Clostridium butyricum* strain. Journal of Biotechnology 77 (2000): 191-208.
- S. Saint-Amans, P. Perlot, G. Goma and P. Soucaille High production of 1,3-propanediol by *Clostridium butyricum* VPI 3266 in a simply controlled fed-batch system. Biotechnol. Lett 16 (1994): 831-836.
- Seader J. D., Ernest J. Henley, Separation Process Principles, John Wiley & Sons, Inc. New York (1998): 163-198

Shiguang Li, Vu A. Tuan, John L. Falconer, Richard D. Noble. Separation of 1,3-propanediol from glycerol and glucose using a ZSM-5 zeolite membrane.

J. Membr. Sci. 191 (2001): 53-59

Yan G, Yu T, Xiao-lin W, Li-xin Y, De-hua Liu. The possibility of the desalination of actual 1,3-propanediol fermentation broth by electrodialysis. Desalination 161 (2004): 169-178.

Zeng AP, Biebl H. Bulk chemicals from biotechnology: the case of 1,3-propanediol production and the new trends. Adv Biochem Eng. 74 (2002): 239-5

APPENDICES

APPENDIX A

EXPERIMENTAL DATA

A-1 Standard calibration curve of 1,3-propanediol and glycerol

Table A-1.1 Standard calibration curve data of 1,3-propanediol

Concentration of 1,3-propanediol (g/100ml)	Area			
	Inj.1	Inj.2	Inj.3	Average
1	426902	359365	344561	376943
2	803076	772178	649706	741653
4	1410585	1427405	1505211	1447734
6	2011679	2028409	2021091	2020393
8	2461633	2518310	2487715	2489219

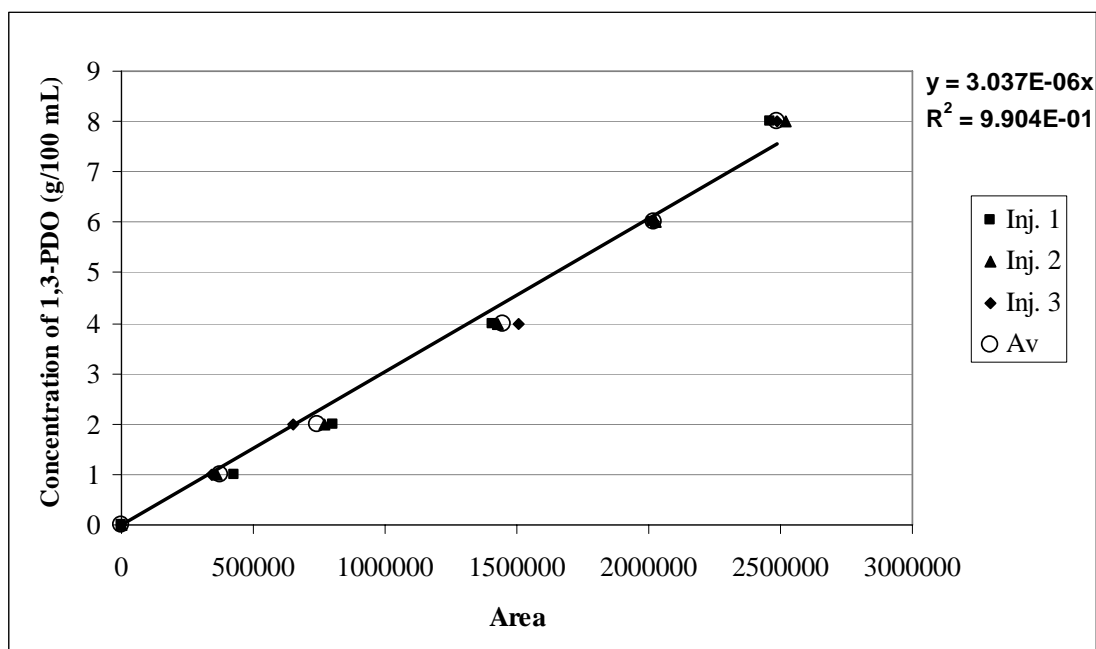


Figure A-1.1 Standard calibration curve of 1,3-propanediol

Table A-1.2 Standard calibration curve data of glycerol

Concentration of Glycerol (g/100 ml)	Area			
	Inj.1	Inj.2	Inj.3	Average
0.5	180495	161682	242749	194975
1	396568	399267	397612	397816
2	641498	663659	690774	665310
4	1367628	1332492	1356125	1352082
6	2112284	2136295	2107288	2118622
8	2886497	2852102	2858824	2865808
10	3583951	3627731	3363714	3525132
12	4243905	4155295	4151364	4183521

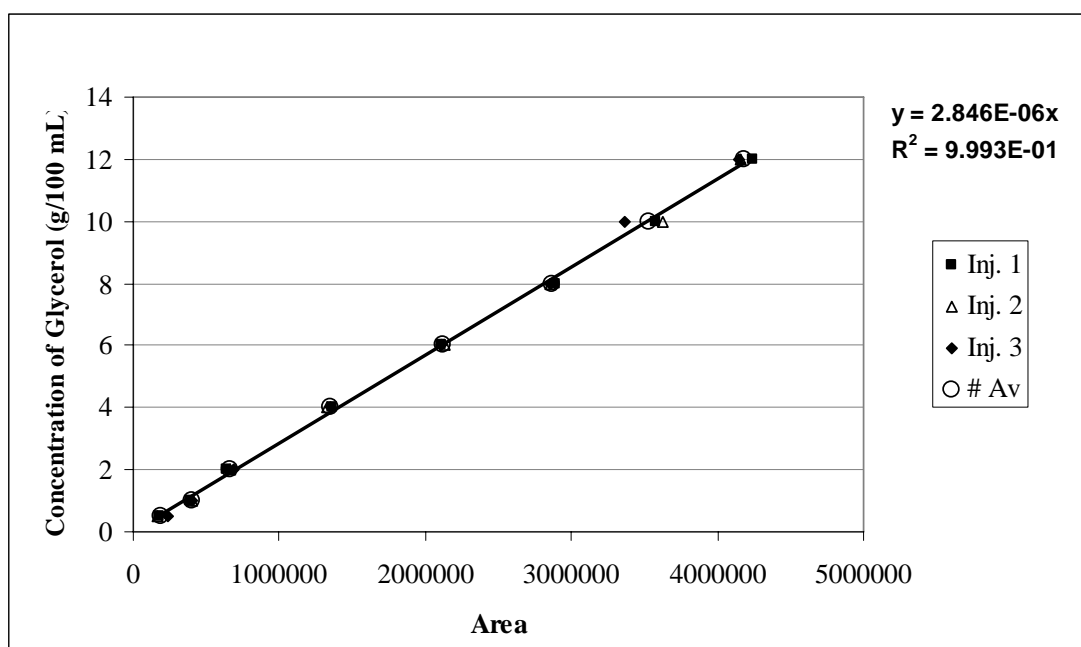


Figure A-1.2 Standard calibration curve of glycerol

A-2 HPLC chromatogram of 1,3-propanediol and glycerol

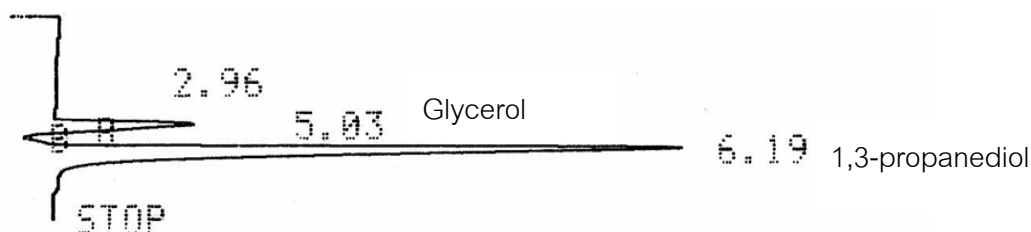


Figure A-2.1 HPLC chromatogram of 1,3-propanediol and glycerol

A-3 Calculating data of liquid-liquid equilibrium of the system using unifac model

Table A-3.1 Liquid-liquid equilibrium of the system 1,3-propanediol (1) + water (2) + ethyl acetate (3) at 303.15 K

Aqueous phase			Organic phase		
1,3-Propanediol	Water	Ethyl Acetate	1,3-Propanediol	Water	Ethyl Acetate
0.0000	0.9833	0.0167	0.0000	0.0210	0.9790
0.1537	0.7973	0.0490	0.0219	0.0277	0.9503
0.2423	0.6597	0.0980	0.0316	0.0309	0.9375
0.2908	0.5513	0.1579	0.0355	0.0321	0.9324
0.3143	0.4642	0.2215	0.0376	0.0326	0.9298
0.3231	0.3930	0.2839	0.0396	0.0331	0.9273
0.3236	0.3341	0.3423	0.0423	0.0335	0.9242
0.3196	0.2845	0.3959	0.0459	0.0339	0.9202
0.3132	0.2424	0.4444	0.0505	0.0343	0.9152
0.3055	0.2062	0.4883	0.0564	0.0346	0.9090
0.2972	0.1748	0.5280	0.0637	0.0349	0.9015
0.2883	0.1473	0.5644	0.0727	0.0351	0.8922
0.2784	0.1230	0.5987	0.0841	0.0353	0.8807
0.2666	0.1013	0.6321	0.0983	0.0357	0.8660
0.2515	0.0819	0.6666	0.1169	0.0365	0.8466
0.2300	0.0645	0.7055	0.1422	0.0387	0.8191
0.2083	0.0495	0.7422	0.2059	0.0495	0.7447

Table A-3.2 Liquid-liquid equilibrium of the system 1,3-propanediol (1) + water (2) + butanol (3) at 303.15 K

Aqueous phase			Organic phase		
1,3-Propanediol	Water	Butanol	1,3-Propanediol	Water	Butanol
0.0000	0.9249	0.0751	0.0000	0.2191	0.7809
0.0451	0.8619	0.0930	0.0540	0.2548	0.6912
0.0878	0.7963	0.1159	0.1027	0.2964	0.6009
0.1265	0.7281	0.1454	0.1434	0.3445	0.5121
0.1594	0.6562	0.1844	0.1738	0.4009	0.4253
0.1835	0.5790	0.2375	0.1906	0.4678	0.3415
0.1919	0.5226	0.2856	0.1915	0.5226	0.2859

A-4 Equilibrium time for extracting 1,3-propanediol

Table A-4.1 Equilibrium time data for extracting 1,3-propanediol and glycerol from aqueous solution with ethyl acetate

No.	Name	Mixing time (min)	Total Volume (mL)	Raffinate Volume (mL)	Weight of Flash (g)	Weight of solution (g)	Weight of evaporated solution (g)
1	Feed 1,3-PDO 60 g/L: glycerol 10 g/L	0	-	20	-	-	-
2	Raffinate phase Exp.1	20	39	19.8	101.4103	121.3839	118.5530
3	Raffinate phase Exp.2	20	39	20	109.4567	129.2080	127.2080
4	Raffinate phase Exp.3	20	39	20.5	109.4552	130.1608	127.8746
5	Raffinate phase Exp.4	40	38	20	101.4093	121.5010	118.8854
6	Raffinate phase Exp.5	40	38	21	109.4565	130.5673	126.9348
7	Raffinate phase Exp.6	40	38.8	21	101.4095	122.7453	119.7553
8	Raffinate phase Exp.7	60	38	22	101.4046	123.6458	119.1951
9	Raffinate phase Exp.8	60	38	21	109.4563	130.4602	127.0577
10	Raffinate phase Exp.9	60	38.5	20.5	101.4104	121.9407	119.7377

Table A-4.2 Mass fraction of 1,3-propanediol and glycerol in raffinate phase at different mixing time

No.	Name	Mixing time (min)	Area (1,3-PDO)	Area (Glycerol)	Mass fraction of 1,3-PDO	Mass fraction of glycerol
1	Feed 1,3-PDO 60 g/L: glycerol 10 g/L	0	1939984	393612	0.059	0.011
2	Raffinate phase Exp.1	20	2044779	378822	0.053	0.009
3	Raffinate phase Exp.2	20	1884255	341482	0.051	0.009
4	Raffinate phase Exp.3	20	1926882	361066	0.052	0.009
5	Raffinate phase Exp.4	40	1888500	368895	0.050	0.009
6	Raffinate phase Exp.5	40	1831368	354361	0.046	0.008
7	Raffinate phase Exp.6	40	1878177	347432	0.049	0.008
8	Raffinate phase Exp.7	60	1926448	378317	0.046	0.009
9	Raffinate phase Exp.8	60	1917164	375886	0.048	0.009
10	Raffinate phase Exp.9	60	1816029	362728	0.049	0.009

A-5 Experimental data of liquid-liquid equilibrium of the 1,3-propanediol-water-ethyl acetate system at 303.15 K

Table A-5 Experimental solubility curve of the system 1,3-propanediol (1) + water (2) + ethyl acetate (3) at 303.15 K

Exp.No.	Aqueous phase			Organic phase		
	Mass (g)			Mass (g)		
	Water	1,3-PDO	EA	Water	1,3-PDO	EA
1	9.95	0.00	0.48	2.09	0.00	10.04
2	9.92	1.02	0.92	1.97	0.22	10.00
3	10.01	3.00	1.15	2.03	0.60	9.93
4	10.04	6.97	3.15	1.90	0.87	9.99
5	4.94	4.96	2.49	2.26	1.21	9.91

A-6 Tie line data of liquid-liquid equilibrium of the 1,3-propanediol-water-ethyl acetate at 303.15 K

Table A-6.1 Experimental tie line data of the system 1,3-propanediol (1) + water (2) + ethyl acetate (3) at 303.15 K

No.	Name	Total Volume (mL)	Raffinate Volume (mL)	Weight of Flash (g)	Weight of solution (g)	Weight of evaporated solution (g)
1	Feed 1,3-PDO 60 g/L	-	20	-	-	-
2	Raffinate phase #1	37.8	18	109.4514	128.0652	126.4518
3	Raffinate phase #2	37	19	109.4501	128.4077	126.4692
4	Feed 1,3-PDO 200 g/L	-	20	-	-	-
5	Raffinate phase #2	38	19.5	109.4497	128.8337	126.9160
6	Raffinate phase #7	38	20	109.4504	129.0014	127.0111
7	Feed 1,3-PDO 300 g/L	-	20	-	-	-
8	Raffinate phase #3	37.5	19	109.4498	128.3136	125.6225
9	Raffinate phase #8	37.8	20	109.4509	129.4300	127.0743
10	Feed 1,3-PDO 400 g/L	-	20	-	-	-
11	Raffinate phase #4	38	20	109.4517	129.7682	127.0879
12	Raffinate phase #9	38	20	109.4512	129.6343	126.9564
13	Feed 1,3-PDO 500 g/L	-	20	-	-	-
14	Raffinate phase #5	37	20	109.4491	129.5072	125.3928
15	Raffinate phase #10	37	20	109.4515	129.5613	126.2055

Table A-6.2 Experimental mass of the system 1,3-propanediol (1) + water (2) + ethyl acetate (3) at 303.15 K in raffinate phase

No.	Name	Area (1,3-PDO)	Mass of PDO (g)	Mass of Ethyl acetate (g)	Mass of Water (g)
1	Feed 1,3-PDO 60 g/L	2013304	1.22		18.84
2	Raffinate phase #1	2062518	1.02	1.61	15.98
3	Raffinate phase #2	2056988	1.05	1.94	15.97
4	Feed 1,3-PDO 200 g/L	1485925	4.51		15.71
5	Raffinate phase #2	1467376	3.87	1.92	13.59
6	Raffinate phase #7	1560989	4.22	1.99	13.34
7	Feed 1,3-PDO 300 g/L	2083744	6.33		13.98
8	Raffinate phase #3	2107349	5.13	2.69	11.05
9	Raffinate phase #8	2040162	5.39	2.36	12.24
10	Feed 1,3-PDO 400 g/L	1546764	9.40		11.07
11	Raffinate phase #4	1495365	7.73	2.68	9.90
12	Raffinate phase #9	1599353	8.27	2.68	9.23
13	Feed 1,3-PDO 500 g/L	1720484	10.45		10.07
14	Raffinate phase #5	1896213	8.89	4.11	7.05
15	Raffinate phase #10	1808280	8.94	3.36	7.81

A-7 Data of the Othmer-Tobias and Hand plot

Table A-7 Experimental tie line data correlation to plot Othmer-Tobias and Hand

Concentration of 1,3-propanediol (g/L)	$\ln[(1-W33)]/w33$	$\ln[(1-w22)]/W22$	$\ln(w13/w33)$	$\ln(w12/w22)$
60	-1.54	-1.74	-4.33	-2.74
200	-1.40	-0.68	-3.02	-1.21
300	-1.30	-0.48	-2.68	-0.91
400	-1.24	-0.02	-2.35	-0.35
500	-1.03	0.53	-2.03	0.18

A-8 Solubility data of 1,3-propanediol in ethyl acetate as function of temperature

Table A-8 Experimental solubility of 1,3-propanediol in ethyl acetate at 303.15 K, 313.15 K, 323.15 K

Ex. No.	Temperature (°C)	Mass (g)		Solubility Of 1,3-propanediol in ethyl acetate (g/L)
		Ethyl acetate	1,3-PDO	
1	30	15.01	1.53	84.61
2	30	15.02	1.68	92.17
3	30	15.00	1.72	93.90
4	40	15.05	2.41	127.04
5	40	15.01	2.45	129.16
6	40	15.02	2.53	132.85
7	50	15.01	3.94	193.45
8	50	15.01	4.05	197.65
9	50	15.00	3.98	194.94

A-9 Calculating data of liquid-liquid equilibrium of the system using unifac model at 313.15 K and 323.15 K

Table A-9.1 Liquid-liquid equilibrium of the system 1,3-propanediol (1) + water (2) + ethyl acetate (3) at 313.15 K

Aqueous phase			Organic phase		
Water	1,3-propanediol	Ethyl acetate	Water	1,3-propanediol	Ethyl acetate
98.127	0	1.873	2.28	0	97.72
79.701	15.123	5.176	3.026	2.352	94.622
65.945	23.962	10.093	3.417	3.488	93.096
55.11	28.821	16.069	3.583	3.988	92.429
46.401	31.168	22.431	3.663	4.26	92.078
39.287	32.009	28.704	3.725	4.508	91.767
33.388	31.979	34.633	3.788	4.815	91.396
28.432	31.457	40.111	3.855	5.216	90.929
24.218	30.661	45.121	3.923	5.732	90.345
20.596	29.711	49.693	3.991	6.384	89.625
17.451	28.657	53.892	4.061	7.2	88.739
14.697	27.501	57.803	4.139	8.217	87.644
12.264	26.197	61.539	4.239	9.495	86.266
10.101	24.645	65.254	4.391	11.133	84.476
8.163	22.635	69.201	4.666	13.301	82.034
7.268	21.331	71.401	4.895	14.661	80.444
5.599	17.039	77.362	5.228	15.95	78.822
5.426	16.697	77.876	5.426	16.691	77.882

Table A-9.2 Liquid-liquid equilibrium of the system 1,3-propanediol (1) + water (2) + ethyl acetate (3) at 323.15 K

Aqueous phase			Organic phase		
Water	1,3-propanediol	Ethyl acetate	Water	1,3-propanediol	Ethyl acetate
97.909	0	2.091	2.461	0	97.539
79.669	14.865	5.465	3.287	2.51	94.203
65.916	23.675	10.408	3.762	3.825	92.413
55.086	28.536	16.378	3.986	4.454	91.56
46.381	30.875	22.744	4.101	4.802	91.097
39.267	31.678	29.055	4.188	5.103	90.709
33.367	31.572	35.061	4.276	5.456	90.267
28.41	30.936	40.654	4.373	5.907	89.72
24.194	29.993	45.813	4.478	6.482	89.04
20.569	28.859	50.571	4.594	7.208	88.198
17.423	27.585	54.992	4.726	8.117	87.157
14.667	26.167	59.166	4.888	9.259	85.854
12.234	24.547	63.219	5.105	10.705	84.191
10.069	22.592	67.338	5.439	12.578	81.983
8.128	19.821	72.051	5.713	14.138	80.149

A-10 Experimental data of liquid-liquid equilibrium of the system using unifac model at 313.15 K and 323.15 K

Table A-10.1 Experimental data of the system 1,3-propanediol (1) + water (2) + ethyl acetate (3) at 313.15 K

No.	Name	T _{Ext.} (°C)	Total Vol. (mL)	Raf. Vol. (mL)	Weight of Flash (g)	Weight of solution (g)	Weight of evaporated solution (g)
C1	Feed 1,3-PDO 60 g/L	-	-	20	-	-	-
1	Raffinate phase #1	40	37.0	20.5	109.4552	129.6108	127.0609
C2	Feed 1,3-PDO 60 g/L	-	-	20	-	-	-
2	Raffinate phase #2	40	35.2	19.5	109.4517	128.6983	126.9326
C3	Feed 1,3-PDO 200 g/L	-	-	20	-	-	-
3	Raffinate phase #1	40	37.5	19.5	109.4617	128.9243	126.8172
C4	Feed 1,3-PDO 200 g/L	-	-	20	-	-	-
4	Raffinate phase #2	40	38.0	19.5	109.4535	129.0695	127.0634
C5	Feed 1,3-PDO 300 g/L	-	-	20	-	-	-
5	Raffinate phase #1	40	37.0	19.5	109.4549	129.0968	126.8095
C6	Feed 1,3-PDO 300 g/L	-	-	20	-	-	-
6	Raffinate phase #2	40	35.5	20.5	109.455	129.77	127.3817
C7	Feed 1,3-PDO 400 g/L	-	-	20	-	-	-
7	Raffinate phase #1	40	37.5	20.5	109.4567	130.0434	126.2404
C8	Feed 1,3-PDO 400 g/L	-	-	20	-	-	-
8	Raffinate phase #2	40	38.0	20.5	109.4552	130.1131	126.9091
C9	Feed 1,3-PDO 500 g/L	-	-	20	-	-	-
9	Raffinate phase #1	40	37.0	20.5	109.4555	130.1313	126.8911
C10	Feed 1,3-PDO 500 g/L	-	-	20	-	-	-
10	Raffinate phase #2	40	36.0	21	109.4545	130.1105	127.2173

Table A-10.2 Experimental mass of the system 1,3-propanediol (1) + water (2) + ethyl acetate (3) at 313.15 K

No.	Name	T _{Ext.} (°C)	Area (1,3- PDO)	Mass of PDO (g)	Mass of Ethyl acetate (g)	Mass of Water (g)
C1	Feed 1,3-PDO 60 g/L	-	1952270	1.19	-	18.87
1	Raffinate phase #1	40	2056438	1.10	2.55	16.50
C2	Feed 1,3-PDO 60 g/L	-	1846254	1.12	-	18.93
2	Raffinate phase #2	40	1953088	1.04	1.77	16.55
C3	Feed 1,3-PDO 200 g/L	-	1429185	4.34	-	15.87
3	Raffinate phase #1	40	1448909	3.78	2.11	13.57
C4	Feed 1,3-PDO 200 g/L	-	1399511	4.25	-	15.96
4	Raffinate phase #2	40	1374287	3.61	2.01	13.85
C5	Feed 1,3-PDO 300 g/L	-	1962598	5.96	-	14.33
5	Raffinate phase #1	40	1979838	5.10	2.29	12.25
C6	Feed 1,3-PDO 300 g/L	-	2058665	6.25	-	14.06
6	Raffinate phase #2	40	2029959	5.50	2.39	12.42
C7	Feed 1,3-PDO 400 g/L	-	1374282	8.35	-	12.06
7	Raffinate phase #1	40	1481674	7.33	3.80	9.32
C8	Feed 1,3-PDO 400 g/L	-	1374282	8.35	-	12.06
8	Raffinate phase #2	40	1405784	7.24	3.20	10.07
C9	Feed 1,3-PDO 500 g/L	-	1661764	10.09	-	10.40
9	Raffinate phase #1	40	1636149	8.40	3.24	8.92
C10	Feed 1,3-PDO 500 g/L	-	1764941	10.72	-	9.81
10	Raffinate phase #2	40	1777210	9.60	2.89	8.16

Table A-10.3 Liquid-liquid equilibrium of the system 1,3-propanediol (1) + water (2) + ethyl acetate (3) at 313.15 K

Exp. No.	Water-rich phase			Solvent-rich phase		
	W ₁₂	W ₂₂	W ₃₂	W ₁₃	W ₂₃	W ₃₃
1,3-Propanediol (1)- Water (2)- Ethyl acetate (3) System						
1	5.476885	81.87204	12.65107	0.542511	15.67296	83.78453
2	5.19786	82.07691	12.72524	0.740459	19.29056	79.96899
3	19.41056	69.76034	10.8291	3.41043	13.90276	82.68681
4	18.57485	71.1167	10.30846	3.761954	12.53494	83.7031
5	26.03861	62.28507	11.67632	5.338803	13.23048	81.43072
6	27.09186	61.15168	11.75645	4.946113	10.78061	84.27328
7	35.83748	45.56508	18.59744	6.486186	17.42929	76.08452
8	35.28411	49.09394	15.62195	6.898023	12.35263	80.74934
9	45.85231	35.90456	18.24314	8.925507	18.15691	72.91758
10	46.4976	39.49582	14.00658	8.065267	11.91286	80.02187

Table A-10.4 Experimental data of the system 1,3-propanediol (1) + water (2) + ethyl acetate (3) at 323.15 K

No.	Name	T _{Ext.} (°C)	Total Vol. (mL)	Raf. Vol. (mL)	Weight of Flash (g)	Weight of solution (g)	Weight of evaporated solution (g)
C1	Feed 1,3-PDO 60 g/L	-	-	20			
1	Raffinate phase #1	50	36	20	109.4551	129.0405	126.9887
C2	Feed 1,3-PDO 60 g/L	-	-	20			
2	Raffinate phase #2	50	37	20	109.4565	129.1217	127.2129
C3	Feed 1,3-PDO 200 g/L	-		20			
3	Raffinate phase #1	50	38	19.4	109.4541	128.8309	127.1165
C4	Feed 1,3-PDO 200 g/L	-		20			
4	Raffinate phase #2	50	37	19	109.4508	128.7738	126.9954
C5	Feed 1,3-PDO 300 g/L	-		20			
5	Raffinate phase #1	50	35.8	20	109.4516	129.3559	127.2450
C6	Feed 1,3-PDO 300 g/L	-		20			
6	Raffinate phase #2	50	37	20	109.4570	129.5028	127.3252
C7	Feed 1,3-PDO 400 g/L	-		20			
7	Raffinate phase #1	50	37	21	109.4560	130.3498	127.2628
C8	Feed 1,3-PDO 400 g/L	-		20			
8	Raffinate phase #2	50	38	21	109.4570	130.3096	127.2846
C9	Feed 1,3-PDO 500 g/L	-		20			
9	Raffinate phase #1	50	35.9	20	109.4557	129.5302	126.8795
C10	Feed 1,3-PDO 500 g/L	-		20			
10	Raffinate phase #2	50	34	21	109.4557	130.5503	127.7694

Table A-10.5 Experimental mass of the system 1,3-propanediol (1) + water (2) + ethyl acetate (3) at 323.15 K

No.	Name	T _{Ext.} (°C)	Area (1,3-PDO)	Mass of PDO (g)	Mass of Ethyl acetate (g)	Mass of Water (g)
C1	Feed 1,3-PDO 60 g/L	-	1952270	1.19		18.87
1	Raffinate phase #1	50	1996298	1.07	2.05	16.46
C2	Feed 1,3-PDO 60 g/L	-	1846254	1.12		18.93
2	Raffinate phase #2	50	1897867	1.03	1.91	16.90
C3	Feed 1,3-PDO 200 g/L	-	1429185	4.34		15.87
3	Raffinate phase #1	50	1417131	3.77	1.71	13.92
C4	Feed 1,3-PDO 200 g/L	-	1429185	4.34		15.87
4	Raffinate phase #2	50	1430585	3.70	1.78	13.51
C5	Feed 1,3-PDO 300 g/L	-	1962598	5.96		14.33
5	Raffinate phase #1	50	2008590	5.39	2.11	12.41
C6	Feed 1,3-PDO 300 g/L	-	2058665	6.25		14.06
6	Raffinate phase #2	50	2115319	5.65	2.18	12.22
C7	Feed 1,3-PDO 400 g/L	-	1374282	8.35		12.06
7	Raffinate phase #1	50	1382698	7.38	3.09	10.56
C8	Feed 1,3-PDO 400 g/L	-	1374282	8.35		12.06
8	Raffinate phase #2	50	1360794	7.29	3.02	10.71
C9	Feed 1,3-PDO 500 g/L	-	1736293	10.55		9.97
9	Raffinate phase #1	50	1810565	9.38	2.65	8.04
C10	Feed 1,3-PDO 500 g/L	-	1557286	9.46		11.01
10	Raffinate phase #2	50	1569494	8.54	2.78	9.80

Table A-10.6 Liquid-liquid equilibrium of the system 1,3-propanediol (1) + water (2) + ethyl acetate (3) at 323.15 K

Exp. No.	Water-rich phase			Solvent-rich phase		
	W ₁₂	W ₂₂	W ₃₂	W ₁₃	W ₂₃	W ₃₃
1,3-Propanediol (1)- Water (2)- Ethyl acetate (3) System						
1	5.464666	84.10308	10.43226	0.757566	15.88539	83.35704
2	5.195269	85.1855	9.619236	0.583019	13.05833	86.35865
3	19.41351	71.74933	8.83716	3.371157	11.46155	85.16729
4	19.48238	71.15252	9.3651	3.867396	14.27048	81.86212
5	27.27033	62.0438	10.68587	3.94979	14.28941	81.7608
6	28.18297	60.9539	10.86312	3.868474	11.7781	84.35343
7	35.10427	50.21636	14.67937	6.575014	10.20812	83.21687
8	34.67937	50.93769	14.38294	6.763154	8.641152	84.59569
9	46.73946	40.05622	13.20431	7.926079	13.14967	78.92425
10	40.44184	46.39105	13.1671	7.672801	10.10054	82.22666

A-11 Experimental data of glycerol addition in feed aqueous stream

Table A-11.1 Experimental data for extraction of 1,3-propanediol from aqueous solution with glycerol at mass ratio of 60 1,3-PDO/12 glycerol

No.	Name	Total Vol. (mL)	Raf. Vol. (mL)	Weight of Flash (g)	Weight of solution (g)	Weight of evaporated solution (g)
1	Feed 1,3-PDO 60 g/L: glycerol 12 g/L	-	20	-	-	-
G1	Raffinate phase #1	39	21	109.4483	130.0389	127.9525
G1R	Raffinate phase #2	38	21	109.4511	129.9361	127.9588
2	Feed 1,3-PDO 200 g/L: glycerol 40 g/L		20	-	-	-
G2	Raffinate phase #3	37.5	20	109.4500	129.4889	127.4982
2R	Feed 1,3-PDO 200 g/L: glycerol 40 g/L		20	-	-	-
G2R	Raffinate phase #4	38	19.5	109.4507	129.2362	127.3798
3	Feed 1,3-PDO 300 g/L: glycerol 60 g/L		20	-	-	-
G3	Raffinate phase #5	37.8	19.5	109.4493	129.3872	127.6264
G3R	Raffinate phase #6	38	20	109.4496	129.2796	127.3131
4	Feed 1,3-PDO 400 g/L: glycerol 80 g/L	-	20	-	-	-
G4	Raffinate phase #7	36.5	19	109.4493	129.1467	127.0888
G4R	Raffinate phase #8	37	19	109.4428	128.8444	126.7181
5	Feed 1,3-PDO 500 g/L: glycerol 100 g/L	-	20	-	-	-
G5	Raffinate phase #9	37	19	109.4428	129.3210	127.0167
G5R	Raffinate phase #10	37	20	109.4519	130.2624	127.5349

Table A-11.2 Experimental mass for system of 1,3-propanediol with glycerol in feed stream at mass ratio of 60 1,3-PDO/12 glycerol

No.	Name	Area (1,3-PDO)	Area (Glycerol)	Mass of PDO (g)	Mass of Gly. (g)	Mass of Ethyl acetate (g)	Mass of Water (g)
1	Feed 1,3-PDO 60 g/L: glycerol 12 g/L	1922838	433234	1.17	0.25	-	18.69
G1	Raffinate phase #1	1922470	454213	1.09	0.24	2.09	17.17
G1R	Raffinate phase #2	1885941	452035	1.08	0.24	1.98	17.19
2	Feed 1,3-PDO 200 g/L: glycerol 40 g/L	1340486	271332	4.07	0.77	-	15.52
G2	Raffinate phase #3	1321395	279922	3.57	0.71	1.99	13.77
2R	Feed 1,3-PDO 200 g/L: glycerol 40 g/L	1442614	322487	4.38	0.92	-	15.11
G2R	Raffinate phase #4	1383237	341582	3.66	0.85	1.86	13.42
3	Feed 1,3-PDO 300 g/L: glycerol 60 g/L	1901729	446939	5.78	1.27	-	13.50
G3	Raffinate phase #5	1754643	428510	4.68	1.07	1.76	12.43
G3R	Raffinate phase #6	1768878	426254	4.79	1.08	1.97	12.00
4	Feed 1,3-PDO 400 g/L: glycerol 80 g/L	1277332	252173	7.76	1.44	-	11.49
G4	Raffinate phase #7	1291572	276040	6.56	1.31	2.06	9.77
G4R	Raffinate phase #8	1305354	266522	6.60	1.26	2.13	9.41
5	Feed 1,3-PDO 500 g/L: glycerol 100 g/L	1594808	342535	9.69	1.95	-	9.24
G5	Raffinate phase #9	1533677	346279	7.66	1.62	2.30	8.29
G5R	Raffinate phase #10	1602748	369727	8.26	1.79	2.73	8.03

Table A-11.3 Liquid-liquid equilibrium of the system 1,3-propanediol (1) + water (2) + ethyl acetate (3) + glycerol (4) at 303.15 K at mass ratio of 60 1,3-PDO/12 glycerol

Exp. No.	Water-rich phase				Solvent-rich phase			
	W ₁₂	W ₄₂	W ₂₂	W ₃₂	W ₁₃	W ₄₃	W ₂₃	W ₃₃
1,3-Propanediol (1)- Water (2)- Ethyl acetate (3)- Glycerol (4) System								
1	5.30	1.17	83.39	10.13	0.47	0.03	9.29	90.21
2	5.26	1.18	83.91	9.65	0.59	0.03	9.72	89.67
3	17.82	3.54	68.71	9.93	3.12	0.40	10.90	85.59
4	18.52	4.28	67.81	9.38	4.23	0.41	9.95	85.41
5	23.45	5.37	62.35	8.83	6.54	1.20	6.36	85.90
6	24.14	5.45	60.49	9.92	5.97	1.15	9.08	83.80
7	33.30	6.67	49.59	10.45	7.43	0.75	10.63	81.18
8	34.01	6.51	48.52	10.96	6.97	1.04	12.44	79.55
9	38.54	8.15	41.72	11.59	12.13	1.97	5.70	80.20
10	39.71	8.58	38.60	13.11	9.07	1.04	7.72	82.17

Table A-11.4 Experimental data for extraction of 1,3-propanediol from aqueous solution with glycerol at mass ratio of 60 1,3-PDO/8 glycerol

No.	Name	Total Vol. (mL)	Raf. Vol. (mL)	Weight of Flash (g)	Weight of solution (g)	Weight of evaporated solution (g)
6	Feed 1,3-PDO 60 g/L: glycerol 8 g/L	-	20	-	-	-
G6	Raffinate phase #1	38	20	109.4534	129.1375	124.9944
G6R	Raffinate phase #2	38	20	109.4513	129.0213	126.6219
7	Feed 1,3-PDO 200 g/L: glycerol 26.7 g/L	-	20	-	-	-
G7	Raffinate phase #3	38	19.5	109.4533	129.0398	127.0873
G7R	Raffinate phase #4	38	20	109.4538	129.3507	127.3893
8	Feed 1,3-PDO 300 g/L: glycerol 40 g/L		20	-	-	-
G8	Raffinate phase #5	37	19.5	109.4498	128.9498	127.0952
G8R	Raffinate phase #6	38	19.5	109.4520	129.2214	127.2292
9	Feed 1,3-PDO 400 g/L: glycerol 53.3 g/L	-	20	-	-	-
G9	Raffinate phase #7	38	21	109.4534	130.0202	127.5549
G9R	Raffinate phase #8	38.5	20	109.4535	129.8904	127.5181
10	Feed 1,3-PDO 500 g/L:glycerol 66.67 g/L	-	20	-	-	-
G10	Raffinate phase #9	36	19.5	109.4497	129.1203	126.4946
G10R	Raffinate phase #10	37	19.5	109.4541	129.0291	126.5806

Table A-11.5 Experimental mass for system of 1,3-propanediol with glycerol in feed stream at mass ratio of 60 1,3-PDO/8 glycerol

No.	Name	Area (1,3-PDO)	Area (Glycerol)	Mass of PDO (g)	Mass of Gly. (g)	Mass of Ethyl acetate (g)	Mass of Water (g)
6	Feed 1,3-PDO 60 g/L: glycerol 8 g/L	1809295	262968	1.10	0.15		18.84
G6	Raffinate phase #1	2026110	303389	0.95	0.13	4.14	14.46
G6R	Raffinate phase #2	1837910	285480	0.97	0.14	2.40	16.06
7	Feed 1,3-PDO 200 g/L: glycerol 26.7 g/L	1293404	251775	3.93	0.72		15.70
G7	Raffinate phase #3	1268680	236761	3.34	0.58	1.95	13.71
G7R	Raffinate phase #4	1247808	229392	3.38	0.58	1.96	13.98
8	Feed 1,3-PDO 300 g/L: glycerol 40 g/L	1878418	272208	5.71	0.77		13.96
G8	Raffinate phase #5	1827539	280678	4.84	0.70	1.85	12.11
G8R	Raffinate phase #6	1823938	271343	4.79	0.67	1.99	12.32
9	Feed 1,3-PDO 400 g/L: glycerol 53.3 g/L	1336831	244980	8.12	1.39		11.17
G9	Raffinate phase #7	1272973	252865	7.06	1.31	2.47	9.72
G9R	Raffinate phase #8	1237008	243011	6.53	1.20	2.37	10.34
10	Feed 1,3-PDO 500 g/L: glycerol 66.67 g/L	1545145	290369	9.39	1.65		9.77
G10	Raffinate phase #9	1545676	298742	7.79	1.41	2.63	7.85
G10R	Raffinate phase #10	1561893	284933	7.96	1.36	2.45	7.80

Table A-11.6 Liquid-liquid equilibrium of the system 1,3-propanediol (1) + water (2) + ethyl acetate (3) + glycerol (4) at 303.15 K at mass ratio of 60 1,3-PDO/8 glycerol

Exp. No.	Water-rich phase				Solvent-rich phase			
	W ₁₂	W ₄₂	W ₂₂	W ₃₂	W ₁₃	W ₄₃	W ₂₃	W ₃₃
1,3-Propanediol (1)- Water (2)- Ethyl acetate (3)- Glycerol (4) System								
1	4.82	0.68	73.46	21.05	0.90	0.10	26.22	72.77
2	4.95	0.72	82.07	12.26	0.79	0.05	16.79	82.37
3	17.05	2.98	70.00	9.97	3.46	0.78	11.69	84.07
4	16.98	2.92	70.24	9.86	3.33	0.82	10.42	85.43
5	24.83	3.57	62.09	9.51	5.36	0.48	11.51	82.64
6	24.23	3.38	62.32	10.08	5.38	0.63	9.66	84.33
7	34.34	6.39	47.28	11.99	6.76	0.51	9.27	83.46
8	31.93	5.88	50.58	11.61	9.35	1.13	4.91	84.60
9	39.59	7.17	39.89	13.35	10.40	1.58	12.50	75.53
10	40.68	6.95	39.86	12.51	8.75	1.79	12.08	77.38

Table A-11.7 Experimental data for extraction of 1,3-propanediol from aqueous solution with glycerol at mass ratio of 60 1,3-PDO/4 glycerol

No.	Name	Total Vol. (mL)	Raf. Vol. (mL)	Weight of Flash (g)	Weight of solution (g)	Weight of evaporated solution (g)
11	Feed 1,3-PDO 60 g/L: glycerol 4 g/L	-	20	-	-	-
G11	Raffinate phase #1	37.8	19.3	109.4543	129.1123	126.2308
G11R	Raffinate phase #2	38	20	109.4523	129.0362	125.7825
12	Feed 1,3-PDO 200 g/L: glycerol 13.33 g/L	-	20	-	-	-
G12	Raffinate phase #3	38	21	109.4536	129.8739	127.8501
G12R	Raffinate phase #4	38	21	109.4527	129.9218	127.7479
13	Feed 1,3-PDO 300 g/L: glycerol 20 g/L		20			
G13	Raffinate phase #5	37.2	20.5	109.4503	129.8802	127.3711
G13R	Raffinate phase #6	38	20.5	109.4531	129.8655	127.4859
14	Feed 1,3-PDO 400 g/L: glycerol 26.67 g/L	-	20			
G14	Raffinate phase #7	37.5	19.7	109.4521	129.1495	126.9481
G14R	Raffinate phase #8	37.5	20	109.4533	129.2236	126.8418
15	Feed 1,3-PDO 500 g/L: glycerol 33.33 g/L	-	20	-	-	-
G15	Raffinate phase #9	38	21	109.4549	130.5616	126.7887
G15R	Raffinate phase #10	37	21	109.4543	130.4668	127.3975

Table A-11.8 Experimental mass for system of 1,3-propanediol with glycerol in feed stream at mass ratio of 60 1,3-PDO/4 glycerol

No.	Name	Area (1,3-PDO)	Area (Glycerol)	Mass of PDO (g)	Mass of Gly. (g)	Mass of Ethyl acetate (g)	Mass of Water (g)
11	Feed 1,3-PDO 60 g/L: glycerol 4 g/L	1829071	197592	1.11	0.11		18.85
G11	Raffinate phase #1	1978291	203686	0.97	0.09	2.88	15.72
G11R	Raffinate phase #2	1966363	208924	0.98	0.10	3.25	15.25
12	Feed 1,3-PDO 200 g/L: glycerol 13.33 g/L	1523764	170981	4.63	0.49		15.21
G12	Raffinate phase #3	1442382	157948	4.11	0.42	2.02	13.87
G12R	Raffinate phase #4	1534586	153369	4.33	0.41	2.17	13.56
13	Feed 1,3-PDO 300 g/L: glycerol 20 g/L	1897893	133483	5.76	0.38		14.22
G13	Raffinate phase #5	1808617	128363	4.87	0.32	2.51	12.73
G13R	Raffinate phase #6	1857804	134450	5.04	0.34	2.38	12.65
14	Feed 1,3-PDO 400 g/L: glycerol 26.67 g/L	1284313	144863	7.80	0.82		11.93
G14	Raffinate phase #7	1288847	156620	6.76	0.77	2.20	9.97
G14R	Raffinate phase #8	1307261	156097	6.89	0.77	2.38	9.72
15	Feed 1,3-PDO 500 g/L: glycerol 33.33 g/L	1546353	170731	9.39	0.97		10.30
G15	Raffinate phase #9	1531116	180827	7.82	0.87	3.77	8.65
G15R	Raffinate phase #10	1522615	181330	8.14	0.91	3.07	8.90

Table A-11.9 Liquid-liquid equilibrium of the system 1,3-propanediol (1) + water (2) + ethyl acetate (3) + glycerol (4) at 303.15 K at mass ratio of 60 1,3-PDO/4 glycerol

Exp. No.	Water-rich phase				Solvent-rich phase			
	W ₁₂	W ₄₂	W ₂₂	W ₃₂	W ₁₃	W ₄₃	W ₂₃	W ₃₃
1,3-Propanediol (1)- Water (2)- Ethyl acetate (3)- Glycerol (4) System								
1	4.92	0.47	79.94	14.66	0.84	0.11	18.44	80.60
2	5.00	0.50	77.89	16.61	0.79	0.09	21.68	77.44
3	20.12	2.06	67.90	9.91	3.34	0.42	8.67	87.58
4	21.17	1.98	66.23	10.62	1.90	0.52	10.65	86.93
5	23.82	1.58	62.31	12.28	5.85	0.37	9.70	84.09
6	24.69	1.67	61.98	11.66	4.52	0.24	9.77	85.48
7	34.30	3.91	50.62	11.18	6.37	0.34	11.94	81.35
8	34.86	3.90	49.19	12.05	5.63	0.33	13.66	80.38
9	36.61	4.05	41.68	17.66	9.86	0.67	8.74	80.74
10	38.26	4.27	43.04	14.43	8.38	0.43	7.65	83.54

A-12 Experimental data of 1,3-propanediol extraction with solvent mixture of ethyl acetate and ethanol

Table A-12.1 Experimental data for extraction of 1,3-propanediol from aqueous solution with solvent mixture at volume ratio 95:5 and 90:10 (ethyl acetate:ethanol)

No.	Name	Total Vol (mL)	Raf Volume (mL)	Weight of Flash (g)	Weight of solution (g)	Weight of evaporated solution (g)
a	Feed 1,3-PDO 60 g/L	-	20	-	-	-
1	Volume ratio = 95:5	36.5	20.5	109.4567	129.6317	126.9043
2	Volume ratio = 90:10	37.5	21	109.4537	130.2319	127.4485
b	Feed 1,3-PDO 200 g/L	-	20	-	-	-
1	Volume ratio = 95:5	36.9	20	109.4570	129.4089	126.3874
2	Volume ratio = 90:10	42	26	109.4550	135.5131	131.8833
c	Feed 1,3-PDO 300 g/L	-	20	-	-	-
1	Volume ratio = 95:5	38	21.5	109.4570	130.6175	127.4367
2	Volume ratio = 90:10	38	22	109.4598	131.0843	127.4268

Table A-12.2 Experimental mass for 1,3-propanediol + water + solvent mixture system at volume ratio 95:5 and 90:10 (ethyl acetate:ethanol)

No.	Name	Area (1,3-PDO)	Mass of PDO (g)	Mass of Ethyl acetate (g)	Mass of Water (g)
a	Feed 1,3-PDO 60 g/L	2125453	1.29	-	18.77
1	Ex-Ea:Et = 95:5	1903314	1.01	2.73	16.52
2	Ex-Ea:Et = 90:10	1794336	0.98	2.78	16.99
b	Feed 1,3-PDO 200 g/L	1363192	4.14	-	16.06
1	Ex-Ea:Et = 95:5	1341693	3.39	3.02	13.43
2	Ex-Ea:Et = 90:10	1334220	4.45	3.63	17.74
c	Feed 1,3-PDO 300 g/L	1923474	5.84	-	14.45
1	Ex-Ea:Et = 95:5	1779985	4.86	3.18	13.36
2	Ex-Ea:Et = 90:10	1740394	4.74	3.66	13.44

Table A-12.3 Liquid-liquid equilibrium of the system 1,3-propanediol (1) + water (2)
+ solvent mixture (3) at 303.15 K

Exp. No.	Water-rich phase			Solvent-rich phase		
	W_{12}	W_{22}	W_{32}	W_{13}	W_{23}	W_{33}
1,3-Propanediol (1)- Water (2)- Ethyl acetate (3) System						
1	4.988371	81.54539	13.46624	1.880572	15.11157	83.00786
2	4.706214	81.87713	13.41666	2.051816	11.64345	86.30473
3	17.10079	67.66943	15.22978	4.791207	16.90612	78.30268
4	15.54374	66.92499	17.53127	4.357648	15.24037	80.40198
5	22.71015	62.42253	14.86732	6.501028	7.213298	86.28567
6	21.72059	61.53037	16.74904	7.483939	6.876446	85.63961

APPENDIX B

DATA CALCULATION

B-1 Experimental equilibrium compositions calculation

In this experiment, the total volume and raffinate volume after extraction were measured as shown in Table A-6.1. The 1,3-propanediol in aqueous solution was extracted with ethyl acetate at 303.15 K and then the raffinate phase was separated from extraction mixture. The raffinate phase was evaporated to separate ethyl acetate from aqueous solution; moreover, the mass of ethyl acetate was measured. Finally, the raffinate phase was analyzed for determining the concentration of 1,3-propanediol. The mass fraction and distribution ratio of 1,3-propanediol can be calculated and presented in following step.

From Table A-6.1, Total volume, $V_{\text{tol}} = 37.8 \text{ mL}$

Raffinate volume, $V_{\text{raf}} = 18 \text{ mL}$

Mass of ethyl acetate, $m_{\text{EA}} = 1.61 \text{ g}$

Raffinate volume after evaporation, $V_{\text{raf, ev}} = V_{\text{raf}} - m_{\text{EA}} / \rho_{\text{EA}}$
 $\rho_{\text{EA}} = 0.902 \text{ g/mL};$ $= 18 - (1.61/0.902)$

So, $V_{\text{raf, ev}} = 16.21 \text{ mL}$

From Table A-6.2, Area of 1,3-propanediol in raffinate = 2062518

From Figure A-1.1, Concentration of 1,3-propanediol = 62.65 g/mL

Thus, Mass of PDO in raffinate, $m_{\text{pdo, raf}} = 62.65 \text{ g/mL} * 16.21 \text{ mL}$
 $= 1.02 \text{ g}$

Mass of water in raffinate, $m_{\text{aq, raf}} = (V_{\text{raf, ev}} - (m_{\text{pdo, raf}} / \rho_{\text{pdo}})) * \rho_{\text{water}}$
 $\rho_{\text{pdo}} = 1.052 \text{ g/ml}, \rho_{\text{water}} = 1 \text{ g/mL};$

$$m_{\text{aq, raf}} = (16.21 - (1.02/1.052)) * 1$$

$$= 15.98 \text{ g}$$

Thus, Total mass in raffinate phase, $m_{\text{tol, raf}} = 1.61 + 1.02 + 15.98 = 18.61 \text{ g}$

Mass fraction of 1,3-PDO in raffinate phase, $w_{\text{pdo, raf}} = 1.02/18.61 = 0.55$

From Table A-6.2, Area of 1,3-propanediol in feed = 2013304

Mass of 1,3-propanediol in feed = 1.22 g

Mass of water in feed = 18.84 g

From mass balance, Mass of 1,3-propanediol in extract, $m_{\text{pdo,ext}} = 1.22 - 1.02 = 0.19 \text{ g}$

Mass of water in extract, $m_{\text{aq,ext}} = 18.84 - 15.98 = 2.86 \text{ g}$

From Table A-6.1, Extract volume, $V_{\text{ext}} = 37.8 - 18 = 19.8 \text{ mL}$

Mass of ethyl acetate in extract, $m_{\text{EA,ext}} = (V_{\text{ext}} - (m_{\text{pdo,ext}}/\rho_{\text{pdo}}) - (m_{\text{aq,ext}}/\rho_{\text{water}})) * \rho_{\text{EA}}$

$$= (19.8 - (0.19/1.052) - (2.86/1)) * 0.902$$

$$m_{\text{EA,ext}} = 15.11 \text{ g}$$

Total mass in extract phase = $0.19 + 2.86 + 15.11 = 18.17 \text{ g}$

Mass fraction of 1,3-PDO in extract phase, $w_{\text{pdo,ext}} = 0.19/18.17 = 0.11 \text{ g}$

Thus, The distribution ratio = $w_{\text{pdo,ext}}/w_{\text{pdo,raf}} = 0.11/0.55 = 0.21$

B-2 Calculation of the number of theoretical stages

B-2.1 Determine the minimum solvent-to-feed ratio (S/F)_{min}

This calculation needs to be completed since the extract composition, E_1 needs to be found. This procedure begins by drawing an operating line from S to R. The raffinate composition, R in this work is 0.01 as shown in Figure B-2.1. Next, each tie line is considered to be a pinch point, and a line drawn from each tie line to the operating line is designated a P_1, P_2, \dots, P_n . The farthest away from R is called P_{min} . After P_{min} has been established, a line is drawn from P_{min} through the feed composition, F on the other side of the equilibrium curve to obtain E_1 . The feed composition, F is synthesized from fermentation broth and is 0.1 as shown in Figure B-2.1. In this study, the mass fraction of 1,3-propanediol in raffinate stream, $x_{1,3\text{-pdo,R}}$ is 0.01 and the mass fraction of 1,3-propanediol in solvent stream, $x_{1,3\text{-pdo,S}}$ is 0. After E_1 is known, a mass balance around the system can be utilized to determine the mixing point, m as shown in the Figure B-2.2. The mass fraction of 1,3-propanediol at the mixing point, $x_{1,3\text{-pdo,m}}$ is 0.35.

From mass balance, $F + S_{\text{min}} = R + E_1 = M$

Solving for S/F_{min} , we will obtain the minimum solvent-to feed ratio as

$$\begin{aligned} \frac{S_{\text{min}}}{F} &= \frac{(x_{1,3\text{-pdo,F}} - x_{1,3\text{-pdo,m}})}{(x_{1,3\text{-pdo,m}} - x_{1,3\text{-pdo,S}})} \\ &= \frac{(0.1 - 0.35)}{(0.35 - 0)} \\ &= 2.03 \end{aligned}$$

So, The minimum solvent-to-feed ratio is 2.03

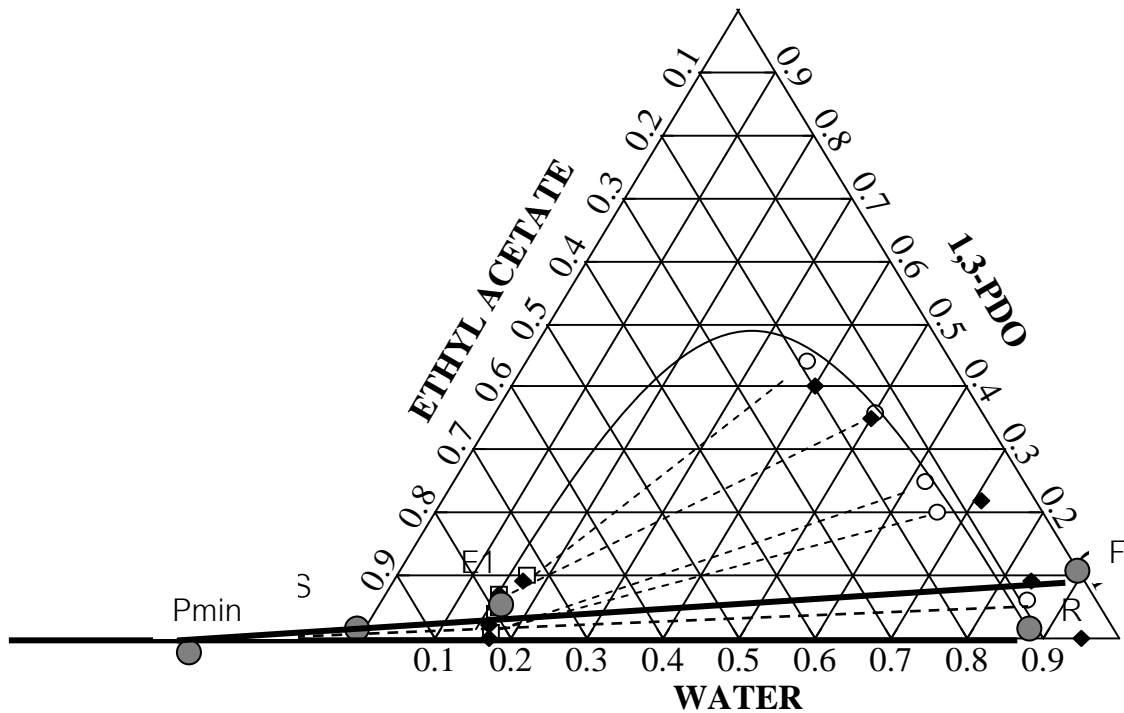


Figure B-2.1 Ternary Diagram of 1,3-PDO+water+ethyl acetate system used to calculate P_{\min} for designing an extractor

Generally, a solvent-to-feed ratio for an extraction system is 1.5 times S/F_{\min} :

$$\begin{aligned} (S/F)_{\text{actual}} &= 1.5(S/F)_{\min} \\ &= 1.5 * 2.03 \\ &= 3.05 \end{aligned}$$

Thus, The actual solvent-to-feed ratio is 3.05

From equation 2.16 (Kremser equation),

$$N = \frac{\ln \left[\left(\frac{X_f - Y_s/m}{X_r - Y_s/m} \right) \left(1 - \frac{1}{E} \right) + \frac{1}{E} \right]}{\ln E} \quad (2.16)$$

The extraction factor, $E = \text{the distribution ratio, } K * (S/F)$

From the experiments of 1,3-propanediol extraction with ethyl acetate,

We obtained the distribution ratio of 1,3-propanediol, $K_{1,3\text{-PDO}} = 0.22$

Then, The extraction factor = $0.22 * 3.05$

$$= 0.671$$

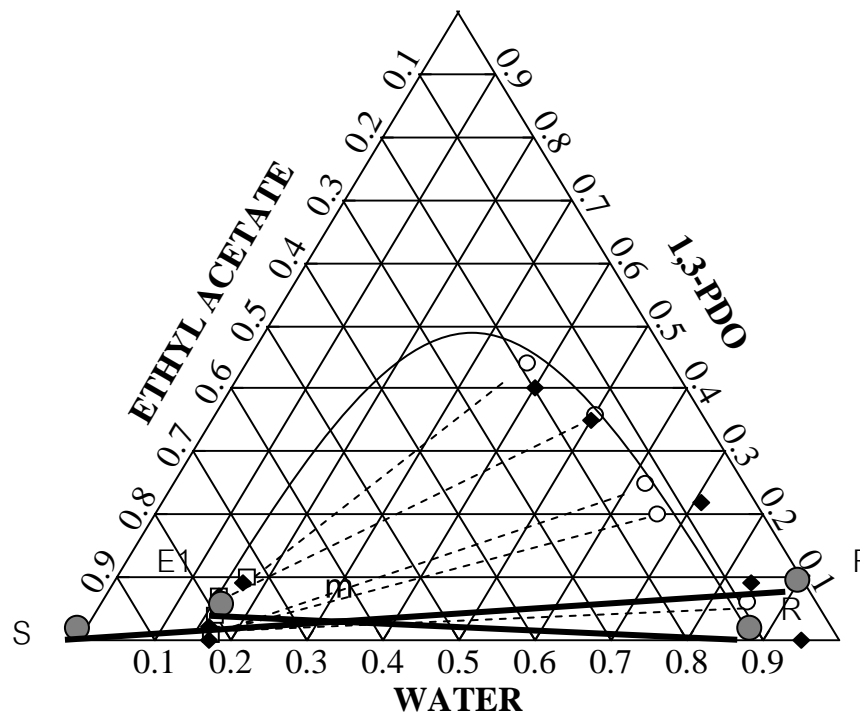


Figure B-2.2 Ternary Diagram of 1,3-PDO+water+ethyl acetate system showing the mixing point based on the $(S/F)_{\min}$, m

In this equation,

The mass fraction of 1,3-propanediol in feed, $X_f = 0.1$

The mass fraction of 1,3-propanediol in solvent, $Y_s = 0$

To determine the number of theoretical stages, NTS, the mass fraction of 1,3-propanediol in raffinate, X_r was plotted with NTS at constant S/F by Kremser equation.

B-3 Error analysis

In experimental work, we frequently plot one variable, such as y , against another, such as x , and then wish to develop an equation that expresses y as a function of x and there are m sets of data points (x_i, y_i) . Our goal in this section in this section is to represent the points by drawing the straight line $y = a + bx$ through them. Thus, we wish to determine suitable values for the intercept a and the slope b , together with a value for the variance σ^2 that indicates how much scatter there is of the y values about

the regression line. We assume that the x_i are known precisely, whereas the y_i are distributed as

$$(N(\alpha + \beta x_i, \sigma^2)) \quad (\text{B.1})$$

mean

That is, the y values are normally distributed about the regression line $y = \alpha + \beta x$ with (constant) variance σ^2 . In this study, x could be the mass fraction of 1,3-propanediol in aqueous phase and y could be the mass fraction of 1,3-propanediol in extract phase at three different temperatures. The regression line is then considered to be the best representation of the data points if the sum of squares of the deviations from the regression line:

$$S = \sum_{i=1}^m (y_i - \alpha - \beta x_i)^2 \quad (\text{B.2})$$

The sum S of squares of the deviations is minimized when its derivatives with respect to α and β are each equated to zero:

$$\frac{\partial S}{\partial \alpha} = -2 \sum_{i=1}^m (y_i - \alpha - \beta x_i) = 0 \quad (\text{B.3})$$

$$\frac{\partial S}{\partial \beta} = -2 \sum_{i=1}^m x_i (y_i - \alpha - \beta x_i) = 0 \quad (\text{B.4})$$

Replacing the model parameters α and β by their estimates a and b , and rearranging, we obtain the simultaneous normal equations in a and b :

$$ma + b \sum_{i=1}^m x_i = \sum_{i=1}^m y_i \quad (\text{B.5})$$

$$a \sum_{i=1}^m x_i + b \sum_{i=1}^m x_i^2 = \sum_{i=1}^m x_i y_i \quad (\text{B.6})$$

Solution of the simultaneous normal equations, (B.5), (B.6), gives:

Slope:
$$b = \frac{m \sum_{i=1}^m x_i y_i - \sum_{i=1}^m x_i \sum_{i=1}^m y_i}{m \sum_{i=1}^m x_i^2 - (\sum_{i=1}^m x_i)^2} \quad (\text{B.7})$$

Intercept:
$$a = \frac{1}{m} \left(\sum_{i=1}^m y_i - b \sum_{i=1}^m x_i \right) \quad (\text{B.8})$$

It can also be shown that the estimate of the variance σ^2 of the y values about the regression line is:

$$\begin{aligned}
s^2 &= \frac{1}{m-2} \sum_{i=1}^m (y_i - a - bx_i)^2 \\
&= \frac{1}{m-2} \left(\sum_{i=1}^m y_i - a \sum_{i=1}^m 1 - b \sum_{i=1}^m x_i \right)^2
\end{aligned} \tag{B.9}$$

Assuming the y_i are independent, the mean and variance of b are given by

$$\mu = \sum_{i=1}^m a_i \mu_i \tag{B.10}$$

$$\sigma^2 = \sum_{i=1}^m a_i^2 \sigma_i^2 \tag{B.11}$$

in which μ_i and σ_i^2 are the means and variances of the individual y_i . Equations (B.10) and (B.11) will now be used to find the means and variances of the slope b and intercept a of regression.

So
$$\sigma_b^2 = \frac{\sigma^2}{\sum_{i=1}^m (x_i - \bar{x})^2} \tag{B.12}$$

$$\sigma_a^2 = \frac{\sigma^2 \sum_{i=1}^m x_i^2}{m \sum_{i=1}^m (x_i - \bar{x})^2} \tag{B.13}$$

where σ_b^2 is the variances of the slope b and σ_a^2 is the variances of the intercept a .

The results of error analysis calculation were shown in Table B-3. The slopes of this linear regression which are to the distribution ratio of 1,3-propanediol tend to increase about 0.03 when the temperature decreases from 313.15 K to 303.15 K. However, the variance increases as the increase temperature.

Table B-3 Error analysis of experimental results from the effect of temperature

Temperature (K)	303.15	313.15	323.15
Slope: b	0.220	0.192	0.185
Intercept: a	-0.219	-0.170	-0.323
Variance: σ^2	0.044	0.155	0.380
Variance: σ_a^2	0.008	0.015	0.036
Variance: σ_b^2	4.2E-07	2.6E-06	1.6E-05
$K_{1,3-PDO}$	0.220±4.2E-07	0.192±2.6E-06	0.185±1.6E-05

VITA

Mr. Thapagorn Boonsongsawat was born on January, 19, 1983, in Chonburi, Thailand. He received a Bachelor's Degree of Chemical Engineering from the Faculty of Engineering, Chulalongkorn University in 2005. After then he subsequently completed the requirements for a Master's Degree in Chemical Engineering at the Department of Chemical Engineering, Faculty of Engineering, Chulalongkorn University in 2007.

